UNIVERSITÉ DU QUÉBEC À RIMOUSKI

ANALYSE DENDROÉCOLOGIQUE ET DENDROCLIMATIQUE DES GISEMENTS DE BOIS DE LACS DE LA TAÏGA DE L'EST DE L'AMERIQUE DU NORD

Thèse présentée

dans le cadre du programme de doctorat en biologie

en vue de l'obtention du grade de docteur

PAR

© FABIO GENNARETTI

Juillet 2014

Composition du jury :

Étienne Boucher, président du jury, UQAM

Dominique Arseneault, directeur de recherche, UQAR

Yves Bégin, codirecteur de recherche, INRS-ETE

Joël Guiot, examinateur externe, CEREGE

Hubert Morin, examinateur externe, UQAC

Dépôt initial le 12 mars 2014 Dépôt final le 04 juillet 2014

À Aurore

REMERCIEMENTS

Je remercie tous ceux qui de près ou de loin ont contribué à ce projet. En premier lieu, mon directeur de recherche, le professeur Dominique Arseneault, et mon codirecteur, le professeur Yves Bégin. Merci Dominique pour tout le temps que nous avons passé ensemble sur le terrain, ces moments ont été inoubliables, pour les échanges d'idées continus que nous avons eu et pour tes innumérables conseils dans la rédaction des articles. Merci Yves pour avoir dirigé de façon magistrale durant ces années le projet ARCHIVES dont mon projet de doctorat a représenté une petite contribution. Ton leadership a vraiment été essentiel.

Je remercie ensuite toutes les personnes du laboratoire d'écologie historique et de dendrochronologie de l'UQAR qui m'ont accueilli à Rimouski et m'ont fait sentir chez moi: Séb, Gab, André, Raph, Marie, Val, Julia, Ben, Tas, Victor et Louis. Merci aussi à tous les membres du projet ARCHIVES pour avoir échangé et collaboré avec moi, vous êtes trop nombreux pour vous nommer sans oublier quelqu'un d'important, et merci à Yves Bouthillier, Pierre-Paul Dion, Maud Naulier et encore Julia Autin, Sébastien Dupuis et Benjamin Dy qui m'ont aidé sur le terrain et au laboratoire.

Un remerciement spécial est dédié à ma famille. En premier lieu à Aurore qui m'a supporté durant toutes ces années et qui est devenue, sans trop le vouloir, une dendrochronologue avec moi, et ensuite à ma famille en Italie qui m'a toujours aidé sans jamais bien comprendre ce que je faisais au Québec. Je vous aime.

Mon doctorat a été une contribution du projet ARCHIVES et a été financé par le CRSNG, Hydro-Quebec, Ouranos, ArcticNet, EnviroNord et le Centre d'Études Nordiques.

RÉSUMÉ

Le but de cette thèse a été de reconstituer des processus écologiques et des changements climatiques dans la taïga du Québec au cours des deux derniers millénaires pour comprendre des aspects qui ont fortement influencé l'évolution de ce territoire majestueux. Pour obtenir des résolutions spatiale et temporelle très fines, nous avons utilisé comme indicateur paléoécologique et paléoclimatique les cernes annuels de croissance de bois subfossiles que nous avons récupéré dans six lacs.

Les gisements de bois subfossiles structurent les écosystèmes littoraux et supportent les réseaux trophiques des lacs. De plus, ils peuvent représenter des puits de carbone à long terme. Dans le premier chapitre de la thèse, nous avons décrit les gisements actuels de bois subfossiles dans les portions littorales des lacs et nous avons établi le temps de résidence des bois dans l'eau en les datant par dendrochronologie ou par le radiocarbone. Cette datation nous a aussi permis d'identifier précisément les incendies qui ont brulé les forêts riveraines durant le dernier millénaire. Ce chapitre a montré que les interactions entre écosystèmes terrestres et aquatiques dans la taïga sont fortement influencées par les incendies, dont les effets peuvent persister pendant des siècles à cause des fortes réductions des apports de bois dans les lacs à la suite des feux dans les forêts riveraines. À échelle locale, la quantité de bois et de carbone préservée dans les gisements littoraux dépend de l'histoire des feux du dernier millénaire qui est propre à chaque site. À échelle régionale, les incendies limitent significativement le carbone séquestré dans les gisements littoraux de bois. Ces gisements représentent une proportion négligeable du stock total de carbone de la taïga malgré la grande abondance de lacs et le long temps de résidence du bois dans l'eau (jusqu'à cinq millénaires pour les bois enfouis).

Dans le deuxième chapitre, nous avons combiné un inventaire détaillé de la forêt riveraine actuelle de deux lacs avec la datation par dendrochronologie des bois subfossiles accumulés dans les zones littorales adjacentes à ces forêts. Notre objectif a été de vérifier si les variations de structure et de composition de la forêt riveraine actuelle pouvaient être attribuées à différentes histoires des feux au cours du dernier millénaire et de montrer les impacts des incendies passés sur la mortalité des arbres, leur densité et leur croissance. Un nombre très important de subfossiles (n = 1037) a permis de reconstituer la dynamique millénaire des forêts avec une fine résolution spatiale (quelques centaines de mètres carrés) et temporelle (annuels) sans précédent. Nos résultats ont contribué à expliquer comment la diversité du paysage actuel de la taïga reflète l'histoire des feux du dernier millénaire qui varie de site en site. Les incendies ont

eu des effets persistants et cumulatifs résultant en une ouverture progressive du couvert forestier avec l'exclusion du sapin baumier qui est un arbre sensible au feu. Le paysage de la taïga est un mosaïque de peuplements forestiers caractérisés par différents temps depuis le dernier feu et différentes trajectoires de structure de la forêt après feu.

Dans le troisième chapitre, nous avons utilisé le réseau de séries dendrochronologiques millénaires développés à partir des bois subfossiles pour produire une reconstitution régionale des températures de juillet-août des 1100 dernières années. Notre réseau a comblé une lacune importante dans le réseau nord-hémisphérique d'indicateurs paléoclimatiques de résolution annuelle utilisés pour reconstituer les températures du dernier millénaire (voir rapport du GIEC). De plus, notre reconstitution a fourni une preuve directe que le climat du Nord-Est de l'Amérique du Nord est particulièrement sensible au forçage volcanique. En effet, elle a montré que des grandes éruptions successives ont déclenché le commencement de périodes plus froides dans la région d'étude qui ont persisté pendant plusieurs décennies. En particulier, deux séries d'éruptions, centrées sur l'éruption du Samalas en 1257 et celle du Tambora en 1815, ont coïncidé avec deux changements abrupts de régime des températures. Ces changements ont marqué respectivement le début du Petit Âge glaciaire et de sa phase la plus froide dans le Nord-Est de l'Amérique du Nord. Notre reconstruction a montré également un Optimum climatique médiéval bien défini, qui a inclus quelques décennies significativement plus chaudes que les 10 dernières années.

Mots clés : changements de régime des températures; débris ligneux littoraux; écologie des feux; forçage volcanique; interactions forêt-lac; interactions végétation-climat; Optimum climatique médiéval; Petit Âge glaciaire; séries dendrochronologiques millénaires; trajectoires de structure et composition des forêts

ABSTRACT

The aim of this thesis was to reconstruct ecological processes and climate change in the taiga of Quebec over the last two millennia to understand factors that have strongly influenced the evolution of this majestic region. To obtain the finest spatial and temporal resolution in our analysis, we used annual growth rings of subfossil logs collected in six lakes as paleoecological and paleoclimatic proxies.

Deposits of subfossil logs determine the structure of lake littoral ecosystems and support their food webs. Moreover, they may represent long-term carbon sinks. In the first chapter of the thesis, we described present-day stocks of subfossil logs in the selected littoral zones and established log residence time in the lakes by tree-ring or radiocarbon dating. Dating also allowed precise identification of each fire that burned the riparian forests during the last millennium. This chapter showed that interactions between terrestrial and aquatic ecosystems in the taiga are strongly influenced by wildfires whose effects can persist for centuries because of strong postfire reductions of log recruitments in lakes. At a local scale, the amount of logs and carbon preserved in littoral stocks depends on the fire history of the last millennium that is specific to each site. At a regional scale, wildfires limit significantly the amount of carbon sequestered in littoral stocks of logs. These stocks represent a negligible fraction of the total taiga carbon storage despite the abundance of lakes and the long residence time of littoral logs (up to five millennia for buried logs).

In the second chapter, we combined a detailed inventory of the present-day riparian forest situated along the shoreline of two lakes with the tree-ring dating of the subfossil logs accumulated in the littoral zones facing these shores. Our objective was to determine whether changes in current riparian forest structure and composition within a given site could be attributed to different fire histories over the last millennium and to show the impacts of past fires on tree mortality, density and growth. Using our impressive paleoecological dataset (n = 1037 logs) in combination with our present-day forest inventory, we were able to reconstruct millennial forest dynamics with an unprecedented high spatial (few hundreds of square meters) and temporal (annual) resolution. Our findings help explain how the present-day landscape diversity in the taiga reflects the fire history of the last millennium, which varies from site to site. Fires have caused persistent and cumulative impacts resulting in a progressive opening of the forest cover along with exclusion of balsam fir, a fire-sensitive tree species. The taiga landscape is a mosaic of forest stands characterized by different times since fire and different postfire forest structure trajectories.

In the third chapter, we used our network of millennial tree-ring chronologies developed from the collected subfossil logs to produce a regional reconstruction of July-August temperatures over the last 1100 years. Our network filled a wide gap in the north-hemispheric network of paleoclimate proxies with annual resolution used for temperature reconstructions of the last millennium (see IPCC report). Moreover, our reconstruction provided direct field evidence that the climate of Northeastern North America is particularly sensitive to volcanic forcing. Indeed, successive large eruptions triggered the beginning of cold episodes in the study area that persisted for decades. In particular, two series of eruptions, centered around the Samalas event in 1257 and the Tambora event in 1815, coincided with two abrupt temperature regime shifts. In Northeastern North America, these shifts marked the onset of the Little Ice Age and the beginning of its coldest phase, respectively. Our reconstruction also showed a well-expressed Medieval Climate Anomaly, which included a few decades significantly warmer than the last 10 years.

Keywords : fire ecology; forest-lake interactions; large woody debris; Little Ice Age; Medieval Climate Anomaly; millennial tree-ring chronologies; plant-climate interactions; temperature regime shifts; trajectories of forest structure and composition; volcanic forcing

TABLE DES MATIÈRES

LISTE DES TABLEAUX

LISTE DES FIGURES

LISTE DES ABRÉVIATIONS, DES SIGLES ET DES ACRONYMES

ACF	Autocorrelation function.
AD	Anno Domini.
AIC	Akaike information criterion.
AMS	Accelerator mass spectrometry.
ANOVA	Analysis of variance.
apr. J.-C.	Après Jésus-Christ.
ARCHIVES	Projet d'analyse rétrospective des conditions hydroclimatiques à l'aide des indicateurs de leur variabilité à l'échelle séculaire.
BC	Before Christ.
BP	Before present.
CEN	Centre d'études nordiques.
CRSNG-RDC	Conseil de recherches en sciences naturelles et en génie du Canada - Subvention de recherche et développement coopératifs.
CRU	Climatic research unit.
DBH	Diameter at breast height.
DOI	Digital object identifier.

DPI	Dots per inch.
ECCOREV	Écosystèmes continentaux et risques environnementaux.
EPS	Expressed population signal.
GDL	Gros débris ligneux.
GIEC	Groupe d'experts intergouvernemental sur l'évolution du climat.
GIS	Geographic information system.
HMM	Hidden Markov models.
INRS-ETE	Institut national de la recherche scientifique - Centre eau terre environnement.
IPCC	Intergovernmental panel on climate change.
IREQ	Institut de recherche d'Hydro-Québec.
LWD	Large woody debris.
PCA	Principal component analysis.
MCMC	Monte Carlo Markov chain simulations.
NENA	Northeastern North America.
NSERC	Natural Sciences and Engineering Research Council of Canada.
PDF	Probability density function.
Rbar	Mean correlation between pairs of tree-ring individual series.
RCS	Regional curve standardization.
RMSE	Root-mean-square error.

SD	Standard deviation.
SE	Standard error.
SEA	Superimposed epoch analysis.
SI	Supporting information.
STREC	Summer temperature reconstruction for Eastern Canada.
UQAR	Université du Québec à Rimouski.

INTRODUCTION GÉNÉRALE

Deux questions principales ont animé ce projet doctoral: comment les perturbations et la variabilité climatique des deux derniers millénaires ont-elles façonné le paysage actuel de la taïga du Québec? et comment le climat de cette région a-t-il fluctué au cours des deux derniers millénaires? La réponse à ces deux questions est bien évidement très complexe et ne peut être exhaustive. De plus, plusieurs chercheurs ont auparavant été passionnés par ces mêmes questions et des réponses partielles sont déjà connues. L'originalité de notre contribution par rapport aux travaux antérieurs a été de montrer des processus écologiques et des fluctuations climatiques au cours des deux derniers millénaires avec une résolution spatiale et temporelle extrêmement fine, ce qui est rare dans l'Est de l'Amérique du Nord. Pour ce faire, nous avons choisi d'utiliser comme indicateur paléoécologique et paléoclimatique les cernes de croissance des arbres et donc la dendrochronologie.

Le mot dendrochronologie est un néologisme qui dérive du grec *dendron* qui signifie arbre et *khronos* qui signifie temps. La dendrochronologie est en effet la méthode scientifique permettant la datation de l'année de formation des cernes de croissance des arbres par l'analyse de la variabilité interannuelle de leur largeur. Cette méthode permet des datations absolues précises à l'année près et a été développée au début du XX^{e} siècle principalement grâce aux intuitions de l'astronome A. E. Douglass. Celui-ci comprit qu'il était possible d'utiliser les informations liées aux cernes de croissance des arbres et il arriva en 1929 à déterminer les années de construction de plusieurs ruines aztèques grâce à l'interdatation de certains échantillons de bois avec une série de référence (Douglass, 1929). Aujourd'hui les longues séries dendrochronologiques (séries temporelles de largeur des cernes de croissance des arbres) sont utilisées dans

plusieurs domaines comme par exemple pour la datation de restes archéologiques et d'œuvres d'art et pour la calibration des datations radiocarbone (Kuniholm, 2000; Friedrich *et al.*, 2004). En paléoécologie, ces séries permettent de reconnaitre et comprendre les processus importants qui ont déterminé la structure et la composition des forêts, comme les épidémies d'insectes et les incendies du passé (Swetnam *et al.*, 2009; Boulanger *et al.*, 2012b). De plus, les séries dendrochronologiques sont reconnues comme étant les meilleurs indicateurs de résolution annuelle du climat de l'Holocène et sont souvent utilisées pour les reconstitutions climatiques (Jones, Osborn et Briffa, 2001; Mann et Jones, 2003; Briffa, Osborn et Schweingruber, 2004; Cook, Esper et D'Arrigo, 2004; Moberg *et al.*, 2005; Rutherford *et al.*, 2005; D'Arrigo, Wilson et Jacoby, 2006; Jansen *et al.*, 2007; Juckes *et al.*, 2007).

En forêt boréale, les arbres morts qui tombent dans l'eau dans des zones lacustres aux caractéristiques favorables (présence de sédiments fins, zone lacustre protégée des vagues, bonne profondeur près de la rive) peuvent se conserver durant des siècles ou des millénaires. De plus, les apports de bois mort dans l'eau sont constants sur de longues périodes, si l'interface forêt-lac est abrupte, si la rive est à l'abri des vents dominants et si les incendies sont rares (Gennaretti, Arseneault et Bégin, 2014). Enfin, l'état de conservation des arbres récupérés permet souvent leur datation par dendrochronologie (Guyette et Cole, 1999; Eronen *et al.*, 2002; Guyette *et al.*, 2002). Pour toutes ces raisons, les arbres subfossiles puisés dans la portion littorale de certains lacs boréaux sont un excellent matériel pour des analyses dendrochronologiques qui ont pour but de répondre à des questions écologiques ou de produire des reconstitutions climatiques sur de longues périodes. Une résolution spatiale et temporelle très fine peut être obtenue dans les analyses car les cernes sont formés annuellement et, dans certains lacs, les bois ne subissent pas de déplacements significatifs. Ces bois contiennent donc des informations importantes quant à l'histoire de la forêt riveraine située devant eux (Gennaretti, Arseneault et Bégin, 2014).

L'objectif de ma thèse a été d'effectuer une analyse dendroécologique et dendroclimatique des gisements de bois de lacs de la taïga de l'Est de l'Amérique du Nord. À partir des bois subfossiles échantillonnés dans six lacs sélectionnés pour leurs caractéristiques favorables, j'ai développé un réseau de séries dendrochronologiques millénaires qui ont permis de:

1 - Comprendre l'influence des incendies du dernier millénaire sur les apports de restes d'arbre dans la zone littorale des lacs étudiés;

2 - Analyser le temps de résidence des bois subfossiles dans l'eau et les facteurs qui influencent leur conservation;

3 - Étudier les effets des incendies passés sur la structure et la composition actuelles des peuplements forestiers de la taïga;

4 - Analyser la croissance plurimillénaire des forêts riveraines et la force du signal commun d'origine climatique préservé dans les cernes;

5 - Effectuer une reconstitution climatique du dernier millénaire dans la région d'étude qui a pu être comparée avec les reconstitutions les plus accréditées;

6 - Vérifier l'occurrence dans la région d'étude des fluctuations climatiques qui ont caractérisé le dernier millénaire (Optimum climatique médiéval et Petit Âge glaciaire);

7 - Quantifier, à échelle régionale, l'intensité du réchauffement climatique actuel.

8 - Déterminer les forçages climatiques les plus influents sur la variabilité régionale du climat au cours du dernier millénaire.

Dans son rapport de 2007, le Groupe d'experts Intergouvernemental sur l'Évolution du Climat (GIEC) avait souligné la mauvaise couverture spatiale et le manque de réplication des données qui permettent de reconstituer l'histoire du climat au cours du dernier millénaire (Jansen *et al.*, 2007). Récemment le GIEC a publié un nouveau rapport

et les résultats relatifs à la variabilité climatique des deux derniers millénaires sont essentiellement fondés sur les travaux du consortium PAGES 2K (Pages 2k Consortium, 2013). Malgré les avancements accomplis durant les dernières années, le climat des deux derniers millénaires en Amérique du Nord a seulement été reconstitué à partir d'indicateurs de basse résolution, comme les pollens conservés dans les sédiments lacustres (Viau, Ladd et Gajewski, 2012; Trouet *et al.*, 2013). Par contre, des reconstitutions fiables qui utilisent des indicateurs de résolution annuelle comme des cernes d'arbres couvrent seulement les 800 dernières années (Pages 2k Consortium, 2013). Ce manque de données génère beaucoup d'incertitude lorsque l'on cherche à comparer le réchauffement climatique du dernier siècle avec la variabilité naturelle du climat au cours des derniers millénaires. Cette thèse peut donc susciter beaucoup d'intérêt dans la communauté scientifique internationale car elle a permis d'améliorer la couverture spatiale et temporelle du réseau de séries dendrochronologiques utilisé pour les reconstitutions climatiques millénaires. En effet, la forêt boréale nord américaine est une des régions pour lesquelles les longues séries dendrochronologiques sensibles aux températures sont actuellement très rares (D'Arrigo *et al.*, 2009).

La mise en place de notre réseau de séries dendrochronologiques a également permis de répondre à des questions écologiques. Grâce aux chronologies produites et à la découverte d'échantillons avec des traces de feu, nous avons été capables de dater les incendies du dernier millénaire qui ont affecté les forêts riveraines dans chacun des sites d'étude. Ceci a permis d'étudier l'influence des incendies aussi bien sur les apports de restes d'arbre dans les zones littorales des lacs que sur l'état actuel des pessières à lichens riveraines de la taïga québécoise. Les incendies sont la principale cause de changements écologiques en forêt boréale nordique (Morneau et Payette, 1989; Arseneault et Payette, 1992; Arseneault et Payette, 1997a; Lavoie et Sirois, 1998; Girard, Payette et Gagnon, 2008; Payette, Filion et Delwaide, 2008). La variation de leur intensité et de leur fréquence a des répercussions sur les transferts entre écosystèmes terrestres et lacustres

(Marchand, Prairie et del Giorgio, 2009), sur la structure des peuplements forestiers, sur la répartition spatiale et sur l'abondance des espèces forestières (Payette, 1993).

De plus, cette thèse a eu des retombées appliquées car elle s'est insérée dans le projet ARCHIVES (http://archives.ete.inrs.ca/). Ce projet multidisciplinaire qui a regroupé plusieurs chercheurs de différents pays a eu pour objectif d'évaluer les variations à long terme des réserves d'eau contenues dans les immenses réservoirs hydroélectriques du secteur boréal du Québec. Dès 1983, des niveaux d'eau extrêmement bas ont été enregistrés dans les réservoirs hydroélectriques de la Grande Rivière causés par des précipitations en dessous de la moyenne des 30 années précédentes (Roy, Mathier et Bobée, 1995). Le projet ARCHIVES a visé à reconstituer le climat passé pour calibrer les projections climatiques futures dans le Québec boréal et fournir des outils nécessaires pour une meilleure gestion des réservoirs. Dans le cadre d'ARCHIVES, les données de ce doctorat ont servi d'intrant à d'autres projets, dont: (1) une maîtrise qui a visé à déterminer la meilleur façon d'intégrer des arbres vivants et des arbres subfossiles dans les séries dendrochronologiques pour des analyses paléoclimatiques, (2) une maîtrise qui a eu pour objectif de comprendre l'influence des niveaux d'eau sur les arbres riverains, (3) et enfin un doctorat qui a visé à reconstituer le climat à partir des isotopes de la cellulose dans les cernes des arbres subfossiles que nous avons échantillonné. La fusion des résultats de ces projets permettra d'améliorer et de valider les reconstitutions climatiques effectuées.

Cette thèse est divisée en trois chapitres qui correspondent à trois publications scientifiques. Ces chapitres sont liés par l'utilisation de l'information que l'on peut extrapoler des gisements de bois de lacs et ont permis de mieux comprendre des processus qui ont fortement marqué l'évolution de la taïga de l'Est de l'Amérique du Nord au cours des deux derniers millénaires. Les questions abordées dans les trois chapitres sont très différentes. Cependant, dans l'ensemble, cette thèse a montré le lien réel, scientifique et conceptuel qui existe entre l'évolution écologique et climatique du territoire étudié et a montré des problèmes et des enjeux généraux associés à la

transformation à long terme des paysages forestiers. Au fur et à mesure que nous avons avancé dans les chapitres et dans les analyses, nous avons pris en compte une échelle spatiale de plus en plus grande. Tout d'abord, nous avons analysé le recrutement des bois subfossiles dans chaque portion littorale étudiée. Cela nous a permis de démontrer que les interactions entre écosystèmes terrestres (pessières à lichens riveraines) et aquatiques dans la taïga sont fortement influencées par les incendies qui provoquent des effets pouvant s'étaler sur plusieurs siècles. Ensuite, nous avons élargie l'échelle spatiale de l'analyse et nous nous sommes intéressés à la dynamique à long-terme des forêts riveraines de notre région d'étude. Plus précisément nous avons essayé de démontrer la connexion entre la diversité actuelle des pessières à lichens riveraines de la taïga et le climat et l'histoire des feux du dernier millénaire. Enfin, dans le troisième chapitre de la thèse nous nous sommes intéressés à la variabilité du climat régional au cours du dernier millénaire et nous avons aussi essayé de comprendre les forçages globaux qui déterminent cette variabilité.

Interactions forêt-lac: le rôle du bois subfossile dans la portion littorale.

Les écosystèmes sont rarement des systèmes fermés et les mouvements de nutriments, détritus, proies et consommateurs de ressources sont communs entre plusieurs habitats. Ces mouvements peuvent influencer localement la quantité de ressources disponibles, les réseaux trophiques et la dynamique des communautés et des populations (Polis, Anderson et Holt, 1997). Par exemple, un lac est spatialement défini par ses rives, la surface de l'eau et les sédiments lacustres mais des nutriments et des sources d'énergie peuvent traverser ces frontières, générant des inputs ou des outputs d'origines météorologiques, géologiques ou biologiques (Hasler, 1975). En effet, les réseaux trophiques des lacs sont souvent alimentés par des ressources biologiques allochtones provenant en partie de la végétation riveraine comme les restes d'arbre et de branches qui tombent dans l'eau dans la zone littorale (Gros Débris Ligneux, GDL). Les GDL qui proviennent de la forêt riveraine apportent non seulement une quantité substantielle de matériel organique aux écosystèmes aquatiques mais ajoutent également

une certaine hétérogénéité et complexité à la structure des habitats littoraux (Glaz, 2008). Les GDL sont très importants pour plusieurs organismes aquatiques des lacs et des rivières en créant des refuges et des zones d'ombre et en gardant la température de l'eau en dessous de seuils (Sargent *et al.*, 2011). Les GDL de la zone littorale représentent donc l'habitat idéal pour plusieurs communautés de microorganismes (Tank et Webster, 1998; Vadeboncoeur et Lodge, 2000; Collier, Smith et Halliday, 2004), invertébrées (Lester, Wright et Jones-Lennon, 2007; Scealy, Mika et Boulton, 2007; Hrodey, Kalb et Sutton, 2008; Glaz, Nozais et Arseneault, 2009) et poissons (Fausch et Northcote, 1992; Everett et Ruiz, 1993).

Les changements affectant les milieux littoraux structurés par des GDL sont très lents. Le recrutement des bois et leur dégradation doivent être analysés sur des échelles temporelles de l'ordre de plusieurs siècles (Guyette et Cole, 1999; Harmon *et al.*, 2004). Pour cette raison, les GDL accumulés dans la zone littorale des lacs et rivières peuvent contribuer au stockage d'une portion de carbone qui serait rapidement perdu dans les écosystèmes terrestres (Guyette, Dey et Stambaugh, 2008). En effet, le bois mort peut demeurer dix fois plus longtemps dans les écosystèmes d’eau douce que dans les écosystèmes terrestres avoisinants (Guyette *et al.*, 2002).

L'accumulation et la quantité totale de GDL dans la zone littorale des lacs peuvent être fortement influencées par l'histoire des perturbations anthropiques, comme par exemple l'exploitation forestière ou le développement résidentiel (Guyette et Cole, 1999; Marburg, Turner et Kratz, 2006; Boucher, Arseneault et Sirois, 2009; Glaz, Nozais et Arseneault, 2009). Il y a, par contre, très peu de connaissances sur les variations du taux de recrutement des GDL à la suite de perturbations naturelles. Récemment, il a été démontré que les incendies qui affectent les peuplements riverains provoquent dans les lacs boréaux du Québec une augmentation de la respiration planctonique et donc une augmentation ultérieure de la minéralisation et des émissions de carbone (Marchand, Prairie et del Giorgio, 2009). Cet aspect peut avoir un impact important sur le bilan de carbone à échelle du paysage, mais les incendies provoquent aussi des altérations

d'apports de bois mort dans l'eau qui ont des répercussions sur de longues périodes et qu'il faut considérer dans le bilan total.

Dans le premier chapitre de cette thèse, nous avons examiné l'influence des incendies du dernier millénaire sur les apports de restes d'arbre dans la zone littorale de cinq lacs de la taïga québécoise. Nous avons aussi analysé les facteurs qui influencent le temps de résidence et l'état de préservation du bois subfossile dans l'eau de ces lacs et la quantité de carbone séquestrée dans ces gisements. Les objectifs spécifiques de ce chapitre ont été les suivants:

Objectif 1 - Déterminer l'impact des incendies du dernier millénaire sur les apports de restes d'arbre dans la zone littorale des lacs étudiés.

Hypothèse - Les incendies causent des apports massifs de restes d'arbre dans l'eau et des interruptions d'apports qui varient en fonction de la sévérité de ces perturbations.

Objectif 2 - Analyser le temps de résidence des arbres subfossiles dans des lacs boréaux et la quantité maximale de biomasse préservée dans ces gisements.

Hypothèse 1 - Les arbres subfossiles peuvent se conserver des millénaires dans la zone littorale de lacs boréaux.

Hypothèse 2 - Le temps de résidence des restes d'arbre dans l'eau dépend de leurs conditions de préservation (substrat, degré d'enfouissement, profondeur dans l'eau, distance de la rive, etc.).

Hypothèse 3 - À l'échelle locale, d'importants volumes de bois et quantités de carbone peuvent se conserver dans des gisements de GDL.

Cette partie de la thèse a été basée sur la datation par dendrochronologie des GDL puisés dans les lacs sélectionnés pour mettre en place notre réseau de sites d'échantillonnage. Cette datation nous a permis d'identifier les incendies qui ont affecté chaque site et d'examiner les changements de régime d'apports de GDL dans les lacs

durant les derniers millénaires. Le principal résultat de ce chapitre a été de démontrer que les interactions entre les écosystèmes terrestres et aquatiques dans les régions boréales nordiques sont fortement influencées par les incendies dont les effets peuvent perdurer durant des siècles. En effet, les incendies brulent les forêts riveraines et modifient les apports de GDL dans les lacs en produisant souvent des interruptions d'apports. Ce sont des modifications à long terme (de l'ordre des siècles) a cause de la lente décomposition des GDL qui structurent les écosystèmes littoraux des lacs boréaux. Les GDL, et particulièrement ceux qui sont enfouis dans les sédiments et qui sont plus éloignés de la rive, peuvent avoir des temps de résidence dans les zones littorales très longs, jusqu'à cinq millénaires. En conclusion, dans la région d'étude les volumes de bois et les quantités de carbone séquestrées dans les gisements de GDL dans les lacs dépendent de l'histoire des incendies qui a varié de site en site durant les derniers millénaires. Cependant, à l'échelle du paysage, le carbone séquestré dans les gisements de GDL littoraux représente une portion minime du carbone séquestré en région boréale.

L'impact des incendies dans la taïga.

La zone boréale du Nord-Est de l'Amérique du Nord est divisée en trois grandes sous-zones qui couvrent trois bandes latitudinales: la forêt boréale continue (au sud), la taïga dominée par les pessières à lichens qui s'étend du 52^{e} au 55^{e} parallèle (au centre) et la toundra forestière (au nord) (Saucier *et al.*, 2003). Les associations entre les quelques espèces forestières présentes dans ces écosystèmes boréaux sont le résultat d'interactions complexes entre le climat, le contexte biophysique et les perturbations durant l'Holocène (de Lafontaine et Payette, 2010). Par exemple, les incendies forestiers sont un des facteurs les plus importants pour la caractérisation des processus associées aux écosystèmes terrestres dans le biome boréal (Rowe et Scotter, 1973).

Plusieurs études ont estimé le cycle de feux (le temps nécessaire pour brûler une superficie équivalente à l'aire d'étude) pour des portions de forêt boréale canadienne et les résultats varient selon les secteurs entre 40 et 600 ans (Payette *et al.*, 1989; Larsen,

1997; Bergeron *et al.*, 2001; Héon, 2009; Boulanger *et al.*, 2012a). Les feux dans cette région sont en général très sévères et très étendus, car ils atteignent la cime des arbres, et couvrent de très grandes superficies pouvant atteindre plusieurs milliers de kilomètres carrés (Johnson, 1992; Amiro *et al.*, 2001; Arseneault, 2001; Stocks *et al.*, 2003; Héon, 2009).

La fréquence, la sévérité et le comportement des incendies dans la zone boréale ont un impact majeur sur l'état de la forêt actuelle et ont créé une mosaïque caractérisée par des grandes variations de structure et de composition de la végétation (Johnson, 1992; Arseneault, 2001). Par exemple, l'épinette noire et le pin gris sont les espèces qui dominent le paysage de la taïga québécoise car ils sont très bien adaptés aux feux grâce à leur cônes semi-sérotineux ou sérotineux (cônes qui s'ouvrent et libèrent des graines viables suite aux incendies; Black et Bliss, 1980; Rudolph et Laidly, 1990; Viereck et Johnston, 1990). Des études ont montré que la fréquence des incendies influence les processus de rétablissement après feu de ces espèces. Des intervalles courts entre les feux (< 60 ans) peuvent expliquer l'expansion du pin et au contraire des intervalles longs (> 220 ans) sont la cause de la prépondérance de l'épinette (Le Goff et Sirois, 2004). Cette raison explique la distribution actuelle du pin gris qui, durant l'Holocène, a connu une expansion du sud-ouest vers le centre du Québec, s'arrêtant où la fréquence des feux diminue en raison d'un climat plus humide (Payette, 1993). L'abondance du sapin baumier dépend aussi de l'histoire des feux. Cet arbre est l'un des moins bien adaptés aux incendies en région boréale (Payette, 1993). Il a été supposé que les perturbations causées par les incendies au nord du 49^{e} parallèle ont provoqué la diminution de l'abondance du sapin et l'omniprésence des espèces les plus adaptées au feu. Aujourd'hui le sapin dans la taïga représenterait un vestige d'une expansion historique vers le nord causée par une fréquence mineure des perturbations (Sirois, 1997; Arseneault et Sirois, 2004; Boucher, Arseneault et Hétu, 2006; de Lafontaine et Payette, 2010).

En conclusion, les incendies sont la principale perturbation et la principale cause de changements écologiques en forêt boréale nordique (Morneau et Payette, 1989).

Durant le dernier millénaire, l'intensité des incendies, un intervalle de temps réduit entre les feux et un climat moins favorable ont provoqué une mauvaise régénération et des changements de structure de la végétation dans toute la zone boréale (Arseneault et Payette, 1992; Arseneault et Payette, 1997a; Lavoie et Sirois, 1998; Johnstone, 2006; Johnstone et Chapin, 2006; Girard, Payette et Gagnon, 2008; Payette, Filion et Delwaide, 2008; Johnstone *et al.*, 2010).

La région d'étude de cette thèse correspond à la taïga québécoise au nord des dernières coupes forestières, à l'est des derniers peuplements de pin gris, qui se retrouvent une dizaine de kilomètres plus à l'ouest, et à la limite nord de l'aire de répartition du sapin baumier (Payette, 1993). Dans cette zone, le paysage est composé d'une mosaïque de pessières à lichens établies après feu, mais comme le cycle de feu semble assez lent, plusieurs forêts sont très vieilles. Cette mosaïque est le résultat des changements climatiques et des perturbations qui ont eu lieu durant l'Holocène. Le deuxième chapitre de cette thèse a eu comme objectif de comprendre les liens entre les incendies historiques, le climat et la structure et composition actuelle des forêts riveraines de la taïga du Québec. Plus précisément, l'objectif et les hypothèses de ce chapitre ont été les suivants:

Objectif - Analyser les impacts des incendies historiques sur les pessières à lichens de la taïga du Québec.

Hypothèse 1 - Dans la taïga du Québec, les incendies du dernier millénaire ont causé des impacts persistants et cumulatifs qui ont provoqué une diminution de la densité des arbres dans les peuplements les plus affectés. Ces impacts sont encore visibles même si le dernier feu a eu lieu il y a quelques siècles.

Hypothèse 2 - Les incendies récurrents durant les deux derniers millénaires ont causé la diminution de l'abondance du sapin baumier et aujourd'hui nous ne retrouvons cette espèce que dans les peuplements qui ont été à l'abri des feux sévères.

Hypothèse 3 - Des peuplements adjacents peuvent être caractérisés par une structure et une composition de la forêt très différentes qui dépendent de leur histoire de feu respective.

Ce chapitre a été basé sur la comparaison de l'état actuel des pessières à lichens sur la rive des lacs échantillonnés avec les données provenant des arbres subfossiles puisés dans les portions littorales de ces lacs. L'analyse des forêts actuelles a permis d'identifier des portions homogènes par leur structure et leur composition. Ensuite, les données dendrochronologiques provenant des arbres subfossiles nous ont fourni pour chaque portion des informations sur l'occurrence des incendies dans le passé, sur les changements de densité des arbres des forêts riveraines et sur leur croissance séculaire. Ces données nous donnent une perspective à long terme avec une résolution spatiale et temporelle très fine qui a aidé à comprendre comment la diversité du paysage actuel dans la taïga du Québec dépend de l'histoire des incendies de chaque site au cours du dernier millénaire. Le paysage de cette région est une mosaïque de pessières à lichens établies plus au moins récemment après feu et chaque feu a entrainé par la suite dans chaque site une trajectoire différente de structure et composition de la forêt. De plus, la variabilité climatique du dernier millénaire a influencé la croissance et la mortalité des arbres à l'échelle locale. En effet, la croissance des forêts était plus rapide durant l'Optimum climatique médiéval et une période froide à la fin du Petit Âge glaciaire (durant la première moitié du XIX^{e} siècle) a provoqué une diminution de la croissance et la mort de plusieurs arbres dans les peuplements étudiés.

La dendrochronologie et les reconstitutions climatiques.

La connaissance de la variabilité climatique du passé est cruciale pour la compréhension des changements climatiques actuels et la modélisation des changements climatiques futurs. Cependant, les enregistrements des stations météorologiques ne sont pas assez longs et donc ne fournissent pas des informations sur la variabilité climatique à l'échelle des siècles (Jones, Osborn et Briffa, 2001). Actuellement, il existe différents

types d'indicateurs (en anglais "*proxies*") pouvant être utilisés pour reconstituer l'histoire du climat du dernier millénaire (Jones *et al.*, 2009). Parmi ces indicateurs, les séries dendrochronologiques sont l'une des principales sources de données utilisées, en raison de leur résolution annuelle et de l'ubiquité des arbres (D'arrigo et Jacoby, 1993; Mann, Bradley et Hughes, 1998; Briffa, 2000; Jones, Osborn et Briffa, 2001; Helama *et al.*, 2002; Mann et Jones, 2003; Briffa, Osborn et Schweingruber, 2004; Cook, Esper et D'Arrigo, 2004; Cook *et al.*, 2004; Rutherford *et al.*, 2005; D'Arrigo, Wilson et Jacoby, 2006; D'Arrigo *et al.*, 2009). Les cernes de croissance des arbres sont des indicateurs climatiques uniques qui permettent d'analyser des variations de courte (annuelle) et de longue période (séculaire) (Briffa, 2000; Esper, Cook et Schweingruber, 2002).

Dans les écosystèmes tempérés et boréaux, il a été possible de construire plusieurs séries dendrochronologiques millénaires en combinant des arbres vivants, des arbres subfossiles et des restes archéologiques. Par exemple, nous pouvons citer les séries de plus de 7000 ans produites en Scandinavie en utilisant des restes d'arbres (pin sylvestre) prélevés dans des lacs (Eronen *et al.*, 2002; Grudd *et al.*, 2002), les séries millénaires de mélèze développées en Sibérie et dans les Alpes (Hantemirov et Shiyatov, 2002; Naurzbaev *et al.*, 2002; Büntgen *et al.*, 2005), la chronologie de 3585 ans de genévrier (*Sabina przewalskii* Kom.) produite avec des arbres vivants et des restes archéologiques dans le plateau tibétain (Shao *et al.*, 2009), les séries plurimillénaires de chêne du centre et du nord de l'Europe (Kelly *et al.*, 2002; Leuschner *et al.*, 2002; Spurk *et al.*, 2002; Friedrich *et al.*, 2004), les chronologies de pin bristlecone dans le sud-ouest américain qui remontent jusqu'à 8500 ans (Ferguson, 1979; Ferguson et Graybill, 1983) et, en ce qui concerne l'hémisphère sud, les séries produites en Tasmanie et Nouvelle Zélande par Cook et al. (Cook *et al.*, 2006).

Malgré ces progrès, les reconstitutions climatiques sont encore très incertaines et la couverture spatiale et temporelle du réseau de *proxies* millénaires doit être améliorée. En effet, la quantité de données disponibles est insuffisante pour estimer de façon précise à l'échelle régionale l'importance du réchauffement climatique actuel par rapport

aux fluctuations naturelles des deux derniers millénaires (Jansen *et al.*, 2007; Pages 2k Consortium, 2013). Par exemple, le réseau de séries dendrochronologiques est certainement plus développé dans l'hémisphère nord mais, pour certaines régions, les longues chronologies sont presque inexistantes. En particulier dans la forêt boréale nord-américaine, les séries sont rares à cause de la courte longévité des arbres (rarement plus de 300 ans; la plus vieille épinette noire trouvée avait 504 ans; Payette *et al.*, 1985) et de la haute fréquence des incendies forestiers (Arseneault *et al.*, 2013). Le réchauffement actuel dans les hautes latitudes nord est extrêmement prononcé et la rareté de témoins climatiques pour le dernier millénaire en Amérique du Nord est particulièrement grave car il affecte la qualité des prédictions futures (voir le cinquième rapport du GIEC; Stocker *et al.*, 2013).

Un autre problème concerne la façon d'utiliser les *proxies*, surtout les séries dendrochronologiques, pour produire des reconstitutions climatiques. Cet aspect a causé de nombreuses critiques sur la validité des reconstitutions, comme par exemple la fameuse critique de McIntyre et McKitrick (McIntyre et McKitrick, 2005) sur la reconstitution de Mann et al. (Mann, Bradley et Hughes, 1998). En effet, parmi les facteurs qui peuvent influencer les résultats des reconstitutions, nous pouvons citer: la méthode choisie pour assimiler les *proxies*, la saison choisie pour la reconstitution, la validité spatiale de la reconstitution et surtout la qualité du réseau de *proxies* utilisé (Rutherford *et al.*, 2005). Pour cette raison, il est nécessaire de produire de nouvelles séries de *proxies* sensibles aux facteurs climatiques, de sélectionner des séries avec une bonne réplication sur toutes les périodes couvertes, de bien comprendre la réponse des *proxies* au climat et enfin d'utiliser des méthodes de reconstitution permettant la quantification des erreurs (Briffa et Matthews, 2002; Jones *et al.*, 2009; Franke *et al.*, 2013). Un autre facteur qui a récemment ajouté de l'incertitude aux reconstitutions basées sur les séries dendrochronologiques a été le problème de la "Divergence", c'est à dire la tendance qu'ont plusieurs indices dendrochronologiques à sous-estimer l'augmentation récente des températures (Jacoby et D'Arrigo, 1995; Briffa *et al.*, 1998;

Wilmking *et al.*, 2005; D'Arrigo *et al.*, 2008). Les causes de ce problème sont mal connues et sans doute multiples, comme par exemple: des relations non linéaires entre la croissance des arbres et le climat, une sensibilité importante des arbres à la sécheresse avec l'augmentation des températures et des artefacts méthodologiques dus au processus de standardisation des séries de croissance (D'Arrigo *et al.*, 2008). Enfin, un autre aspect qui a été souligné est l'importance de produire des reconstitutions ayant une validité locale ou régionale et non pas seulement de grandes reconstitutions à échelle hémisphérique. En effet, certaines fluctuations climatiques du passé, comme l'Optimum climatique médiéval, se sont produites durant des périodes différentes selon la région considérée, et c'est pourquoi, les grandes reconstitutions qui utilisent plusieurs *proxies* éparpillés sur le globe peuvent être incapables de montrer ces fluctuations climatiques (D'Arrigo, Wilson et Jacoby, 2006).

Les reconstitutions climatiques basées sur des données dendrochronologiques peuvent être utilisées pour évaluer l'influence des forçages climatiques sur la variabilité du climat à échelle régionale et hémisphérique. Par exemple, ces données ont été utilisées pour évaluer les effets du forçage solaire (Breitenmoser *et al.*, 2012), du forçage orbital (Esper *et al.*, 2012), du forçage volcanique (D'Arrigo, Wilson et Anchukaitis, 2013; Esper *et al.*, 2013) et pour déterminer si l'ampleur du réchauffement climatique récent d'origine anthropique est sans précédent par rapport aux fluctuations des derniers siècles (Sidorova *et al.*, 2013; Tingley et Huybers, 2013). En ce qui concerne le forçage volcanique, l'effet refroidissant sur le climat global des cendres volcaniques et des gouttelettes d'acide sulfurique émises dans l'atmosphère lors des grandes éruptions est bien connu, malgré les désaccords qui existent sur la force et la durée de ces effets (Miller *et al.*, 2012; Esper *et al.*, 2013). Récemment des données de terrain (Miller *et al.*, 2012) et des modélisations climatiques (Stenchikov *et al.*, 2009; Otterå *et al.*, 2010; Zhong *et al.*, 2011; Zanchettin *et al.*, 2012; Schleussner et Feulner, 2013) ont montré que des grandes éruptions successives peuvent entraîner le début de périodes froides qui peuvent persister pour plusieurs décennies ou des siècles si des rétroactions océaniques

ou liées à la glace de mer se mettent en place. Par contre, le réseau nord hémisphérique de séries dendrochronologiques sensibles aux températures semble montrer que les plus fortes éruptions du dernier millénaire ont produit des baisses de température qui ont toujours duré moins de dix ans (Breitenmoser *et al.*, 2012; D'Arrigo, Wilson et Anchukaitis, 2013; Esper *et al.*, 2013). Cette discordance a fait douter de la possibilité de bien reconstituer les baisses de température d'origine volcanique avec la dendroclimatologie (Mann, Fuentes et Rutherford, 2012). Cependant, une sensibilité plus au moins forte aux effets du forçage volcanique selon la région considérée pourrait en partie expliquer cette discordance (D'Arrigo, Wilson et Anchukaitis, 2013). En particulier, le Nord-Est de l'Amérique du Nord, pour lequel les longues séries dendrochronologiques sont très rares, semble être très sensible au volcanisme (Jacoby, Ivanciu et Ulan, 1988; Briffa *et al.*, 2001; Miller *et al.*, 2012).

Un des objectifs de cette thèse a été de produire une reconstitution climatique régionale à partir de la construction d'un réseau de séries dendrochronologiques millénaires dans la taïga du Québec. Les séries dans notre région d'étude sont très rares mais le caractère exceptionnel de nos sites, témoigné par le grand nombre d'arbres subfossiles récoltés en parfait état de conservation, a permis la production de séries locales hautement répliquées couvrant les 1400 dernières années pour chaque site. Grace à cette réplication, il a été possible de produire une reconstitution climatique avec une bonne robustesse statistique. Actuellement, la compréhension de la variabilité climatique du dernier millénaire à l'échelle régionale représente un défi très important pour la communauté scientifique internationale. Notre réseau de séries dendrochronologiques millénaires hautement répliquées suscitera donc un grand intérêt car il a permis d'améliorer la représentativité spatiale et temporelle des reconstitutions climatiques. Les objectifs spécifiques de ce chapitre ont été les suivants:

Objectif 1 - Vérifier si un signal commun d'origine climatique est présent dans les séries dendrochronologiques produites.

Hypothèse - Les séries dendrochronologiques produites corrèlent significativement entre elles et avec les données climatiques régionales du dernier siècle.

Objectif 2 - Vérifier l'occurrence, dans notre région d'étude, des oscillations climatiques qui ont caractérisé le dernier millénaire et comparer leurs amplitudes.

Hypothèse - Dans le Nord-Est de l'Amérique du Nord, l'Optimum climatique médiéval plus chaud a été suivi par le Petit Âge glaciaire plus froid et, par la suite, durant le dernier siècle une augmentation significative des températures a été observée.

Objectif 3 - Déterminer les effets du volcanisme sur le climat régional dans le Nord-Est de l'Amérique du Nord durant le dernier millénaire.

Hypothèse - Le Nord-Est de l'Amérique du Nord est particulièrement sensible aux effets refroidissants des grandes éruptions volcaniques et des éruptions successives ont provoqué des baisses soudaines et persistantes des températures.

Ce chapitre repose sur la création de six séries dendrochronologiques millénaires standardisées, une pour chaque lac. Les indices de ces séries ont été comparés aux données climatiques du dernier siècle disponibles pour la région d'étude (températures, précipitations, etc.) pour établir un modèle d'inférence statistique (i.e. fonction de transfert) qui a été utilisé pour la reconstitution paléoclimatique des températures estivales dans le Nord-Est de l'Amérique du Nord. Des données relatives aux dépôts sulfurés dans des carottes glaciaires (Gao, Robock et Ammann, 2008) ont ensuite permis de comparer les dates des éruptions volcaniques les plus fortes des derniers siècles à notre reconstitution pour voir si le volcanisme a influencé le climat de notre région d'étude.

Notre réseau de séries dendrochronologiques millénaires a comblé une lacune importante dans le réseau nord-hémisphérique d'indicateurs paléoclimatiques de résolution annuelle qui peuvent être utilisés pour des reconstitutions des températures.

Notre reconstitution des températures estivales appuie l'hypothèse que le Nord-Est de l'Amérique du Nord est très sensible aux effets du volcanisme et que, dans cette région, des séries d'éruptions volcaniques très fortes ont causé le début de baisses de température significatives et persistantes. En effet, suite à l'Optimum climatique médiéval, durant lequel les décennies les plus chaudes des 1100 dernières années ont eu lieu, une baisse des températures a été observée et a coïncidé avec une série d'éruptions volcaniques centrée sur l'immense éruption du Samalas en 1257 (Lavigne *et al.*, 2013). Ce changement de régime des températures a marqué dans le Nord-Est de l'Amérique du Nord la fin de l'Optimum climatique médiéval et le début du Petit Âge glaciaire. Par la suite, une autre série d'éruptions volcaniques centrée sur l'éruption du Tambora en 1815 (Cole-Dai *et al.*, 2009) a provoqué le début de la période de 40 ans la plus froide des 1100 dernières années à la fin du Petit Âge glaciaire. Durant le dernier siècle, une hausse des températures particulièrement forte a été observée dans le Nord-Est de l'Amérique du Nord, surtout si nous considérons seulement les 30 dernières années (cette affirmation est basée sur les données du Climatic Reasearch Unit; Mitchell et Jones, 2005). Cependant, selon notre reconstitution, qui reproduit bien la hausse des températures du dernier siècle, des températures plus chaudes par rapport aux dernières décennies ont été observées durant certaines décennies de l'Optimum climatique médiéval.

Région d'étude

Pour la création de notre réseau de séries dendrochronologiques nous avons choisi une aire d'étude à l'interface entre la taïga et la toundra forestière dans la région boréale nordique du Québec (54 N, 72 W; Saucier *et al.*, 2003). La topographie de notre région d'étude est vallonnée avec une altitude variant de 380m à 730m avec une moyenne de 500m. Les stations météorologiques du réseau d'Environnement Canada les plus proches sont La Grande IV et Schefferville. Les données de ces deux stations confirment que la région est caractérisée par un climat subarctique continental avec des étés courts et doux et des hivers longs et froids, et avec une température annuelle moyenne en dessous de 0°C (-3,0°C pour La Grande IV et -5,3°C pour Schefferville). En ce qui concerne les précipitations, elles sont plus copieuses en été, mais à Schefferville les précipitations totales annuelles sont plus abondantes (823mm contre 760mm pour La Grande IV). En effet, le climat devient de plus en plus humide vers l'est, parallèlement à une diminution de la fréquence des incendies (Boulanger *et al.*, 2012a).

En dehors des tourbières, des lacs et des endroits ouverts récemment incendiés, la pessière à lichens est l'écosystème dominant dans ce territoire et l'épinette noire (*Picea mariana* (Mill.) B.S.P.) est de loin l'espèce d'arbre la plus abondante. Le bois de l'épinette noire est particulièrement propice pour des analyses dendrochronologiques. En effet, les cernes sont facilement visibles, les cernes manquants sont très rares (cernes non visibles car trop étroits) et nous y retrouvons plusieurs cernes pâles (cernes avec bois final peu différencié), caractérisant des années particulières, qui fournissent un outil de datation supplémentaire (Filion *et al.*, 1986; Arseneault et Payette, 1998). De plus, les épinettes qui tombent dans l'eau dans la zone littorale de lacs aux caractéristiques favorables peuvent se conserver des siècles, voire des millénaires (Gennaretti, Arseneault et Bégin, 2014). Nous avons donc sélectionné des portions littorales de six lacs caractérisées par des gisements importants de bois subfossile pour la réalisation de notre réseau de séries dendrochronologiques à partir d'épinettes vivantes (arbres riverains) et subfossiles.

Notre aire d'étude regroupe une série de caractéristiques favorables. Tout d'abord, malgré qu'elle soit située dans une région éloignée, cette région est accessible grâce à la route Transtaïga. Cette route gravelée commence au kilomètre 542 de la route de la Baie James et s'étend vers l'est sur 666 Km. Elle fut construite dans les années 70 pour permettre l'accès aux centrales hydroélectriques et aux réservoirs situés en amont de la Grande Rivière. Un autre avantage de notre aire d'étude est sa localisation au nord de la forêt boréale (54^{e} parallèle). À ces latitudes, les arbres sont plus sensibles aux facteurs climatiques que dans le sud de la forêt boréale et les seules activités anthropiques qui peuvent avoir perturbé leur croissance ont eu lieu après la construction de la route. Cette région se caractérise également par des écosystèmes forestiers simples dominés par un nombre restreint d'espèces d'arbres: l'épinette noire, le sapin baumier (*Abies balsamea* L.), et le mélèze laricin (*Larix laricina* (Du Roi) K. Koch). Pour cette raison, l'étude des impacts des perturbations naturelles et de la variabilité climatique sur le paysage régional au cours du dernier millénaire est aussi simplifié. Finalement, cette aire d'étude comprend un très grand nombre de lacs par unité de surface, un atout important qui a permis de sélectionner des lacs parmi un vaste choix. Peu de lacs regroupent en effet toutes les caractéristiques qui permettent de construire une longue série dendrochronologique fortement répliquée (i.e. gros gisements de bois subfossile dans la zone littorale, apports continus de bois subfossile dans l'eau au cours des derniers siècles et caractéristiques favorables à la conservation du bois à long terme).

L'analyse des images satellitaires disponibles, l'inspection de plusieurs lacs en canoë ou en plongeant ainsi qu'un pré-échantillonnage ont permis de sélectionner six portions littorales de six lacs facilement accessibles. Ces portions sont caractérisées par une abondance de bois subfossiles dans la zone littorale, des sédiments fins près de la rive pour enfouir et conserver le bois à long terme (i.e. plusieurs millénaires), une interface forêt-lac abrupte à l'abri des vents dominants et une forêt riveraine très ancienne. Étant donné que le sapin baumier se régénère très mal après feu (Payette,

1993), sa présence dans les forêts riveraines des lacs a été utilisée comme indicateur d'ancienneté des peuplements.

Interdatation des bois subfossiles

Malgré que nous abordons des questions d'écologie et de paléoclimatologie différentes dans les trois chapitres de la thèse, les chapitres sont basés sur la datation par dendrochronologie des bois subfossiles échantillonnés dans les six lacs et sur la construction d'une série dendrochronologique locale pour chaque site. Pour cette raison, cette dernière partie de l'introduction générale est dédiée aux techniques d'interdatation des bois subfossiles.

Les arbres subfossiles ont été échantillonnés exhaustivement par un plongeur aidé par deux ou trois assistants sur la portion de la zone littorale retenue dans chaque lac. L'ensemble des arbres dans l'eau ou situés dans la couche superficielle des sédiments a été récupéré comme décrit par Arseneault *et al.* (2013). La longueur des troncs, leur diamètre maximum et minimum, leur alignement par rapport à la berge, leur degré d'enfouissement, leur distance à la rive, leur profondeur, leur forme, les caractéristiques du substrat, les éventuelles traces de feu sur les branches ou les troncs ainsi que la présence ou non d'une souche attachée au tronc ont été systématiquement notés. La position de chaque arbre subfossile a ensuite été cartographiée avec un théodolite. Une section transversale de tronc a été prélevée au niveau du diamètre maximal pour permettre la datation par dendrochronologie. Le ponçage des galettes récoltées a permis la lecture de leurs cernes de croissance. Les espèces ont été identifiées par l'anatomie du bois (épinette noire, sapin baumier ou mélèze laricin). Deux rayons par spécimen ont été numérisés à 6400 DPI afin de mesurer la largeur des cernes annuels de croissance grâce au logiciel OSM (SCIEM, 2007). L'interdatation des échantillons s'est effectué grâce aux logiciels PAST4 (SCIEM, 2011) et COFECHA (Holmes, 1983) en utilisant aussi des chronologies de cernes pâles comme repères chronologiques (Arseneault et Payette,

1998; Dy, 2008). Toutes les données relatives à chaque spécimen récolté ont été ensuite organisées dans une base de données relationnelle.

CHAPITRE 1.
STOCKS ET FLUX MILLÉNAIRES DE GROS DÉBRIS LIGNEUX DANS DES LACS DE LA TAÏGA NORD-AMÉRICAINE

1.1 RESUME EN FRANÇAIS DU PREMIER ARTICLE

Ce premier article, intitulé « *Millennial stocks and fluxes of large woody debris in lakes of the North American taiga* », fut co-rédigé par moi-même ainsi que par les professeurs Dominique Arseneault (UQAR) et Yves Bégin (INRS-ETE). Il fut accepté pour la publication dans sa version finale en novembre 2013 par les éditeurs de la revue *Journal of Ecology* et fut publié en mars 2014. En tant que premier auteur, j'ai participé aux travaux de terrain, à l'analyse des échantillons au laboratoire, au choix des tests statistiques et à la rédaction de l'article. La contribution et le support des professeurs Dominique Arseneault et Yves Bégin, respectivement deuxième et troisième auteurs, ont été essentiels dans toutes les phases de l'étude. Je remercie spécialement le professeur Dominique Arseneault pour avoir fourni l'idée originale et pour sa contribution dans la rédaction.

Pour cet article, nous avons analysé les gisements de gros débris ligneux (GDL) dans des lacs boréaux. Les GDL provenant de la végétation riveraine représentant un support essentiel pour les écosystèmes littoraux des lacs. En effet, leur présence peut augmenter la productivité des écosystèmes lacustres et la stabilité des réseaux trophiques associés. De plus, les GDL peuvent représenter un important puits de carbone à l'échelle locale car ils sont préservés durant des siècles dans les zones littorales. Cependant, une analyse à long terme des stocks et des flux de GDL à l'interface forêt-lac, associée avec

une reconstitution des perturbations passées à l'échelle du site, n'a jamais été possible auparavant.

Nous avons échantillonné les gisements de GDL dans cinq lacs de la taïga du Québec. Les stocks actuels de GDL ont été décris et leur temps de résidence dans la zone littorale a été établi par dendrochronologie ou avec des datations par le radiocarbone. Les pertes de GDL par décomposition et enfouissement dans les sédiments lacustres et les facteurs qui influencent leur temps de résidence ont été identifiés en utilisant des modèles de régression linéaire. Les impacts des incendies des 1400 dernières années sur les flux de GDL à travers l'interface forêt-lac ont été reconstitués séparément pour les cinq lacs à l'aide de modèles de régression linéaire par morceaux. Les dates des incendies à chaque site ont été identifiées à partir des dates de recrutement des GDL calcinés.

Le volume de GDL préservés dans nos sites a varié entre 0,92 et 1,57 m^3 par 100 m de rive et nous avons pu conclure, après avoir extrapolé nos résultats à l'échelle du paysage, que le carbone séquestré dans ces gisements représente une portion minime du carbone séquestré en région boréale. Malgré cela, nos données confirment que le temps de résidence des GDL dans des lacs boréaux est très long. Les 1571 GDL qui ont été datés à l'année près, principalement des troncs d'épinettes noires (*Picea mariana* (Mill.) B.S.P.), sont tombés dans les zones littorales de nos lacs durant les 1400 dernières années, tandis que les GDL qui ont formé des séries dendrochronologiques flottantes, datés par le radiocarbone, ont été préservés de la décomposition jusqu'à cinq millénaires. Les variables les plus influentes dans l'explication de la variation du temps de résidence des GDL ont été leur degré d'enfouissement et leur distance par rapport à la rive. Le taux de recrutement des GDL dans les portions littorales sélectionnées a été en moyenne de 5,8 spécimens par siècle par 100 m de rive. Ce taux et le taux d'établissement d'arbres sur les rives ont été altérés principalement par les 14 incendies qui ont brulé les forêts riveraines durant le dernier millénaire.

Avec ce premier article, nous avons démontré que les interactions entre écosystèmes terrestres et aquatiques dans les régions boréales nordiques sont fortement influencées par les incendies qui provoquent des effets pouvant s'étaler sur plusieurs siècles car le taux de décomposition des GDL qui structurent les zones littorales est très lent. Les stocks actuels de GDL et le carbone séquestré dans leurs gisements dépendent de l'histoire des incendies qui ont affecté les forêts riveraines durant les derniers millénaires.

1.2 MILLENNIAL STOCKS AND FLUXES OF LARGE WOODY DEBRIS IN LAKES OF THE NORTH AMERICAN TAIGA

1.2.1 Summary

1. Large woody debris (LWD) is an important cross boundary subsidy that enhances the productivity of lake ecosystems and the stability of aquatic food webs. LWD may also be an important carbon sink because LWD pieces are preserved for centuries in the littoral zone of lakes and rivers. However, a long term analysis of LWD stocks and fluxes in lakes, coupled with the reconstruction of past disturbances at the site level, has never been attempted.

2. LWD was sampled in five lakes of the Quebec taiga. Actual LWD stocks were described and residence time of the LWD pieces was established using tree-ring and radiocarbon dating. LWD losses by decomposition and burial and other factors influencing LWD residence time were investigated using linear regressions.

3. Impacts of wildfires on LWD fluxes during the last 1400 years were reconstructed separately for the 5 lakes using piecewise regression models. Fire years at each site were identified from the recruitment dates of charred LWD pieces.

4. LWD volume ranged between 0.92 and 1.57 m^3 per 100 m of shoreline and, extrapolating these results to the landscape scale, it was concluded that LWD littoral carbon pools represent a minimal portion of boreal carbon storage.

5. LWD residence time in boreal lakes was confirmed to be very long. Tree-ring dates of 1571 LWD pieces, mainly black spruce (*Picea mariana* (Mill.) BSP.), spanned the last 1400 years, while LWD specimens of older floating chronologies were preserved from decomposition for up to five millennia. The most influential variables explaining variation in LWD residence time were the degree of burial and the distance from the shore.

6. LWD recruitment rates averaged 5.8 pieces per century per 100 m of shoreline. Fourteen wildfires were the primary cause for changes in the rates of tree establishment in the riparian forests and of LWD recruitment in the lakes.

7. *Synthesis:* Interactions between terrestrial and aquatic ecosystems in northern boreal regions are strongly influenced by wildfires whose effects can last for centuries due to the slow large woody debris decay rate. Actual LWD stocks and carbon pools are a legacy of the past fire history.

1.2.2 Introduction

Ecosystems are rarely closed systems and movements of nutrients, detritus and preys and predators are extremely common between adjacent habitats. These movements can influence the structure of ecosystems, the quantity of available resources, the stability of trophic networks and the dynamics of existing communities and populations (Polis, Anderson & Holt 1997). For instance, the trophic networks of lakes can be, in part, considered as spatially subsidized food webs supported by allochthonous resources, such as the remains of trees, branches and leaves from the riparian vegetation falling into the littoral zone (Schindler & Scheuerell 2002; Doi 2009).

Among these subsidies, large woody debris (hereafter "LWD") can supply aquatic ecosystems with a large amount of organic matter and can increase the spatial heterogeneity of the littoral zone (Gurnell *et al.* 2002; Webb & Erskine 2003; Collins *et al.* 2012). LWD represents the ideal habitat for many communities of microorganisms (Tank & Webster 1998; Vadeboncoeur & Lodge 2000; Collier, Smith & Halliday 2004), invertebrates (Lester, Wright & Jones-Lennon 2007; Scealy, Mika & Boulton 2007; Hrodey, Kalb & Sutton 2008; Glaz, Nozais & Arseneault 2009) and fish (Fausch & Northcote 1992; Everett & Ruiz 1993; Hrodey & Sutton 2008).

LWD in aquatic environments may also plays an important role in the long-term sequestration of carbon at the landscape scale (Guyette, Dey & Stambaugh 2008) because dead wood resides longer in water than in terrestrial habitats (Guyette *et al.* 2002; Harmon *et al.* 2004). Carbon storage in LWD can be relevant especially in landscapes where lakes and rivers are very common, such as in the boreal forest. Although many studies have examined the amount of carbon stored in forest ecosystems and soils (Dixon *et al.* 1994; Nabuurs & Mohren 1995), little is known regarding the portion of carbon sequestered in aquatic environments or about the causes of its temporal and spatial variability (but see Guyette *et al.* 2002; Buffam *et al.* 2011). Considering the long residence time of LWD, its quantity and distribution in lakes has to be examined in order to establish accurate carbon budgets.

LWD stocks in the littoral zone of lakes reflect the balance between inputs from the riparian forest and losses through decomposition and burial by sediments. In anthropogenic landscapes, LWD stocks are strongly dependent on the history of human disturbances, such as logging or residential development that influence dead wood production in the riparian environment (Guyette & Cole 1999; Marburg, Turner & Kratz 2006; Glaz, Nozais & Arseneault 2009). In the northern boreal forest, where human activities are less intensive, wildfire is the main disturbance affecting terrestrial and aquatic environments (Payette *et al.* 1989; Marchand, Prairie & del Giorgio 2009; Boulanger *et al.* 2012). It has been established that wildfires have major impacts on LWD stocks and recruitment rates in boreal streams and lakes (Chen, Wei & Scherer 2005; Arseneault, Boucher & Bouchon 2007; Arseneault *et al.* 2013).

Very few studies have documented the dynamics of LWD in lakes. In North America, LWD stocks and their short-term (decadal) variability have been documented in lakes of the northern temperate zone (Marburg, Turner & Kratz 2006; Marburg *et al.* 2009) and dendrochronology has allowed dating of LWD in lakes of the northern temperate and northern boreal forests (Guyette & Cole 1999; Guyette *et al.* 2002; Glaz, Nozais & Arseneault 2009; Arseneault *et al.* 2013). However, no studies have combined

dendrochronology with exhaustive LWD sampling to reconstruct the long-term dynamics of LWD stocks in lakes.

The objectives of this research are: (i) to document the stocks of LWD in five lakes situated in the unmanaged boreal forest of eastern Canada with an exhaustive sampling of a portion of their littoral zone, (ii) to use dendrochronology in order to reconstruct LWD transfers across the forest-lake interface, the impacts of wildfires on such transfers and LWD losses through decomposition and burial over the last millennia and (iii) to identify factors influencing residence time and decomposition of LWD in the littoral zone. In order to allow and improve the tree-ring dating, we deliberately sampled sites with large stocks of LWD. Subsequently, we discuss how these stocks could decrease as a result of disturbances and site conditions.

1.2.3 Materials and methods

Study area

The study area is located in the northern taiga of Quebec, Canada, between latitudes 53°50' N and 54°35' N and longitudes 70°15' W and 72°25' W (Fig. 1). This area is situated at the transition between the spruce-lichen woodland and the forest-tundra and is characterized by a continental subarctic climate with short mild summers and long cold winters.

The vegetation of the region reflects mostly the topography and the past fire history. Forests are strongly dominated by black spruce (*Picea mariana* (Mill.) BSP.), which is well adapted to various fire frequencies. Its semi-serotinuous cones shed seeds after fires, thus allowing rapid post-fire recovery, while its ability to form layers (i.e. to propagate vegetatively through the rooting of the lower branches that are touching the ground) allows stands to persist in the absence of fires (Black & Bliss 1980). Black spruce canopy height and density vary according to the time since the last fire, the

severity of the fire and the topographic position of a given stand (Morneau & Payette 1989; Payette 1993; Lavoie & Sirois 1998; Girard, Payette & Gagnon 2008). Other less abundant tree species include balsam fir (*Abies balsamea* L.) and tamarack (*Larix laricina* (Du Roi) K. Koch).

The study area is located in a remote region where significant human influence is sparse and only recent (last 40 years). Lakes of various sizes are extremely abundant, covering about 25% of the landscape. A portion of the littoral zone of each of the five lakes was selected for this study (Fig. 1, Table 1) according to the criteria developed by Arseneault *et al.* (2013) in order to identify sites of high potential for developing millennial tree-ring chronologies. The selected littoral segments possess features that maximize LWD recruitment (an abrupt forest-lake interface on the leeward side of the lake and an old-growth riparian forest) and LWD preservation (presence, near the shoreline, of a talus at least 1 m deep and, on its bottom, of fine sediments).

LWD stocks and dating

The five sites were exhaustively sampled during several summer field campaigns between 2005 and 2011. Any exposed (i.e. laying on the bottom of the lake) or buried logs with a diameter equal or greater than 4 cm, which makes dendrochronological dating possible, were collected by a diver aided by two-three assistants, as described by Arseneault *et al.* (2013). Most logs were pulled to the shore, although a few heavy or stuck logs were partially cleared of sediments, measured and cut with a hand saw in the water. Buried specimens were located as loose sediments can be systematically probed by hand. Only LWD pieces buried in less than about 20 cm of sediments could be extracted. Once on the shore, LWD pieces were mapped with a total station and their length and maximum diameter were measured in order to calculate the LWD number and volume per 100 m of shoreline, which are two metrics that characterize LWD stocks. The volume of each LWD piece was estimated as the volume of a cylinder multiplied by a form factor of 0.6. The form factor was based on more detailed

measurements on a subset of 1626 LWD pieces from this study (i.e. minimum and maximum diameters and their position on each LWD piece). LWD specimens were also examined to detect the presence of charcoal on the trunk and the branch tips and the presence of main roots still connected or not. A stem cross-section was sampled from each LWD piece so as to maximize the number of measurable tree-rings for dendrochronological dating.

In the lab, tree species were identified from wood anatomy (Hoadley 1990). Two radii were then scanned at 6400 DPI on each cross-section of spruce and fir in order to measure tree-ring widths using the OSM3 software (SCIEM, Austria). Individual series (i.e. average of two radii) were crossdated to the calendar year using local master chronologies as a reference (Arseneault *et al.* 2013) and sequences of light rings as an additional dating tool (Arseneault & Payette 1998). Crossdating was performed using COFECHA (Holmes 1983) and PAST4 (SCIEM, Austria) software. All floating chronologies older than the master chronology and comprising at least two tree-ring series of different LWD pieces, not necessarily from the same lake, were AMS (Accelerator Mass Spectrometry) radiocarbon dated. To do this, wood samples from the innermost tree-rings of selected LWD pieces were sent to the Centre for Northern Studies (CEN) radiochronology laboratory (Université Laval, QC, Canada). Conventional radiocarbon ages were calibrated using CALIB 6.0 (Stuiver & Reimer 1993) and the IntCal09 calibration curve.

LWD residence time and losses

To determine the residence time in the lake of each LWD piece that could be crossdated to the calendar year or into a floating chronology, we estimated its recruitment date in the water from its outermost tree-ring date (hereafter "recruitment date"). The residence time was then determined as the time since the LWD recruitment (2012 minus recruitment date), even if this measure can be overestimated by a few years to a few decades due to the decomposition of outermost tree-rings. Similarly, the pith

date of each LWD piece was used to estimate the date at which the corresponding former tree in the riparian forest had reached the height needed to develop an upper stem portion that later became recruited and conserved as a LWD piece (hereafter "establishment date").

To quantify the rate at which LWD pieces are lost from the littoral stocks by abiotic and biotic decomposition and burial, we identified distinct reference time intervals of negligible losses for exposed and buried specimens. First, the cumulative numbers of exposed and buried LWD samples were plotted separately according to residence time. Samples of all lakes were plotted together in order to smooth out the impact of local disturbances (see Fig. 3a). Second, in the range of observed residence times, for each sequential time interval of 400 years lagged backward in time by 1 year, a linear regression model was fitted on the exposed and buried series until at least two LWD specimens could be included (the number of available specimens decreases backward in time). The successive slopes of these regression models allow the comparison among time intervals as their values depend on the LWD recruitment into the exposed or buried groups during the corresponding time interval and on the cumulated losses. Higher recruitment rates would produce more negative slopes and higher losses would produce less negative slopes. With constant recruitment and no losses, the slopes would be constant. Third, for the exposed and buried series, the time interval with the more negative slope was considered as a reference state with no losses as it displayed a very good linear fit to the data (see Fig. 3a). Indeed, exposed specimens reside for some time in water before being lost through decomposition or superficial burial, whereas buried specimens, after the time needed for burial, reside for some time in superficial sediments before being lost through decomposition or deep burial (i.e. at depth greater than 20 cm). Last, assuming that recruitment of exposed and buried specimens is approximately constant through time when several lakes are averaged, the percentage of LWD losses for each 400 years time interval and each burial category was calculated as: [$Losses$ = 100 - (S_i / S_{ref}) * 100]. In the equation, s_i is the slope of the

regression on the residence time interval of 400 years centered in year *i* and s_{ref} refers to the corresponding reference slope.

In addition, the proportion of the exposed LWD pieces that has been eventually buried relative to the proportion that has been lost through decomposition before burial was estimated from the ratio of the two reference slopes (buried over exposed). We also used the slopes of the most recent time intervals of each burial category to compute the average rate of LWD recruitment across all studied lakes (number of LWD pieces per 100 years per 100 m of shoreline computed as the summation of the 2 slopes x 100 years x 100 m, divided by a total of 3330 m of sampled shoreline).

Factors influencing LWD residence time

Factors influencing LWD residence time in the lakes were analyzed using black spruce LWD samples crossdated to the calendar year or into floating chronologies at sites L18 and L20, where most LWD samples were collected. Residence time was log-transformed to reduce skewness and kurtosis. Multiple linear regressions were then performed with the residence time entered as the dependent variable. The independent variables tested were: the minimum depth in the water of each LWD piece (feet), its minimum distance from the shore (cm), its orientation relative to the shoreline (perpendicular =3; parallel =2; inverted=1), its burial type (completely buried =3; partly buried =2; exposed =1), the type of underlying substratum (fine sediments =5; sand =4; gravel =3; stones =2; wood =1), the aspect of the corresponding littoral zone (from 0 to 2) and the exposure to the wave action of the littoral zone (cm). The computations used to obtain these independent variables and the samples used in the regression models are described in the Appendix S1 in Supporting Information.

Models were fitted to data in the R environment and all the possible models from the different combinations of the independent variables were ranked according to their Akaike information criterion (AIC). Because models with smaller AIC are better fitted, only models with a delta AIC ($\Delta i = AICi - AICmin$) smaller than two were retained

(Burnham & Anderson 2002). The selected models were checked for normality and homogeneity of variance of the residuals and absence of multicollinearity to verify that the assumptions of regression were met. For each lake, the relative contribution of the independent variables that were significant in all the alternative best models was estimated by an analysis of variance (ANOVA).

Wildfire impacts on LWD fluxes

Impacts of wildfires on LWD fluxes during the last 1400 years were reconstructed separately for the five selected lakes using piecewise regression models. Due to their longer sampled shore distances and more complex fire history in comparison to the other lakes, L18 and L20 were divided into three different segments and the results of only two segments are shown here for each lake, while the other segment is shown in Supporting information (Fig. S1).

For each site or shore segment, piecewise regression models were fitted to the cumulative number of LWD pieces according to their establishment and recruitment date using the "segmented" package of the R software (Muggeo 2008). Piecewise regressions allow identifying patterns in data using a set of linear regressions linked by breakpoints (see Appendix S2 for technical aspects). The slopes of the piecewise regression segments were then used to estimate the recruitment rates of LWD pieces into the littoral zones (hereafter "recruitment rates") and the establishment rates in the riparian forests of upper stem portions that later generated LWD pieces (hereafter "establishment rates").

Past fires were dated at each site from the recruitment dates of charred LWD pieces (Appendix S2). Breakpoints from the piecewise regressions were then associated to a wildfire date on the condition that they coincided with either: (i) the limits of a period of reduced establishment or recruitment around a fire date; (ii) the beginning of a period of increased establishment or recruitment after a fire; or (iii) the limits of a massive LWD recruitment event due to a fire. We used these breakpoints, along with associated fire dates and segment's slopes, to compute three metrics of past fire impacts

on establishment and recruitment rates (see Table 5). First, the time needed for the normalization of the establishment rate was computed as the length of the time interval between a fire and the following breakpoint marking increasing establishment rate. Second, the time needed for the normalization of the recruitment rate was computed as the length of the time interval between a fire and the breakpoint after the subsequent reduction of recruitment or massive recruitment (a massive recruitment was defined as an input greater than 20 LWD pieces per 100 years per 100 m of shoreline over less than 50 years). Third, the fire-induced recruitment reduction (%) was computed using the following formula: [*Recruitment reduction* = $((S_a - S_b) / S_b) * 100$]. In the equation, S_a is the slope of the segment following the fire and S_b is the slope of the segment preceding the fire.

1.2.4 Results

LWD stocks and dating

A total of 2194 LWD pieces were sampled along 3330 m of shoreline in the 5 lakes (Table 1). A very large proportion of these LWD specimens had no roots, confirming that they represent the upper stem portions of former riparian trees (Table 1). Most samples were black spruce with minor components of balsam fir (4%) and tamarack (3%). Exposed LWD pieces were more abundant than buried ones (62% vs 38%), although buried specimens had higher diameters, lengths and volumes than exposed ones at all lakes, except L1 (Table 2). LWD number varied among lakes at between 50.6 and 84.2 specimens per 100 m of shoreline, whereas LWD volume ranged between 0.92 and 1.57 m^3 per 100 m of shoreline (Table 2).

Tree-ring dating was very successful with 72% of all LWD pieces being crossdated to the calendar year (Table 1). LWD recruitment dates were nearly continuous during the last 1400 years (Fig. 2). The oldest tree-rings crossdated to the calendar year ranged between AD 569 and AD 651 depending on the site (Table 1). An

additional 3% of all LWD pieces were crossdated into 7 floating chronologies, each comprising from 2 to 51 pieces and spanning from 143 to 460 years (Tables 3). Radiocarbon dating indicated that 68 out of the 73 LWD pieces that compose these chronologies fell in the water between the 7th century BC and the 6th century AD, whereas 5 LWD pieces were even older and have been preserved from decomposition for 4 or 5 millennia (Table 3).

LWD residence time and losses

LWD mean residence time in the five lakes varied between 472 and 588 years (Table 1). As expected, exposed specimens had shorter mean residence time than buried ones (386 ± 287 vs. 794 ± 556 years, considering all lakes). All exposed LWD specimens had residence times shorter than 1700 years compared to more than 5000 years for buried ones (Fig. 3a).

For residence times of less than 650 years, the decrease in the cumulative number of LWD pieces with increasing residence time was much faster for exposed specimens than for buried ones, indicating a greater recruitment rate into the exposed group (Fig. 3a,b). In fact, buried LWD pieces increased in abundance with residence times up to and including the 400-600 years residence time class (Fig. 3d,e), pointing out that exposed LWD was transferred to the buried compartment, where sedimentary conditions were favorable for burial, only after an average residence time of about 500 years. Furthermore, the ratio of the two reference slopes (Fig. 3a,b) indicated that only about 46% of the exposed pieces eventually become buried, whereas 54% decay before burial.

Losses of exposed LWD pieces were much faster than of buried ones. The method based on the reference states estimated that 50% of the exposed pieces have been lost through decomposition or burial in less than 612 years, while 50% of the buried specimens have been lost through decomposition or deep burial after a residence time of 1044 years (Fig. 3c). Moreover, about 8% of the buried specimens resided in surficial sediments for more than 1500 years and up to 5 millennia (Fig. 3a). Because buried

LWD pieces were generally older and larger than exposed ones (Fig. 3a and Table 2), their relative importance increased with residence time, especially when LWD volume was considered (Fig. 3f). The lower number of tree-rings confirmed the faster decomposition of exposed LWD pieces as compared to buried ones. The quartiles of the number of measurable tree-rings per residence time classes of 200 years were always lower for exposed than for buried LWD samples, except for the most recent class (Fig. 4). Based upon linear trends calculated on the median numbers of tree-rings, exposed and buried LWD pieces lost through decomposition an average of 3.16 ± 0.57 and 0.92 ± 0.75 rings per century (mean ± SE), respectively.

Factors influencing LWD residence time

The results of the linear regression models retained to explain LWD residence time as a function of multiple variables at L18 and L20 were similar. Total variance explained ranged between 42% and 50% (Table S1) with burial type (26%-35% of the variance explained) and distance from the shore (15%-10%) being the most significant variables (Table 4). Although the remaining variables retained in the models differed between lakes L18 and L20, these variables explained only a tiny fraction of the total variance (less than 2% per each variable; Table 4). Exposure to wave action was significant at L18 but the sign of its coefficient opposed our expectation. Depth in the water, orientation and substratum were significant only at L20 (Table S1).

Wildfire impacts on LWD fluxes

At least 14 wildfires influenced the LWD fluxes across the forest-lake interface in the 5 selected lakes during the last 1400 years but no fire occurred after AD 1848 (Figs 2 and 5). The number of fires per shore segment varied between zero (L20 shore 2) and five (L22). Shore 2 at L20, the only site that has escaped fire over the last 1400 years, displayed a very regular recruitment rate of 13.4 LWD pieces per 100 years per 100 m of shoreline over about 600 years (AD 1254-1834; Figs 5 and 6, Table S2). The remaining sites were characterized by generally lower, but highly variable, recruitment rates that

were dependent on their respective fire histories (Fig. 6). Recruitment rates during the last 500 years that were characterized by low LWD losses by decomposition and deep burial varied from 0.5 LWD pieces per 100 years per 100 m during AD 1668-1768 at L12 to 23.7 pieces per 100 years per 100 m during AD 1722-1731 at shore 2 of L18 (Table S2). Recruitment rates averaged 5.8 LWD pieces per 100 years per 100 m across all sites (computed from the slopes of the most recent time intervals of 400 years for each burial category; Fig. 3b).

Piecewise regressions models were efficient in reconstructing wildfire impacts on LWD fluxes. From the 14 wildfires identified from charred LWD specimens, 10 and 9 corresponded to breakpoints in the recruitment and establishment data, respectively (Tables 5 and S2). Conversely, 54% and 58% of the breakpoints in the recruitment and establishment data, respectively, could be associated to a fire date (Table S2). Fire events often caused a typical response, including the presence of charred LWD pieces, along with the reduction and subsequent normalization of the establishment and recruitment rates (Figs 5 and 6, Table 5). Most fire events caused large reductions of LWD recruitment rates, varying from -46 to -94%, and many years were sometimes required for the normalization of the LWD fluxes (Table 5). For example, the AD 1126 fire at L22 caused a recruitment reduction by -65% for 225 years (Table 5). However, only two fires, the AD 1729 fire at shore 2 of L18 and the presumed AD 1673 fire at L22 (not confirmed by charred LWD), generated massive LWD recruitments (i.e. more than 20 LWD pieces per 100 years per 100 m in less than 50 years; Figs 5 and 6, Table 5). Furthermore, an increasing establishment rate of upper stem portions on the shores was often observed with a post-fire delay ranging from 0 to 143 years (Table 5). The duration of the time periods needed for the normalization of the establishment and recruitment rates after fires were intercorrelated ($r=0.84$; $P < 0.01$) because the first trees to establish in the riparian forest after a fire were generally the first to be subsequently recruited as LWD pieces. Finally, heterogeneity of fire effects increased with the length

of the sampled shore, as shown by the contrasting recruitment trends between shore sections at L18 and L20 (Figs 2 and 5).

1.2.5 Discussion

Residence time, decomposition and burial of LWD pieces

Once they enter in the littoral ecosystem, tree trunks may accumulate and form stocks spending a long residence time outside of sediments as exposed LWD (mean residence time of 386 years in our sites; Fig. 7). The slow decomposition of wood in a lake littoral environment is related to several factors: first, the low oxygen concentration compared to terrestrial environments that restricts microbial colonization of LWD pieces; second, the absence of wood boring organisms that is a peculiarity of freshwater habitats; third, the lower physical fragmentation caused by flowing water compared to streams and rivers (Harmon *et al.* 2004). Furthermore, our study area in the northern taiga of Quebec is characterized by a continental subarctic climate and carbon decomposition is limited by low temperatures (Davidson & Janssens 2006). For all these reasons, decomposition of exposed LWD in this region appears to occur mainly on the outer surface of wood pieces, leaving their interior relatively unaltered (Savard *et al.* 2012). This pattern is also suggested by the smaller number of measurable tree-rings of exposed as compared to buried specimens of similar residence times (Fig. 4). This centripetal pattern of wood decomposition depends on the action of physical agents such as waves and ice, as well as of biotic agents such as bacteria, fungi and algae that form biofilms on the surface of exposed LWD (Tank & Webster 1998; Collier, Smith & Halliday 2004; Guyette, Dey & Stambaugh 2008). However, the long residence time of exposed LWD pieces implies that LWD stocks are resistant to riparian disturbances as they would continue to structure littoral ecosystems over several centuries even after complete deforestation of the riparian environment (Fig. 7).

Marburg, Turner & Kratz (2006) found that areas with low exposure to wind and waves are important sites of littoral LWD accumulation within lakes in Wisconsin, USA. In our models no strong relation was obtained between the LWD residence time and the aspect of the littoral zone or its exposure to wave action (Table 4). Exposure was significant only at L18, but the sign of its coefficients did not correlate with our expectations and it only explained a small fraction of the total variance (Tables 4 and S1). Three hypotheses can explain this contrasting result. First, the exposure of the littoral zone may be important for the LWD accumulation but does not influence the length of the LWD residence time. Second, this result may depend on our sampling design that focused on the most important LWD stocks of our study area which almost systematically occur along shoreline segments protected from dominant winds (Arseneault *et al.* 2013). This design was necessary in order to develop the master tree-ring chronologies needed for crossdating the LWD samples to the calendar scale. Third, LWD pieces are not significantly redistributed in our lakes contrary to what happens in the lakes studied by Marburg, Turner & Kratz (2006). This is shown by the relatively high proportion of specimens oriented perpendicularly to the lakeshore with their base toward the riparian forest at all our sites (Table 1). The stability of the LWD stocks is also revealed by the contrasting LWD recruitment trends between consecutive shore sections with different fire histories at L18 and L20 (Figs 2 and 5, Table S2).

About half of the LWD pieces that enter the littoral zone of our lakes eventually become buried (Fig. 7). Even if we did not assess the decay rate of littoral wood in term of density lost per unit of time, we conclude that buried LWD specimens are much more persistent than exposed ones. This is confirmed by their slower losses (Fig. 3c), longer residence time (Fig. 7), greater diameter, length and volume (Fig. 3f and Table 2) and greater number of measurable tree rings (Fig. 4). Superficially buried specimens have formed relatively dense LWD stocks, which are similar to the exposed stocks on a volume basis (Fig. 7). Burial type and distance from shore have been the most influential factors for the long-term LWD preservation at the studied sites (Table 4). This result

suggests that the upper stem portions of the tallest trees growing near the shore are more likely to generate persistent LWD. In comparison to shorter trees, upper portions of tall trees have better chances of falling at greater distances from the shoreline where sediment accumulation and burial are faster. The process of wood decomposition in sediments is poorly known but its slow rate probably reflects pronounced anoxic conditions which suggest that buried trees are mostly decayed through abiotic hydrolyses (Guyette, Dey & Stambaugh 2008). Although deeply buried stocks (i.e. more than 20 cm deep) could not be quantified (Fig. 7), we estimate that they are much less important than superficial stocks. This is suggested by the discontinuous occurrence of deep loose fine sediments in the littoral zone, along with the occurrence of LWD pieces more than five millennia old in the superficial sediment layer (Fig. 3a).

Some studies have already reported that tree trunks buried in lake and river sediments can be several millennia old (Hyatt & Naiman 2001; Eronen *et al.* 2002; Guyette, Dey & Stambaugh 2008). In our lakes about 8% of the buried LWD pieces resided in superficial sediments for more than 1500 years and up to five millennia (Fig. 3a). Since our study area was deglaciated about 7000 years ago (Dyke 2004), it is likely that the superficial sediment layer still comprises some of the first trees that colonized the region. Although these buried specimens probably only played a minor ecological role, they nevertheless form an important deposit of highly valuable materiel for developing millennial tree ring chronologies. Such chronologies would be useful for reconstructing long-term climate change and millennial forest dynamics. The old age of some LWD pieces also suggests that several of the undated specimens (25% of all sampled LWD pieces) could not be crossdated because they are older than the master chronology. As these specimens are probably scattered in time over several centuries or even millennia, they would not have contributed significantly to our computations of LWD fluxes (Figs 5 and 6, Table S2) or losses (Fig. 3c).

Fire recurrence vs. LWD fluxes

Our study highlights the important role of wildfires in regulating interactions between terrestrial and aquatic ecosystems in boreal landscapes. Despite the fact that we deliberately located our sampling sites within an area of relatively low fire occurrence (Boulanger *et al.* 2012) and selected shore segments with old forests, all sites possessed at least one shore segment that burned at least once and at least 14 wildfires occurred at our sites during the last 1400 years. These fire events were the main disturbances of the LWD fluxes across the forest-lake interfaces (Figs 2 and 5).

The observed variability of the fire impacts (Table 5) most likely reflects varying fire severity. Depending on the fire severity (i.e. proportion of fire-killed trees), fire impacts on LWD fluxes would vary from almost unnoticeable (no charred LWD pieces, absence of massive recruitments, short normalization periods) to very important (charred LWD pieces, massive LWD recruitments, long normalization periods; Figs 5 and 6, Table 5). A similar long-term pattern of varying fire severity and associated LWD recruitment rate has already been observed along a small boreal stream (Arseneault, Boucher & Bouchon 2007). Varying fire severity along the shoreline probably explains the contrasting histories of the LWD recruitment rate between consecutive shore sections at L18 and L20 (Figs 2 and 5).

Some empirical and simulation studies have shown that severe natural disturbances such as fire and insects outbreaks trigger massive LWD recruitments into adjacent aquatic ecosystems (Bragg 2000; Chen, Wei & Scherer 2005). However, the millennial perspective provided by our study indicates that the net result of disturbances in riparian forests is to reduce the long-term LWD recruitment rates relative to values measured in absence of disturbances (Figs 2 and 7). Indeed, riparian trees have to reach a minimum height before being available to generate LWD pieces from their upper stem portions. Consequently, any disturbance resetting height growth to the ground level would interrupt the transfer of LWD pieces across the forest-lake interface and would

reduce the long-term LWD recruitment rate, despite the possible short-term massive recruitment of disturbance-killed trees. Although black spruce seedlings generally establish massively during the first few post-fire years (Sirois 1995), complete stand recovery is slow (Auclair 1985; Morneau & Payette 1989) and several decades are needed for the recovering stand to reach the minimum height to generate LWD pieces. This explains the long time periods observed in our sites for the post-fire normalization of the establishment and recruitment rates (Table 5).

Stand-replacing wildfire is the main natural disturbance in the unmanaged boreal forest of northern Quebec, with annual burn rates that decrease eastward from the extremely high rate of 2.5% per year along the James Bay coast to about 0.2% per year in our study area (Payette *et al.* 1989; Boulanger *et al.* 2012). The time needed for the post-fire normalization of the LWD recruitment rate has a mean value of 115 years at our sites (Table 5). Comparing these durations to the supra-regional fire occurrence gradient, we conclude that fire is a major factor limiting LWD stocks and recruitment rate at large spatial and temporal scales. LWD recruitment in boreal lakes would cease almost completely if a severe wildfire occurs every 100 years, as is currently the case to the west of our study area. A preliminary survey of some lakes in this fire-prone region revealed to us almost non-existent LWD stocks in littoral ecosystems. By the same line of reasoning, the anticipated increase of fire frequency and total area burned in the North American boreal forest (Girardin & Mudelsee 2008; Balshi *et al.* 2009) would imply a progressive large-scale decrease of future LWD stocks in boreal lakes.

Our method, based on piecewise regressions fitted to establishment and recruitment data, was powerful enough to detect changes in LWD fluxes due to past fire disturbances. Piecewise regression can be a useful tool for identifying ecological thresholds and discontinuities in data (Toms & Lesperance 2003). In our analysis, most fires were detected by the piecewise regressions (Fig. 5, Table 5) and the majority of the breakpoints could be explained by the occurrence of fires (Table S2). However, not all wildfires corresponded to breakpoints and not all breakpoints depended on wildfires.

Impacts of low severity fires (e.g. AD 1696 fire at L18 shore 1; Fig. 5, Table 5), of fires recurring with short time intervals among them (e.g. AD 1622, 1668 and 1729 fires at L18 shore 2; Fig. 5, Table 5) and of recent wildfires (e.g. AD 1813 and 1848 fires at L22; Fig. 5) have been more difficult to detect. On the other hand, breakpoints may also have occurred in response to alternative disturbances (e.g. windstorms or changes in lake water level) as well as to continuous LWD losses related to physical and biochemical decomposition or deep burial (Fig. 3c).

Carbon storage in boreal littoral LWD

Stocks of littoral LWD may represent an important, but poorly studied carbon sink at the landscape scale because of their slow decay rate (Guyette *et al.* 2002; Guyette, Dey & Stambaugh 2008). Our exhaustive sampling of large stocks of LWD at several sites allows for the estimation of the maximum amount of carbon stored in aquatic LWD in boreal lakes, considering separately stocks of exposed and superficially buried LWD. First, we can estimate the wood density of each LWD piece (kg/m^3) according to its residence time in water (years) by using the equation developed by Guyette & Stambaugh (2003): [*density* = 1000 * Exp(ln(0.41) - 0.00011 * *residence time*)]. In the equation, 0.41 is the specific gravity of black spruce wood (Forest Products Laboratory 2010) and for undated LWD pieces we used the mean residence time of the corresponding burial category (386 years and 794 years for exposed and buried LWD pieces, respectively). Second, multiplying the volume of each LWD piece by its wood density and considering that the mass of softwood is about 52.1% carbon (Birdsey 1992), LWD volume can be transformed to LWD biomass and LWD carbon storage. The results suggest that the LWD biomass in our lakes is 470 kg per 100 m of shoreline (273 and 197 kg per 100 m of shoreline for exposed and buried specimens, respectively) and that the corresponding LWD carbon storage is 245 kg C per 100 m of shoreline (142 and 103 kg C per 100 m of shoreline for exposed and buried specimens, respectively).

In our study area, an average of 2.68 km of lakeshore is found per km^2 of landscape (value calculated in a GIS). Based on the observation that mature riparian trees tend to fall in the direction of the dominant winds (Arseneault *et al.* 2013), about half of the total shoreline length would allow LWD accumulation in the littoral zone. Multiplying the obtained total (exposed plus buried) LWD volume, biomass and carbon content per km of shore length by 1.34, the maximal LWD volume in the region can be estimated at 16.32 m^3 per km^2, with maximal LWD biomass at 6294 kg per km^2 and maximal LWD carbon storage at 3279 kg C per km^2. Although these values are rough estimates and are not considering deeply buried LWD stocks, they are based on lakes with an exceptional amount of LWD and thus reveal that the maximum amount of carbon that can be sequestered by LWD stocks in the littoral zone of boreal lakes is extremely low. Despite the extreme abundance of lakes in our study area and the long residence time of LWD pieces, the associated carbon storage in littoral areas represents less than 0.05% of the total amount of carbon sequestered in boreal black spruce forest ecosystems on a per area basis (Kane & Vogel 2009). It has been recently pointed out that all boreal carbon stocks must be urgently quantified and preserved because the boreal forest corresponds to about one-third of the global forests and comprises roughly 30% of the stored terrestrial carbon (Bradshaw, Warkentin & Sodhi 2009). Even if large amount of carbon can be sequestered in boreal wetlands and lake sediments (Buffam *et al.* 2011), our results indicate that the LWD littoral carbon pools represent a negligible portion of the boreal carbon storage.

1.2.6 Acknowledgments

The authors wish to thank Julia Autin, Yves Bouthillier, Pierre-Paul Dion, Sébastien Dupuis, Benjamin Dy, Joëlle Marion and Antoine Nicault for field and laboratory assistance and Aurore Catalan for technical assistance. This research is a contribution of the ARCHIVES project and was financially supported by NSERC,

Hydro-Quebec, Ouranos, ArcticNet, the EnviroNorth training program and the Centre for Northern Studies (CEN).

1.2.7 Data Accessibility

All data from the manuscript are archived in "Figshare": http://dx.doi.org/10.6084/m9.figshare.826213 (Gennaretti, Arseneault & Begin 2013).

1.2.8 References

Arseneault, D., Boucher, E. & Bouchon, E. (2007) Asynchronous forest-stream coupling in a fire-prone boreal landscape: insights from woody debris. *Journal of Ecology*, **95,** 789-801.

Arseneault, D., Dy, B., Gennaretti, F., Autin, J. & Bégin, Y. (2013) Developing millennial tree ring chronologies in the fire-prone North American boreal forest. *Journal of quaternary science*, **28,** 283-292.

Arseneault, D. & Payette, S. (1998) Chronologie des cernes pâles de l'épinette noire (Picea mariana [Mill.] BSP.) au Québec subarctique : de 706 à 1675 ap. J.-C. *Géographie physique et Quaternaire*, **52,** 219-226.

Auclair, A. N. D. (1985) Postfire regeneration of plant and soil organic pools in a Piceamariana–Cladoniastellaris ecosystem. *Canadian Journal of Forest Research*, **15,** 279-291.

Balshi, M. S., McGuire, A. D., Duffy, P., Flannigan, M., Walsh, J. & Melillo, J. (2009) Assessing the response of area burned to changing climate in western boreal North America using a Multivariate Adaptive Regression Splines (MARS) approach. *Global Change Biology*, **15,** 578-600.

Birdsey, R. A. (1992) *Carbon storage and accumulation in United States forest ecosystems.* U.S. Department of Agriculture, Forest Service, Washington, DC.

Black, R. A. & Bliss, L. C. (1980) Reproductive Ecology of Picea Mariana (Mill.) BSP., at Tree Line Near Inuvik, Northwest Territories, Canada. *Ecological Monographs,* **50,** 331-354.

Boulanger, Y., Gauthier, S., Burton, P. J. & Vaillancourt, M. A. (2012) An alternative fire regime zonation for Canada. *International Journal of Wildland Fire,* **21,** 1052-1064.

Bradshaw, C. J. A., Warkentin, I. G. & Sodhi, N. S. (2009) Urgent preservation of boreal carbon stocks and biodiversity. *Trends in Ecology and Evolution,* **24,** 541-548.

Bragg, D. C. (2000) Simulating catastrophic and individualistic large woody debris recruitment for a small riparian system. *Ecology,* **81,** 1383-1394.

Buffam, I., Turner, M. G., Desai, A. R., Hanson, P. C., Rusak, J. A., Lottig, N. R., Stanley, E. H. & Carpenter, S. R. (2011) Integrating aquatic and terrestrial components to construct a complete carbon budget for a north temperate lake district. *Global Change Biology,* **17,** 1193-1211.

Burnham, K. P. & Anderson, D. R. (2002) *Model selection and multimodel inference: a practical information-theoretic approach. 2nd ed.* Springer-Verlag, New York.

Chen, X., Wei, X. & Scherer, R. (2005) Influence of wildfire and harvest on biomass, carbon pool, and decomposition of large woody debris in forested streams of southern interior British Columbia. *Forest Ecology and Management,* **208,** 101-114.

Collier, K. J., Smith, B. J. & Halliday, N. J. (2004) Colonization and use of pine wood versus native wood in New Zealand plantation forest streams: Implications for riparian management. *Aquatic Conservation: Marine and Freshwater Ecosystems,* **14,** 179-199.

Collins, B. D., Montgomery, D. R., Fetherston, K. L. & Abbe, T. B. (2012) The floodplain large-wood cycle hypothesis: A mechanism for the physical and

biotic structuring of temperate forested alluvial valleys in the North Pacific coastal ecoregion. *Geomorphology,* **139-140,** 460-470.

Davidson, E. A. & Janssens, I. A. (2006) Temperature sensitivity of soil carbon decomposition and feedbacks to climate change. *Nature,* **440**, 165-173.

Dixon, R. K., Brown, S., Houghton, R. A., Solomon, A. M., Trexler, M. C. & Wisniewski, J. (1994) Carbon pools and flux of global forest ecosystems. *Science,* **263,** 185-190.

Doi, H. (2009) Spatial patterns of autochthonous and allochthonous resources in aquatic food webs. *Population Ecology,* **51,** 57-64.

Dyke, A. S. (2004) An outline of North American deglaciation with emphasis on central and northern Canada. *Developments in Quaternary Science,* **2,** 373-424.

Eronen, M., Zetterberg, P., Briffa, K. R., Lindholm, M., Merilainen, J. & Timonen, M. (2002) The supra-long Scots pine tree-ring record for Finnish Lapland: Part 1, chronology construction and initial inferences. *Holocene,* **12,** 673-680.

Everett, R. A. & Ruiz, G. M. (1993) Coarse woody debris as a refuge from predation in aquatic communities - An experimental test. *Oecologia,* **93,** 475-486.

Fausch, K. D. & Northcote, T. G. (1992) Large woody debris and salmonid habitat in a small coastal British Columbia stream. *Canadian Journal of Fisheries and Aquatic Sciences,* **49,** 682-693.

Forest Products Laboratory (2010) *Wood handbook—Wood as an engineering material.* U.S. Department of Agriculture, Forest Service, Forest Products Laboratory, Madison, WI.

Gennaretti, F., Arseneault, D. & Bégin, Y. (2013) Data from "Millennial stocks and fluxes of large woody debris in lakes of the North American taiga". *Figshare,* http://dx.doi.org/10.6084/m9.figshare.826213.

Girard, F., Payette, S. & Gagnon, R. (2008) Rapid expansion of lichen woodlands within the closed-crown boreal forest zone over the last 50 years caused by stand disturbances in eastern Canada. *Journal of Biogeography,* **35,** 529-537.

Girardin, M. P. & Mudelsee, M. (2008) Past and future changes in Canadian boreal wildfire activity. *Ecological Applications,* **18,** 391-406.

Glaz, P. N., Nozais, C. & Arseneault, D. (2009) Macroinvertebrates on coarse woody debris in the littoral zone of a boreal lake. *Marine and Freshwater Research,* **60,** 960-970.

Gurnell, A. M., Piégay, H., Swanson, F. J. & Gregory, S. V. (2002) Large wood and fluvial processes. *Freshwater Biology,* **47,** 601-619.

Guyette, R. P. & Cole, W. G. (1999) Age characteristics of coarse woody debris (Pinus strobus) in a lake littoral zone. *Canadian Journal of Fisheries and Aquatic Sciences,* **56,** 496-505.

Guyette, R. P., Cole, W. G., Dey, D. C. & Muzika, R. M. (2002) Perspectives on the age and distribution of large wood in riparian carbon pools. *Canadian Journal of Fisheries and Aquatic Sciences,* **59,** 578-585.

Guyette, R. P., Dey, D. C. & Stambaugh, M. C. (2008) The temporal distribution and carbon storage of large oak wood in streams and floodplain deposits. *Ecosystems,* **11,** 643-653.

Guyette, R. P. & Stambaugh, M. (2003) The age and density of ancient and modern oak wood in streams and sediments. *IAWA Journal,* **24,** 345-353.

Harmon, M. E., Franklin, J. F., Swanson, F. J., Sollins, P., Gregory, S. V., Lattin, J. D., Anderson, N. H., Cline, S. P., Aumen, N. G., Sedell, J. R., Lienkaemper, G. W., Cromack Jr, K. & Cummins, K. W. (2004) Ecology of Coarse Woody Debris in Temperate Ecosystems. *Advances in Ecological Research,* **34,** 59-234.

Hoadley, R. B. (1990) *Identifying wood: accurate results with simple tools.* Taunton Press, Newtown, CT.

Holmes, R. L. (1983) Computer-assisted quality control in tree-ring dating and measurement. *Tree-Ring Bulletin,* **43,** 69-78.

Hrodey, P. J., Kalb, B. J. & Sutton, T. M. (2008) Macroinvertebrate community response to large-woody debris additions in small warmwater streams. *Hydrobiologia,* **605,** 193-207.

Hrodey, P. J. & Sutton, T. M. (2008) Fish community responses to half-log additions in warmwater streams. *North American Journal of Fisheries Management,* **28,** 70-80.

Hyatt, T. L. & Naiman, R. J. (2001) The residence time of large woody debris in the Queets River, Washington, USA. *Ecological Applications,* **11,** 191-202.

Kane, E. S. & Vogel, J. G. (2009) Patterns of total ecosystem carbon storage with changes in soil temperature in boreal black spruce forests. *Ecosystems,* **12,** 322-335.

Lavoie, L. & Sirois, L. (1998) Vegetation Changes Caused by Recent Fires in the Northern Boreal Forest of Eastern Canada. *Journal of Vegetation Science,* **9,** 483-492.

Lester, R. E., Wright, W. & Jones-Lennon, M. (2007) Does adding wood to agricultural streams enhance biodiversity? An experimental approach. *Marine and Freshwater Research,* **58,** 687-698.

Marburg, A. E., Bassak, S. B., Kratz, T. K. & Turner, M. G. (2009) The demography of coarse wood in north temperate lakes. *Freshwater Biology,* **54,** 1110-1119.

Marburg, A. E., Turner, M. G. & Kratz, T. K. (2006) Natural and anthropogenic variation in coarse wood among and within lakes. *Journal of Ecology,* **94,** 558-568.

Marchand, D., Prairie, Y. T. & del Giorgio, P. A. (2009) Linking forest fires to lake metabolism and carbon dioxide emissions in the boreal region of Northern Quebec. *Global Change Biology,* **15,** 2861-2873.

Morneau, C. & Payette, S. (1989) Postfire lichen-spruce woodland recovery at the limit of the boreal forest in northern Quebec. *Canadian Journal of Botany,* **67,** 2770-2782.

Muggeo, V. M. R. (2008) Segmented: an R package to fit regression models with broken-line relationships. *R News,* **8,** 20–25.

Nabuurs, G. J. & Mohren, G. M. (1995) Modelling analysis of potential carbon sequestration in selected forest types. *Canadian Journal of Forest Research,* **25,** 1157-1172.

Payette, S. (1993) The Range Limit of Boreal Tree Species in Quebec-Labrador - an Ecological and Paleoecological Interpretation. *Review of Palaeobotany and Palynology*, **79,** 7-30.

Payette, S., Morneau, C., Sirois, L. & Desponts, M. (1989) Recent Fire History of the Northern Quebec Biomes. *Ecology,* **70,** 656-673.

Polis, G. A., Anderson, W. B. & Holt, R. D. (1997) Toward an integration of landscape and food web ecology: The dynamics of spatially subsidized food webs. *Annual Review of Ecology and Systematics,* **28,** 289-316.

Savard, M. M., Bégin, C., Marion, J., Arseneault, D. & Bégin, Y. (2012) Evaluating the integrity of C and O isotopes in sub-fossil wood from boreal lakes. *Palaeogeography, Palaeoclimatology, Palaeoecology*, **348-349,** 21-31.

Scealy, J. A., Mika, S. J. & Boulton, A. J. (2007) Aquatic macroinvertebrate communities on wood in an Australian lowland river: Experimental assessment of the interactions of habitat, substrate complexity and retained organic matter. *Marine and Freshwater Research,* **58,** 153-165.

Schindler, D. E. & Scheuerell, M. D. (2002) Habitat coupling in lake ecosystems. *Oikos,* **98,** 177-189.

Sirois, L. (1995) Initial phase of postfire forest regeneration in two lichen woodlands of northern Quebec. *Ecoscience,* **2,** 177-183.

Stuiver, M. & Reimer, P. J. (1993) Extended 14C data base and revised CALIB 3.0 14C age calibration program. *Radiocarbon,* **35,** 215-230.

Tank, J. L. & Webster, J. R. (1998) Interaction of substrate and nutrient availability on wood biofilm processes in streams. *Ecology,* **79,** 2168-2179.

Toms, J. D. & Lesperance, M. L. (2003) Piecewise regression: A tool for identifying ecological thresholds. *Ecology,* **84,** 2034-2041.

Vadeboncoeur, Y. & Lodge, D. M. (2000) Periphyton production on wood and sediment: Substratum-specific response to laboratory and whole-lake nutrient manipulations. *Journal of the North American Benthological Society,* **19,** 68-81.

Webb, A. A. & Erskine, W. D. (2003) Distribution, recruitment, and geomorphic significance of large woody debris in an alluvial forest stream: Tonghi Creek, southeastern Australia. *Geomorphology,* **51,** 109-126.

1.2.9 Tables

Table 1-1. Description of the sampled lakes and large woody debris (LWD) pieces

Lake	L1	L12	L18	L20	L22	All sites
Surface area (ha)	13.4	43.1	44.8	35.1	665.6	
Length of sampled shore (m)	360	540	1150	1010	270	3330
N. of LWD pieces	267	273	627	850	177	2194
Species abundance (%; spruce / tamarack / fir)	93/7/0	96/2/2	95/4/1	91/2/7	92/2/6	93/3/4
LWD pieces with roots (%)	1.5	3.7	1.0	0.1	3.4	1.2
LWD oriented perpendicularly to the shore (%)	58.0	50.8	54.7	60.0	56.5	56.9
N. of charred (trunk / branch tips)	0/1	0/2	4/12	0/3	2/4	6/22
N. of crossdated to the calendar year	178	219	426	613	135	1571
N. of crossdated into floating chronologies	20	4	9	39	1	73
Average N. of tree-rings per dated LWD piece (mean ± SD) *	121±37	118±35	115±38	116±39	108±38	116±38
LWD mean residence time (mean ± SD; years) *	505±451	514±341	472±365	588±547	557±308	535±452
Oldest tree-ring crossdated to the calendar year (year AD)	639	569	594	651	648	569

* Including LWD samples of the floating chronologies.

Table 1-2. Large woody debris (LWD) stocks in the littoral zone of the five studied lakes. Buried LWD includes completely buried and partly buried specimens. LWD pieces correspond to wood pieces with a maximum diameter equal or greater than 4 cm

Lake	Burial	N.	Average N. of tree-rings (mean±SD)	Average diameter (mean±SD; cm)	Average length (mean±SD; cm)	Average volume (mean±SD; m^3)	N. per 100 m of shore	Volume per 100 m of shore (m^3)
	Buried	69	112.3±40.3	8.8±2.3	331.8±193.7	0.0142±0.0149	19.2	0.2729
L1	Exposed	198	116.6±36.6	9.1±3.0	359.7±186.2	0.0175±0.0246	55.0	0.9649
	Total	267	115.5±37.6	9.0±2.8	352.5±188.6	0.0167±0.0225	74.2	1.2378
	Buried	124	114.6±35.2	10.8±3.0	441.4±210.0	0.0265±0.0216	23.0	0.6078
L12	Exposed	149	116.3±37.7	10.3±2.9	374.8±176.2	0.0211±0.0194	27.6	0.5834
	Total	273	115.5±36.5	10.5±2.9	405.0±195.5	0.0236±0.0206	50.6	1.1913
	Buried	190	94.4±40.5	9.1±3.1	424.6±243.3	0.0196±0.0216	16.5	0.3241
L18	Exposed	437	102.2±42.3	8.4±2.8	340.4±216.9	0.0156±0.0317	38.0	0.5931
	Total	627	99.9±41.9	8.6±2.9	365.9±228.5	0.0168±0.0291	54.5	0.9172
	Buried	389	107.8±39.5	9.6±2.9	406.8±236.3	0.0211±0.0247	38.5	0.8124
L20	Exposed	461	105.4±42.4	8.8±3.4	364.3±194.6	0.0166±0.0245	45.6	0.7558
	Total	850	106.5±41.1	9.2±3.2	383.8±215.8	0.0186±0.0247	84.2	1.5681
	Buried	68	109.0±50.0	9.9±2.9	368.1±199.4	0.0188±0.0184	25.2	0.4746
L22	Exposed	109	90.1±31.2	9.5±3.3	336.0±176.3	0.0183±0.0220	40.4	0.7383
	Total	177	97.3±40.4	9.7±3.2	348.3±186.2	0.0185±0.0207	65.6	1.2129
	Buried	840	106.1±40.7	9.6±3.0	406.6±230.3	0.0208±0.0227	25.2	0.5249
Total	Exposed	1354	105.8±40.9	8.9±3.2	354.8±198.5	0.0170±0.0266	40.7	0.6928
	Total	2194	106.0±40.8	9.2±3.1	374.7±212.9	0.0185±0.0252	65.9	1.2180

Table 1-3. Description of the floating chronologies

ID	N. of LWD pieces	Time span (years)	N. of AMS dates	Calibrated age range of the chronology end (years AD/BC) *
CF1	51	460	6	AD 578 / AD 592
CF8	9	266	2	AD 164 / AD 240
CF14	2	178	1	185 BC / 27 BC
CF17	2	192	1	614 BC / 388 BC
CF9	4	186	2	608 BC / 401 BC
CF12	2	143	1	1938 BC / 1848 BC
CF7	3	172	1	3187 BC / 2942 BC

* Determined from the overlap of the two sigma confidence intervals once shifted to the end of their respective chronology.

Table 1-4. ANOVA table for the selected regression models with large woody debris residence time (log-transformed) as dependent variable. * *P*-value <0.05, ** *P*-value <0.01 and *** *P*-value <0.001

Lake	Source of variation	Df	Sum Sq	F value	Variance explained
L18	Burial type	1	13.57	105.68***	0.259
	Distance from the shore	1	7.92	61.68***	0.151
	Exposure to wave action	1	0.78	6.11*	0.015
	Residuals	235	30.18	NA	0.575
L20	Burial type	1	14.43	291.12***	0.353
	Distance from the shore	1	4.15	83.76***	0.102
	Depth in the water	1	0.77	15.45***	0.019
	Orientation	1	0.58	11.77***	0.014
	Substratum	1	0.53	10.66**	0.013
	Residuals	412	20.43	NA	0.500

Table 1-5. Effects of wildfires prior to AD 1750 on the fluxes of large woody debris (LWD) across the forest-lake interface at the studied sites. Two more recent fires at L22 are excluded because their effects on the LWD fluxes are still ongoing (Fig. 5)

Littoral zone	Fire year	Normalization of establishment rate (years)	Normalization of recruitment rate (years)	Post-fire recruitment reduction (%)	Massive recruitment
L1	1241	48	179 *	NA	No
L12	1463	4	90	-46.1	No
L12	1664	20	104	-92.2	No
L18 shore 1	1696	NA	70	-48.7	No
L18 shore 2	1251	143	221	-93.6	No
L18 shore 2	1622	0	NA	NA	No
L18 shore 2	1668	NA	NA	NA	No
L18 shore 2	1729	7	40	-87.5	Yes
L20 shore 1	1592	60	137	-73.8	No
L22	1126	105	225	-64.6	No
L22	1394	64	85	-87.4	No
L22	1673 †	NA	0	-79.4	Yes

* The calculation was performed because an increased LWD recruitment rate was observed after this wildfire even if it did not cause a recruitment reduction (Fig. 5).
† Wildfire deduced from the pattern of recruitment even if no charred LWD pieces were found.
NA indicates that no value could be calculated because piecewise regressions failed in detecting a corresponding breakpoint.

1.2.10 Figures

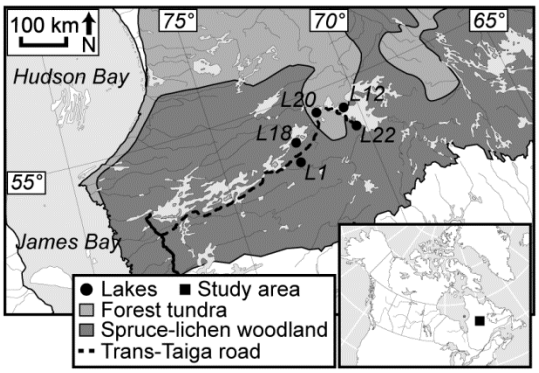

Fig. 1-1. Location of the study area in the northern boreal forest of Quebec, Eastern Canada.

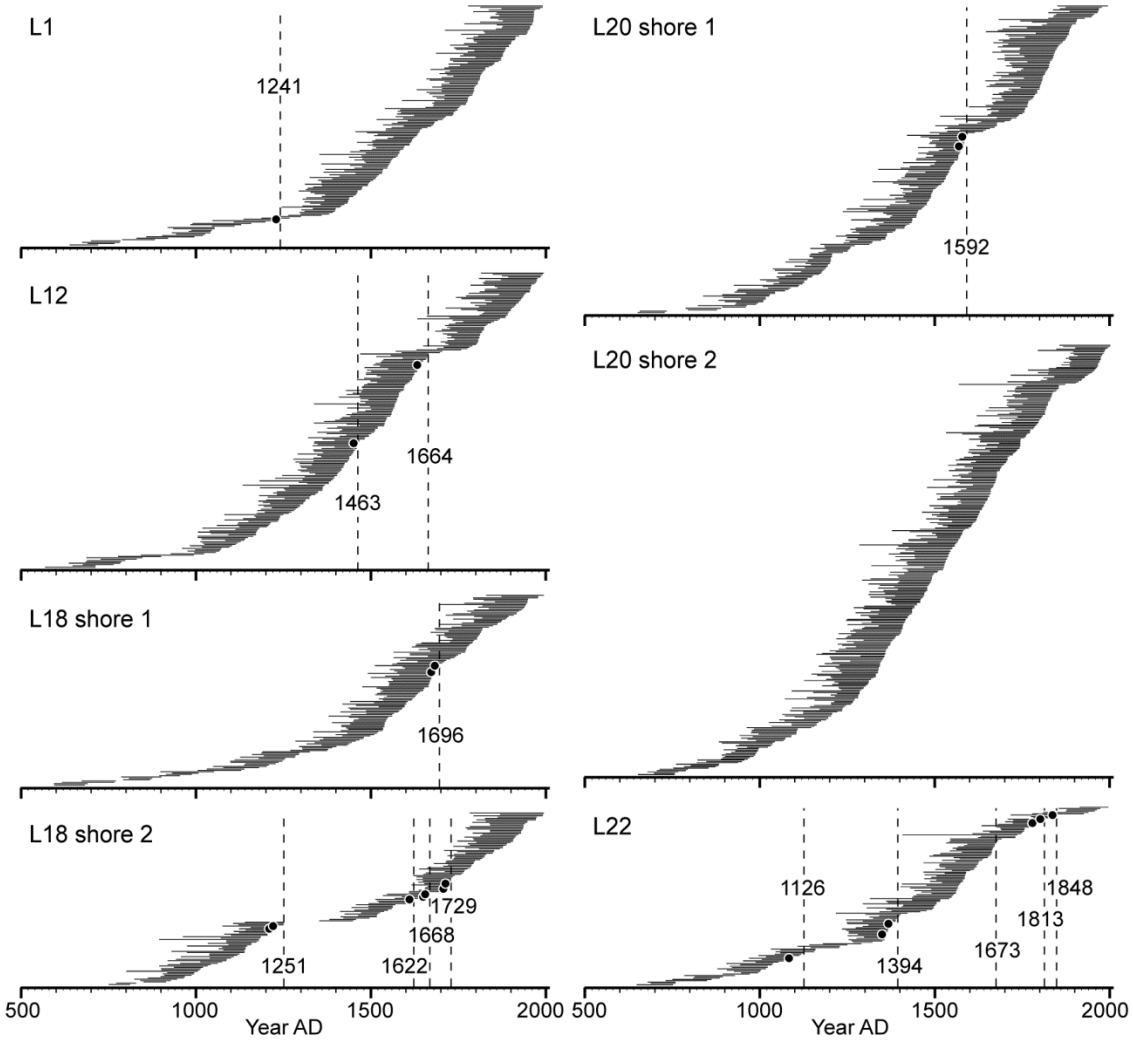

Fig. 1-2. Life spans of large woody debris (LWD) samples from the study sites crossdated to the calendar year. Each horizontal black line refers to one LWD piece and its length indicates the number of tree-rings in the sample. Vertical dashed lines are estimated wildfires dates. Black dots show the end of the life span of charred LWD pieces.

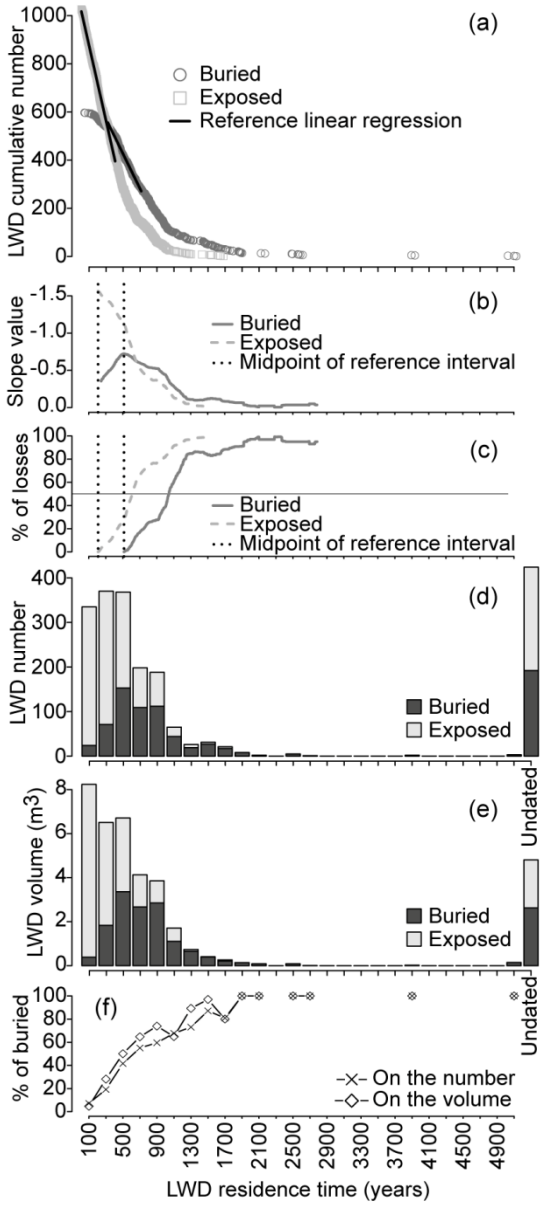

Fig. 1-3. Decay of large woody debris (LWD) abundance according to residence time in lakes. (a) cumulative distributions of buried and exposed LWD pieces; (b) slopes of linear regression models fitted to the cumulative distributions on consecutive residence time intervals of 400 years; (c) percentage of LWD losses by decomposition and burial; (d) number and (e) volume of LWD specimens per residence time classes of 200 years; and (f) percentage of buried specimens. Computations are based on black spruce LWD specimens from all lakes (crossdated into floating and master chronologies). Buried LWD samples include completely buried and partly buried specimens.

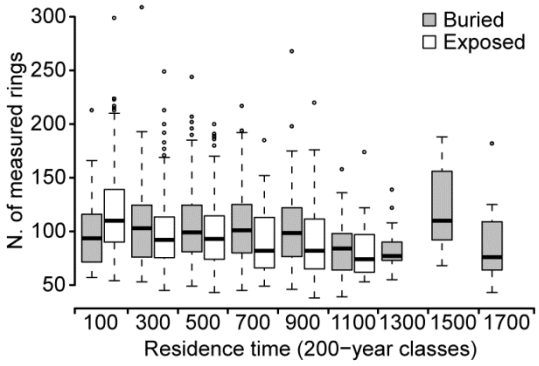

Fig. 1-4. Boxplot of the number of measured tree-rings per large woody debris (LWD) specimen according to residence time classes of 200 years. For each class, quartiles (central bar and box limits), extreme values within 1.5 interquartile ranges from the boxes (whiskers) and outliers (circles) are represented. All dated black spruce specimens from all lakes (master and floating chronologies) are considered, but time classes with less than 10 specimens are excluded. Buried LWD samples include completely buried and partly buried specimens.

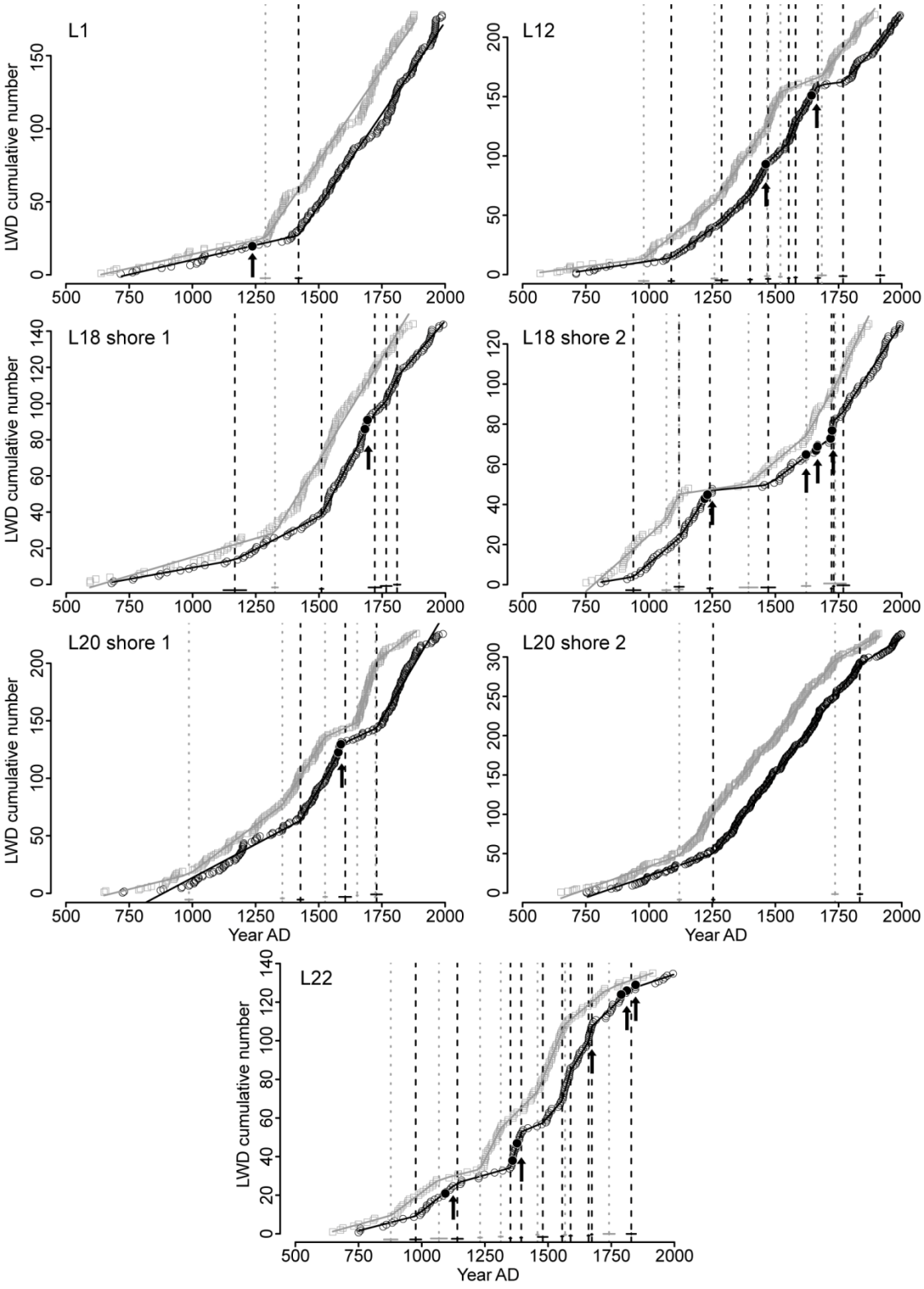
L1
L12
L18 shore 1
L18 shore 2
L20 shore 1
L20 shore 2
L22
LWD cumulative number
Year AD

Fig. 1-5. Cumulative number of large woody debris (LWD) specimens crossdated to the calendar year versus their recruitment (black circles) and establishment (grey squares) dates. Piecewise regression models fitted to the recruitment (black solid line) and establishment (grey solid line) data are also shown, as well as corresponding breakpoint dates (vertical dashed or dotted lines), 95% confidence intervals for the breakpoints (horizontal lines at the base of the dashed or dotted lines), estimated wildfire dates (vertical arrows) and recruitment dates of charred LWD pieces (black dots).

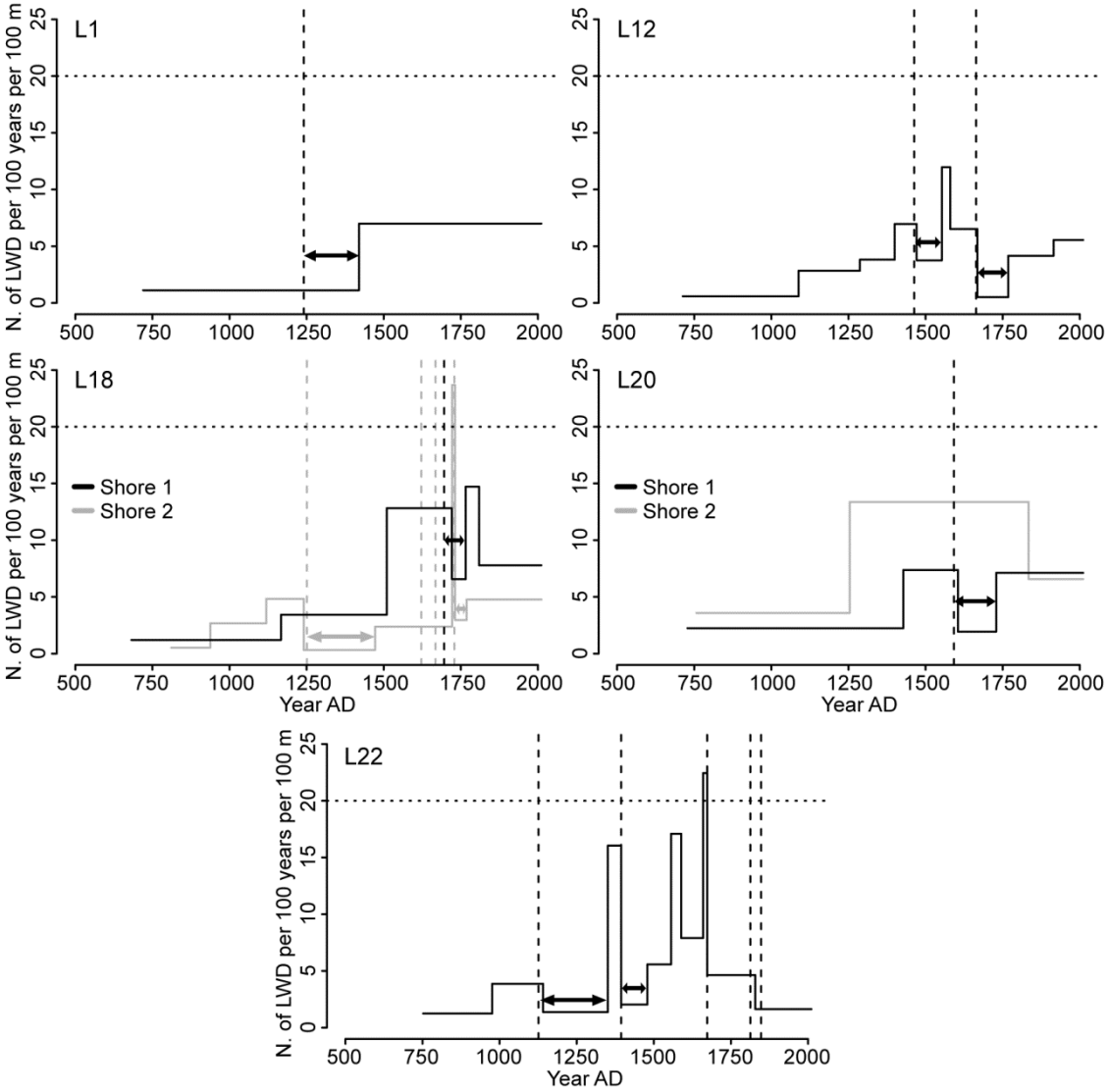

Fig. 1-6. Large woody debris (LWD) recruitment rates in the five littoral zones during the last 1400 years as reconstructed through piecewise regressions. Vertical dashed lines are estimated wildfires dates. The horizontal dotted line indicates the chosen threshold for a massive recruitment. Horizontal arrows show the time needed for the normalization of the recruitment rate after a fire.

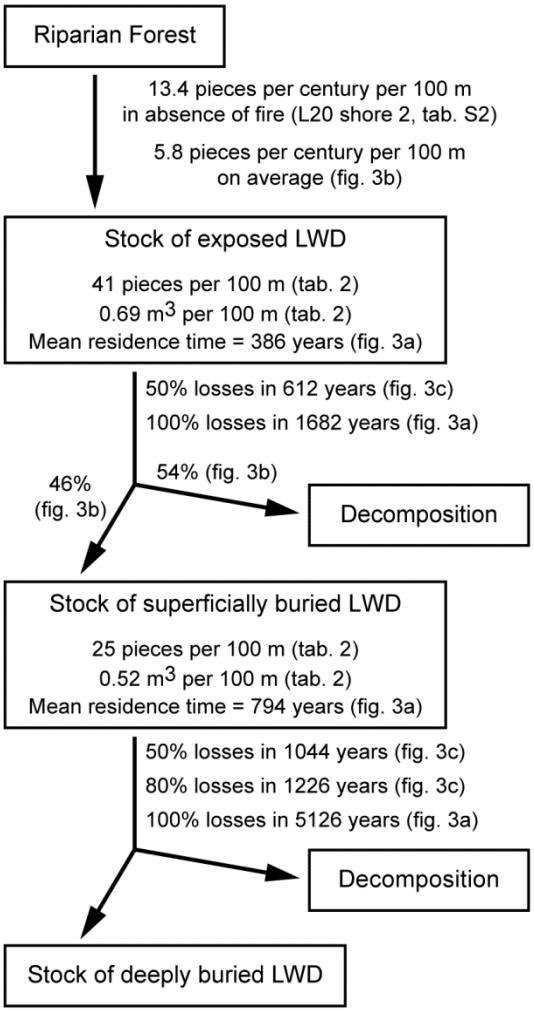

Fig. 1-7. Relative importance of large woody debris (LWD) stocks and fluxes in the studied lakes. The sources of the data are in parentheses.

1.2.11 Supporting information

Appendix S1. Samples and variables used in the regression models to determine factors influencing large woody debris (LWD) residence time.

Factors influencing LWD residence time in lakes were investigated with multiple linear regressions. In this appendix, we describe the samples used in the regression models and the computations to obtain the independent variables.

In total, 239 and 418 black spruce LWD pieces were included in the multiple linear regression models at L18 and L20, respectively. Samples with incomplete data were discarded (100 LWD discarded at L18 and 130 at L20), because they were sampled during a pre-sampling campaign in which not all the independent variables were measured. Specimens recruited during periods of massive or low recruitment due to wildfires (95 LWD pieces at L18 and 87 at L20) were also discarded (see Table 5) to avoid the over- or under-representation of some areas of the littoral zones most affected by fires. Also removed from the models was one negatively influencing outlier per lake.

All categorical independent variables were coded (see main text) such that higher values were assigned to characteristics that would increase LWD residence time. For example, a perpendicular orientation means that a LWD piece has remained undisturbed in the same position after its recruitment into the lake. It was thus hypothesized that a perpendicular orientation has favored LWD preservation because of reduced attrition due to movement. The aspect of the littoral zone was measured at regular intervals with a handheld compass. Aspect was then transformed into a linear metric ranging from zero (SW-W aspect) to two (NE-E aspect), using the following transformation: [aspect = cosine (60 - degrees) + 1] (Beers, Dress & Wensel 1966). SW-W aspect was considered to be the less favorable for LWD preservation as it faces the dominant winds (La Grande IV weather station, Environment Canada 2013). The exposure to wave action was calculated as proposed by Marburg, Turner & Kratz (2006), from the empirical

relationship between maximum wave height and fetch length (Wetzel 2001), weighted by the proportion of wind coming from 12 directions:

$$Exposure = \sum_{i=1}^{12} (0.105 p_i \sqrt{l_i})$$

where exposure is measured in cm (this is a relative measure of exposure that refers to the maximum wave height), p_i is the proportion of wind coming from the direction i obtained from the wind data of the La Grande IV weather station and l_i is the fetch length in cm for the direction i. The fetch length for each LWD piece was calculated in a GIS.

Appendix S2. Technical aspects of computing piecewise regressions models and of dating past fires.

For each site or shore segment, piecewise regression models were fitted to the cumulative number of large woody debris (LWD) pieces according to their establishment and recruitment date using the "segmented" package of the R software (Muggeo 2008; Fig. 5). The breakpoints of these models were selected automatically by increasing the number of starting values provided to the detection algorithm until proper representations of LWD establishment and recruitment were attained. The breakpoint detection algorithm identifies, in each subset of the data defined by the starting values, the point, if any, where the linear relationship between the variables changes. In our case, the starting values were chosen using quantiles or equally spaced intervals according to a visual evaluation of model performance.

Past fires where dated at each site from the recruitment dates of charred LWD pieces (Fig. 2). We considered also that some pieces may have lost their charred marks and may have been more or less eroded. That means that if, in proximity of a charred specimen, some uncharred LWD pieces had a more recent recruitment date immediately

before a clear discontinuity in the temporal trend of recruitment dates, then the fire year was determined from the most recent recruitment preceding the discontinuity.

Supporting References

Beers, T. W., Dress, P. E. & Wensel, L. C. (1966) Aspect transformation in site productivity research. *Journal of Forestry*, **64,** 691-692.

Marburg, A. E., Turner, M. G. & Kratz, T. K. (2006) Natural and anthropogenic variation in coarse wood among and within lakes. *Journal of Ecology*, **94,** 558-568.

Muggeo, V. M. R. (2008) Segmented: an R package to fit regression models with broken-line relationships. *R News*, **8,** 20–25.

Wetzel, R. G. (2001) *Limnology: Lake and River Ecosystems. 3rd ed.* Elsevier academic press, San Diego, CA.

Supporting Tables

Table 1-S1. Alternative linear regression models explaining variation in large woody debris residence time (log-transformed) at sites L18 and L20. Sign and coefficient for each variable in the models are given as well as significant *P*-values (* $P<0.05$, ** $P<0.01$, and *** $P<0.001$). Only models with delta AIC < 2 are shown

Lake	Intercept	Distance from the shore (cm)	Depth in the water (feet)	Burial type	Substratum	Aspect of the littoral zone	Exposure to wave action (cm)	Orientation	Delta AIC	R^2
L18	0.8959**	0.0006***	NA	0.3273***	NA	0.2015	0.0828**	NA	0.00	0.43
	1.2776***	0.0006***	NA	0.3273***	NA	NA	0.0769*	NA	0.32	0.42
	0.8897**	0.0004*	0.0214	0.3201***	NA	0.2047	0.0858**	NA	0.35	0.43
	1.2777***	0.0004**	0.0209	0.3203***	NA	NA	0.0797*	NA	0.77	0.43
	0.8243**	0.0006***	NA	0.3118***	0.0138	0.2133	0.0874**	NA	1.43	0.43
	0.8696**	0.0006***	NA	0.3284***	NA	0.1968	0.0833**	0.0111	1.88	0.43
	0.8304**	0.0004*	0.0203	0.3075***	0.0115	0.2144	0.0895**	NA	1.96	0.44
	1.2407***	0.0006***	NA	0.3157***	0.0104	NA	0.0801*	NA	2.00	0.43
L20	1.9318***	0.0003***	0.0258***	0.1929***	0.0283**	NA	NA	0.0567***	0.00	0.50
	1.9693***	0.0003***	0.0276***	0.1921***	0.0279**	NA	-0.0088	0.0571***	1.34	0.50
	1.9654***	0.0003***	0.0259***	0.1931***	0.0281**	-0.0169	NA	0.0566***	1.98	0.50

Table 1-S2. Estimated wildfire dates and description of piecewise regression models

Littoral zone	Fire year (year AD)	Piecewise regressions on the recruitment data				Piecewise regressions on the establishment data			
		N. of starting values	Breakpoint (year AD)	Slope	N. of LWD samples per 100 years per 100 m	N. of starting values	Breakpoint (year AD)	Slope	N. of LWD samples per 100 years per 100 m
L1	1241	1	**1420**	0.040 0.252	1.114 6.994	1	**1289**	0.038 0.250	1.068 6.933
L12	1463 1664	9	1088 1287 1400 **1471** **1553** 1580 **1668** **1768** 1915	0.032 0.153 0.206 0.376 0.203 0.646 0.352 0.027 0.224 0.300	0.584 2.831 3.815 6.965 3.757 11.969 6.515 0.508 4.156 5.552	9 *	979 1259 **1467** **1520** **1684**	0.028 0.171 0.313 0.522 0.083 0.271	0.520 3.165 5.791 9.670 1.543 5.013
L18 shore 1	1696	6	1167 1510 **1721** **1766** 1809	0.025 0.072 0.269 0.138 0.309 0.164	1.204 3.427 12.819 6.571 14.719 7.786	1	1326	0.041 0.228	1.971 10.871
L18 shore 2	1251 1622 1668 1729	8	938 1119 **1241** **1472** **1722** **1731** **1769**	0.021 0.107 0.193 0.012 0.095 0.947 0.119 0.191	0.521 2.670 4.828 0.311 2.370 23.678 2.963 4.770	6 *	1069 **1119** **1394** **1622** **1736**	0.112 0.254 0.019 0.105 0.217 0.261	2.800 6.338 0.469 2.628 5.425 6.533
L20 shore 1	1592	3	1428 **1605** **1729**	0.117 0.383 0.101 0.370	2.242 7.373 1.935 7.115	5	986 1356 **1525** **1652** 1725	0.055 0.163 0.350 0.100 0.731 0.164	1.051 3.131 6.727 1.915 14.052 3.144
L20 shore 2	No fires	2	1254 1834	0.111 0.414 0.204	3.581 13.361 6.565	2	1120 1736	0.117 0.403 0.180	3.758 13.010 5.813
L22	1126 1394 1673 † 1813 1848	10	976 **1141** **1351** **1394** **1479** 1556 1589 **1660** **1673** 1829	0.034 0.104 0.037 0.433 0.055 0.151 0.462 0.213 0.606 0.125 0.044	1.246 3.867 1.369 16.048 2.029 5.574 17.093 7.896 22.441 4.633 1.631	8 *	877 **1068** **1231** **1313** **1458** **1567** 1741	0.036 0.098 0.033 0.260 0.129 0.321 0.108 0.044	1.331 3.629 1.215 9.633 4.789 11.893 4.004 1.639

Breakpoints explained by the occurrence of a wildfire are in bold.
* Starting values selected using equally-spaced intervals.
† Wildfire deduced from the pattern of recruitment even if no charred LWD piece was found.

Supporting Figures

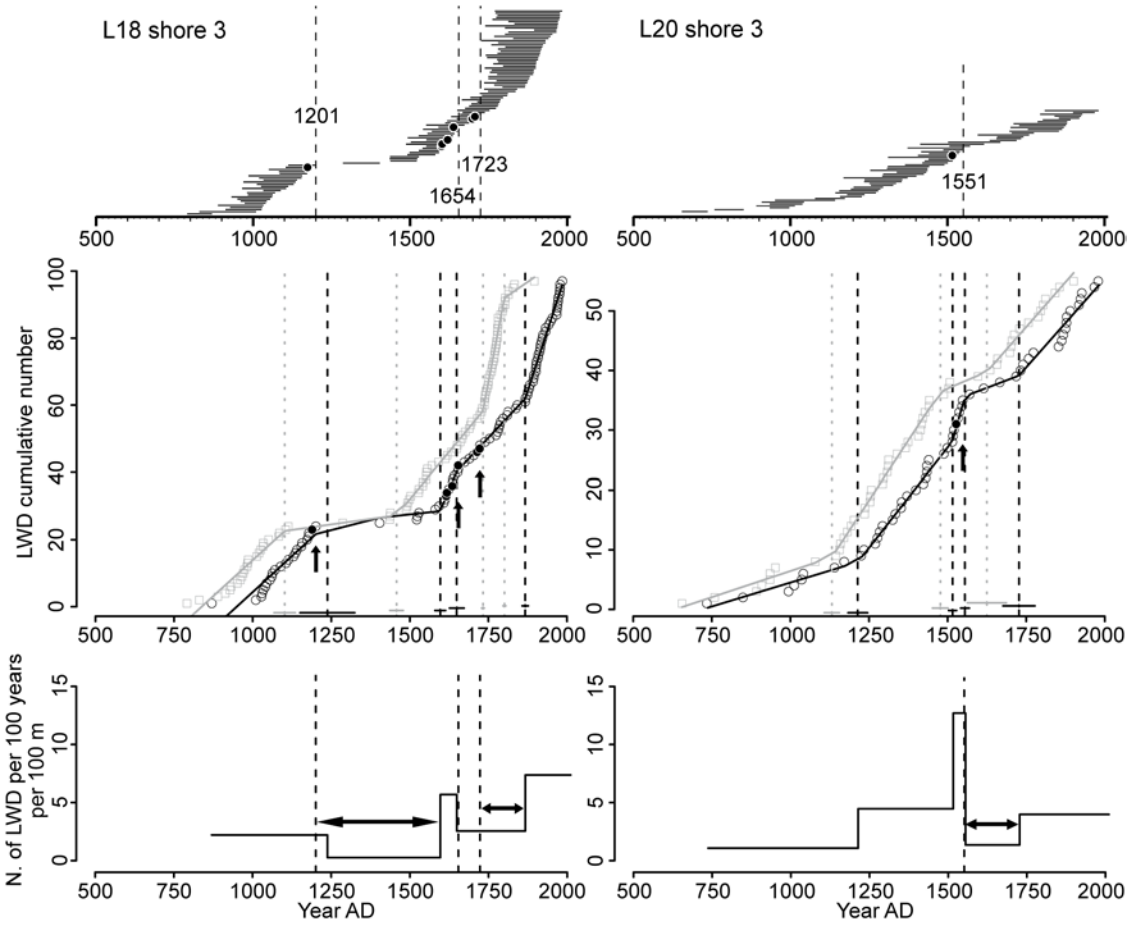

Fig. 1-S1. Wildfire impacts on large woody debris (LWD) fluxes at the shore 3 of L18 (left) and the shore 3 of L20 (right). The upper plots show the life spans of LWD samples crossdated to the calendar year. The middle plots show the piecewise regression models fitted to the recruitment (black) and establishment (grey) data. The bottom plots show the LWD recruitment rates as reconstructed through piecewise regressions. All symbols are as in Figs 2, 5 and 6 of the main manuscript.

CHAPITRE 2.
DYNAMIQUES MILLÉNAIRES DES FORÊTS DE LA TAÏGA DE L'EST CANADIEN SOUS L'INFLUENCE DES INCENDIES

2.1 RÉSUMÉ EN FRANÇAIS DU DEUXIÈME ARTICLE

Le deuxième article de ma thèse, intitulé « *Millennial disturbance-driven forest stand dynamics in the Eastern Canadian taiga reconstructed from subfossil logs* », fut co-rédigé par moi-même ainsi que par les professeurs Dominique Arseneault (UQAR) et Yves Bégin (INRS-ETE). Cet article a été soumis pour la publication aux éditeurs de la revue *Journal of Ecology* en février 2014. La contribution des auteurs est la même que pour le premier article de ma thèse.

Pour cet article, nous avons investigué les impacts des incendies du dernier millénaire sur des forêts de la taïga. Les incendies représentent le principal facteur naturel de perturbation qui produit des changements écologiques en forêt boréale. Malgré cela, la compréhension des effets des incendies du dernier millénaire sur la diversité du paysage actuel est difficile car nous n'avons pas de reconstitutions paleoécologiques qui ont à la fois des résolutions spatiale (quelques centaines de mètres carrés) et temporelle (annuelle) très fines.

Nous avons donc combiné un inventaire détaillé de la forêt riveraine le long de la rive de deux lacs de la taïga de l'est canadien avec l'analyse dendrochronologique des gisements de bois subfossiles accumulés dans la zone littorale adjacente aux forêts étudiées. Cela nous a permis de comparer les impacts des incendies du dernier millénaire entre des peuplements forestiers caractérisés par une structure et une composition

différentes au sein d'un même site. La densité des arbres et les dates des incendies durant les derniers siècles ont été estimées à partir des taux de recrutement des bois subfossiles dans les lacs et de la datation de bois ayant des traces de feu.

L'analyse multivariée des forêts riveraines a révélé respectivement trois et deux sections homogènes (clusters) aux sites L18 et L20. Le cluster 1 de chaque site a été caractérisé par une forêt plus dense, une quantité majeure de bois mort et un pourcentage plus élevé de sapin baumier, une espèce mal adaptée au feu. Respectivement 426 et 611 bois subfossiles (principalement des épinettes noires) ont été datés à l'année près sur les 1400 dernières années aux sites L18 et L20. Leur analyse dendrochronologique a confirmé que chaque cluster riverain, identifié à partir des traits de la forêt actuelle, a connu une histoire spécifique de feux au cours du dernier millénaire (0-5 incendies de sévérité variable) qui a influencé localement la composition de la forêt, la densité des arbres et leur croissance. Chaque feu a déclenché une trajectoire successionnelle spécifique, caractérisée par une diminution de la densité des arbres et un taux de récupération très différents. Nos résultats montrent aussi que la variabilité du climat régional au cours du dernier millénaire a également eu une incidence sur les forêts de nos sites. Les arbres riverains ont poussé plus rapidement durant l'Optimum climatique médiéval alors qu'une période froide au début du XIX^{e} siècle induite par des éruptions volcaniques a coïncidé avec une forte réduction de la croissance et un pic de mortalité des arbres.

Cette étude a fourni une perspective à long terme qui aide à expliquer comment la diversité du paysage actuelle dans la taïga de l'est canadien est liée à l'histoire des feux spécifiques à chaque site. Les incendies ont eu des effets persistants et cumulatifs résultant en une ouverture progressive du couvert forestier avec l'exclusion du sapin baumier. Les paysages actuels sont des mosaïques de peuplements forestiers caractérisés par des temps différents depuis le dernier feu et des trajectoires différentes de structure forestière après feu.

2.2 MILLENNIAL DISTURBANCE-DRIVEN FOREST STAND DYNAMICS IN THE EASTERN CANADIAN TAIGA RECONSTRUCTED FROM SUBFOSSIL LOGS

2.2.1 Summary

1. Although wildfire is the main natural disturbance factor driving changes in the North American boreal forest, understanding how the fire history of the last millennium shaped the present-day landscape diversity is a difficult task due to the lack of paleoecological reconstructions with high spatial (few hundreds of square meters) and temporal (annual) resolutions.

2. We combined a detailed inventory of the present-day riparian forest situated along the shoreline of two lakes of the Eastern Canadian taiga with the dendrochronological dating of the subfossil logs that accumulated in the littoral zones facing these shores. Our objective was to compare the millennial impact of wildfires among stands of various structures and compositions. Past stem densities and fire years were reconstructed from log recruitment rates and dating of charred logs.

3. Multivariate analysis of the present-day riparian forest revealed three and two homogeneous sections per site (i.e. clusters). Cluster 1 at both sites exhibited denser forest, higher dead wood values and a higher percentage of balsam fir, a fire-sensitive species.

4. In total, 426 and 611 subfossil logs (mostly black spruce) were crossdated over the last ~1400 years. Dendrochronological analysis confirmed that each riparian cluster, identified from the traits of the present-day forest, experienced a specific fire history over the last millennium (i.e. 0-5 fires of variable severity) that locally influenced forest composition, tree density and growth. Each fire triggered a specific forest structure trajectory characterized by a different stem density and rate of recovery.

5. Climate variability also impacted our sites. Riparian trees grew faster during the Medieval Climate Anomaly whereas an early 1800's volcano-induced cold episode coincided with a sharp reduction in tree growth and a peak in tree mortality.

6. *Synthesis:* This study provides a long-term perspective that helps explain how the present-day landscape diversity in the Eastern Canadian taiga reflects the site-specific fire history over the last millennium. Fires have caused persistent and cumulative impacts resulting in a progressive opening of the forest cover along with balsam fir exclusion. Present-day landscapes are mosaics of forest stands characterized by different times since fire and different postfire forest structure trajectories.

2.2.2 Introduction

Many ecosystems depend on or are well-adapted to the occurrence of human and natural disturbances (Le Goff & Sirois 2004; Brunbjerg et al. 2012; Newbery et al. 2013). However, disturbances may also produce long-term alterations of the natural landscape (He et al. 2002; Vanderwel, Coomes & Purves 2013), as well as a degradation in ecosystem functioning (Villnäs et al. 2013; Zwicke et al. 2013) or a creation of divergent successional pathways (Folke et al. 2004; Johnstone et al. 2010; Harvey & Holzman 2013). Spatio-temporal variation in disturbance frequency and severity is an agent of ecological diversity in several biomes (Fraterrigo & Rusak 2008).

For example, the North American boreal forest is characterized by large and frequent stand-replacing wildfires (Johnson 1992; Stocks et al. 2003) and is dominated by even-aged communities of fire-adapted species such as black spruce (*Picea mariana* (Mill.) B.S.P.) and jack pine (*Pinus banksiana* Lamb.) (Johnson 1992; Sirois 1995). Although spruce and pine stands recover rapidly after fire due to their serotinous cones (i.e. cones that remain closed and disperse seed following a fire), tree density and forest composition vary according to several factors, such as the magnitude of the pre-fire seed banks (Greene & Johnson 1999), the time since the last fire (Morneau & Payette 1989), the

severity of the fire (Arseneault 2001), and the duration of the preceding fire-free interval (Lavoie & Sirois 1998). In these environments, fire frequency and severity are the dominant drivers of change in forest structure and composition at both the site and landscape levels, and also determine ecosystem net primary production and the regional carbon balance (Bond-Lamberty et al. 2007).

In Eastern Canada, these short-term (decadal to secular) fire effects have been superimposed onto a longer-term, large-scale climate-induced decrease in conifer stem density, which was also mediated by fire disturbance (Payette & Gagnon 1985). The boreal biome of the region is subdivided into three main latitudinal bands from south to north: the closed-crown forest, the spruce-lichen woodland (hereafter referred to as the taiga) and the forest tundra (Fig. 1; Saucier et al. 2003). In the forest tundra zone, black spruce stands occur mostly in the lowlands, while upland spruce stands systematically failed to recover and shifted to treeless ecosystems after fire over the last 600-900 years, following the Medieval Climate Anomaly (Payette & Gagnon 1985; Payette & Morneau 1993; Payette, Filion & Delwaide 2008). Many spruce-lichen woodland and dense forest stands also failed to recover or shifted to more open woodlands after the fires of the 20th century in the closed-crown forest and the taiga zones (Sirois & Payette 1991; Lavoie & Sirois 1998; Girard, Payette & Gagnon 2008; Boiffin & Munson 2013). This generalized fire-climate induced deforestation was accompanied by a decreasing occurrence of fire-sensitive balsam fir (*Abies balsamea* (L.) Mill.) over the last millennia (Arseneault & Sirois 2004; de Lafontaine & Payette 2010). Today, forest stands with abundant fir are scattered in areas less affected by fire, frequently along streams and lakeshores (Sirois 1997; Arseneault, Boucher & Bouchon 2007). It has been hypothesized that these stands are remnants of a previously widespread closed-crown spruce-fir vegetation zone, similar to that occurring further south, established more than 5000 years ago when fires were less frequent due to a more humid climate (Sirois 1997; Arseneault & Sirois 2004; Boucher, Arseneault & Hétu 2006; Ali et al. 2008; de Lafontaine & Payette 2010).

The taiga of Eastern Canada (Fig. 1), comprises a mosaic of spruce-lichen woodlands of various postfire ages, stem densities and fir abundance, along with numerous lakes and peatlands in concave landforms (Fig. S1 in Supporting information). Deciphering how these spatially variable forest structures and compositions reflect long-term fire and climate impacts is a difficult task due to the lack of paleoecological records available to reconstruct millennial forest dynamics with both high spatial and temporal resolutions. Dendrochronology can be used to reconstruct forest dynamics at the stand level with an annual resolution, but such reconstructions are limited to a few centuries because of fast decay of dead wood (Bond-Lamberty & Gower 2008). Conversely, pollen and charcoal and plant macroremains allow the reconstruction of long-term vegetation changes and fire histories (e.g. Carcaillet et al. 2010; Payette et al. 2012; Senici et al. 2013), but provide no direct information on past tree density or growth trends and the dating of disturbances, which in these cases relies on radiocarbon methods, is less precise than with dendrochronology. Furthermore, contrary to fire impacts, pollen data are not stand-specific because of pollen mobility.

In this study, we first conducted a detailed inventory of the present-day riparian forest structure and composition of 2.2 kilometres of shoreline situated along two boreal lakes. Subsequently, we used dendrochronology to analyse the large stocks of submerged subfossil logs that accumulated in the littoral zones facing these same shores in order to reconstruct the millennial impacts of wildfires on riparian forest stands. Our objective was to verify whether variations in the forest structure and composition of the present-day riparian forest at each site can be attributed to varying fire histories during the last millennium. Our hypotheses are that (i) there is a negative correlation between past wildfire frequency and present-day tree density and balsam fir abundance, and that (ii) impacts of past fires have been spatially heterogeneous even within a given site and have persisted over several centuries.

2.2.3 Materials and methods

Study sites and sampling

Two lakes, hereafter called L18 (54.25 N, 72.38 W) and L20 (54.56 N, 71.24 W), were the object of this study. They are located at the interface between the taiga and the forest tundra of Northern Quebec in Eastern Canada (Fig. 1). Black spruce is the prevalent tree species and a mosaic of postfire spruce-lichen woodlands characterizes the region (Fig. S1). Other less abundant tree species include balsam fir and tamarack (Larix laricina (Du Roi) K. Koch). The regional burn rate is about 0.2% per year (Boulanger et al. 2012). The mean annual temperature is -3°C and the average annual precipitation is 760 mm, of which 550 falls as rain (La Grande IV weather station; 22 years of observations, Environment Canada 2014). The region is located in the northern part of the balsam fir range and east of the jack pine range limit. The easternmost jack pine stands are located about 10 kilometres westward of L18.

The two sites are part of a network of lakes selected to study the stocks of subfossil logs in boreal lakes and their fluxes across the forest-lake interface (Gennaretti, Arseneault & Bégin 2014), as well as to develop a dendroclimatic reconstruction of the summer temperatures of Eastern Canada over the last millennium (Gennaretti et al. unpublished data). At each site we selected a lakeshore segment characterized by old-growth forest vegetation (i.e. time since last fire of about 300-400 years; see results) on a well-drained glacial deposit and on the leeward shore of the lake. To characterize the structure and composition of the present-day riparian forest stands, we sampled 39 and 33 plots (10 x 10 m) spaced at 20 m intervals along and adjacent to the lakeshore at L18 and L20, respectively (Fig. 1). Within each plot we recorded the diameter at breast height (DBH) by species (spruce, fir or tamarack) of all living trees and snags ≥ 3 cm DBH. We also recorded the maximum diameter of all stumps and coarse woody debris pieces on the forest floor, excluding specimens with a maximum diameter < 4 cm. Snags were defined as standing dead trees connected to their roots and higher than breast

height, stumps as dead trees connected to their roots and lower than breast height, and coarse woody debris pieces as dead trees on the floor not connected to their roots. The two or three highest living trees (depending on species diversity) at each plot were cored as close to the collar as possible using a Pressler's increment borer. In the laboratory, tree-ring counting on the increment cores (No. = 165) allowed the minimum stand age at each plot to be determined (i.e. maximum number of tree-rings per tree after applying a correction for coring height). Seedlings and saplings (< 2 cm DBH) were counted within two subplots (1 x 10 m) perpendicular to the lakeshore on the two opposite edges of each main plot.

In the littoral zone facing the lakeshore segments, we systematically sampled all subfossil logs found in the water or in the superficial sediments with diameters ≥ 4 cm using the method described by Arseneault et al. (2013). In total, 627 and 848 logs were sampled along 1170 and 990 m of shoreline at L18 and L20, respectively. For each subfossil log, the sampling location was mapped with a total station and a cross-section was collected at its maximum diameter for dendrochronological analysis. In the lab, the tree species were identified using wood anatomy characteristics (spruce, fir or tamarack) and tree-ring width measurements and dendrochronological dating were performed with standard procedures as described by Gennaretti, Arseneault & Bégin (2014). In total, 426 (all black spruce) and 611 (595 black spruce and 16 balsam fir) logs could be crossdated over the last ~1400 years at L18 and L20, respectively. These subfossil logs have not been significantly redistributed along the littoral zone after recruitment into the water as proven by the relatively high proportion of specimens oriented perpendicularly to the lakeshore with their base toward the riparian forest and by the contrasting recruitment trends between consecutive shore sections with different fire histories (Gennaretti, Arseneault & Bégin 2014). Thus, the logs can be used to reconstruct the long term dynamics of the facing riparian forest stands. Subfossil logs that could not be crossdated to the calendar year were discarded from all analyses.

Data analysis

Triplets of consecutive neighbouring plots in the riparian forests were considered for the subsequent analyses so as to obtain 37 and 31 triplets at L18 and L20, respectively (e.g. triplet 1 comprises plots 1, 2 and 3; triplet 2 comprises plots 2, 3 and 4, etc.). Using triplets allowed compiling data within larger and more representative portions of the riparian forests and smoothing out the background noise among plots. Several variables were then developed to characterize the forest structure and composition of each triplet (Table 1). When two variables were strongly correlated ($r > 0.8$ or < -0.8), one of them was excluded from the subsequent analyses to limit redundancy (Tables S3 and S4). In this way, "Nliv", "Ntot", "F%reg", "BAliv" and "a" were excluded for L18, while "Nliv", "Ntot", "Nliv6", "BAliv" and "a" where excluded for L20. Correlation between "F%" and "Ndead" was slightly higher than 0.8 at L18, but the two variables were retained as their association is not straightforward.

We performed a Principal Component Analysis (PCA) on the triplets of each lake using our set of descriptive variables. All variables were scaled to unit variance. Only principal components with eigenvalues > 1 were retained (Figs 2 and S2 to S5). A hierarchical cluster analysis was subsequently used to detect associations among triplets at each site based on a Euclidean distance matrix obtained from the component scores scaled so as to have variance proportional to their corresponding eigenvalues. Ward's method was applied in clustering. Homogeneous clusters of triplets were then defined for each lake by cutting dendrograms at distance two (Figs S6 and S7). Each riparian forest plot was finally considered as a part of a cluster if the majority of the triplets in which it was included belonged to that cluster. Two plots (one per lake) could not be assigned to any cluster because their corresponding triplets were equally distributed amongst more than one cluster (Fig. 1).

Crossdated spruce and fir logs were subsequently assigned to the nearest riparian plot and then to the corresponding cluster. To limit data fragmentation along the

shoreline, logs assigned to a series of less than three contiguous plots belonging to the same cluster were discarded from the subsequent analyses (i.e. logs facing plots 9 and 10 at L18, and those facing plot 1 at L20; Fig. 1). Cluster 3 at L18 was also divided into two sub-clusters for the analysis of the subfossil logs as, even if today the riparian plots are characterized by a similar forest, their histories showed some differences (cluster 3A contains logs assigned to plots 6-8 and 11-15, while cluster 3B contains those assigned to plots 24-32; see Figs 1 and 3).

Tree-ring dating of charred subfossil logs (see Fig. S8 for some examples), along with concurrent variations of log abundance, allowed us to determine when wildfires affected the riparian forest of each cluster during the last millennium. Each identified fire was assigned to the date of its most recent evidence considering that some subfossil logs may have lost their charred marks and may have been more or less eroded (i.e. fire evidences are the outermost tree-ring dates of charred logs or of subfossil logs in proximity of a charred specimen and preceding a clear discontinuity in the temporal trend of outermost tree-ring dates). A detailed analysis of more than 1600 logs from five lakes indicates that our estimated fire dates may precede the actual dates by a few years because an average of three outermost tree-rings per century is lost through decay per log (Gennaretti, Arseneault & Bégin 2014). The relative severity of the wildfires was evaluated from their impacts on the number of subfossil logs produced by the riparian forest and preserved in the adjacent littoral zone. A typical response to fire includes a peak in subfossil log recruitment (this peak is not always detectable when several centuries have elapsed since the fire and many logs are already decomposed), followed by a recruitment reduction as trees grown up after fire have to reach a minimum height before being available to generate subfossil logs from their upper stem portions (Gennaretti, Arseneault & Bégin 2014). Here, a complete interruption or a strong reduction of log recruitment for several years after a fire were used as an indicator that most of the trees were killed and that the stand developed as an even-aged postfire cohort.

The subfossil records of both sites were then divided into discrete fire-free intervals delineated by the estimated wildfire dates. Three fire-free intervals were identified at both sites: AD 682-1251, 1251-1624 and 1729-1994 at L18, and 728-1207, 1207-1592 and 1592-2002 at L20. The recruitment rates of subfossil logs (number recruited per 100 years per 100 m of shoreline based on their outermost tree-ring dates) were computed for each of these intervals in order to compare the relative openness of the riparian forest cover between clusters at each site (Figs 3 and 4). Assuming that the number of subfossil logs produced by the riparian forest in a cluster is directly related to the density of large riparian trees during a fire-free interval which in turn is influenced by fire occurrence and severity, regular and high recruitment rates were attributed to a dense mature forest cover and low rates to an open cover. However, because subfossil logs progressively decay, these recruitment rates fade out when moving backward in time and cannot be compared among different fire-free intervals. To allow this comparison, we used the presence at each site of a cluster that has escaped fire over the entire study period (see results). For each site, we standardized the number of subfossil logs that were living each year per 100 m of shoreline in each fire-affected cluster by dividing it with the number of logs in the cluster that had escaped fire. These ratios show the relative openness of the riparian forest cover among fire-free intervals and clusters (Fig. 5).

The smoothed average age-related growth curves of the subfossil logs recruited during different fire-free intervals were compared among clusters and fire-free intervals at each lake. For each interval and cluster, all individual ring width series were aligned according to cambial age and averaged. Firs and specimens with missing pith were discarded. A spline with a 50% frequency cut-off and time-varying response (starting from 10 years and increasing by one each year; Melvin et al. 2007) was then used as smoothing algorithm to generate the smoothed growth curves. These growth curves allowed us to detect the most important temporal and spatial shifts of riparian forest growth in response to disturbances and climate change (Figs 6, 7, S9 and S10).

2.2.4 Results

Partitioning of the present-day riparian forest

Principal component and cluster analyses identified three and two clusters of homogeneous riparian forest stands at L18 and L20, respectively (Figs 1 and 2). At L18, the first principal component (31% of the variance explained) differentiated cluster 1 from clusters 2 and 3, based on its higher percentages of fir, higher densities of snags and stumps, and higher densities of living trees, especially of small size classes (Figs 2 and S2 and Table 2). The second principal component (24% of the variance explained) differentiated cluster 3 from clusters 1 and 2, based on its lower densities of large-sized trees (≥ 12 cm DBH) and higher densities of saplings and seedlings that together influenced the coefficient "b" of the power function models (Figs 2 and S2 and Table 2). Compared to cluster 1 and 3, cluster 2 displayed intermediate characteristics and lower densities of saplings and seedlings. At L20, the two clusters differed mainly by their first principal component scores (35% of the variance explained). In comparison to cluster 2, cluster 1 was associated with higher fir percentages, higher basal areas of dead trees and higher densities of regeneration, dead trees and living trees ≥ 2 cm DBH (Figs 2 and S3 and Table 2).

Past fires, subfossil recruitment and riparian tree density

At least four wildfires of varying severities affected the riparian forest at L18 during the last millennium (Fig. 3). Cluster 1, which is today characterized by denser forest with more abundant fir, was clearly less severely affected by these wildfires than clusters 2 and 3, and escaped stand-replacing fires over at least the last 1200 years. A fire event completely interrupted the recruitment of subfossil logs in clusters 2 and 3B and strongly reduced the recruitment in cluster 3A at AD 1251, indicating severe tree mortality in the riparian environment. The fire may have partially burned the forest of cluster 1, where the recruitment of subfossil logs slightly decreased, but several

individuals survived. Because fires generally reduce the recruitment of subfossil logs for about 120 years in these boreal lakes (Gennaretti, Arseneault & Bégin 2014), the interruption that lasted for at least 200 years at clusters 2 and 3 after the AD 1251 event suggests the occurrence of a second fire before about AD 1400. This presumed fire most likely killed trees established after AD 1251 before they could become high enough to generate subfossil logs with diameters ≥ 4 cm. Three subsequent closely spaced fires burned across the riparian forest of clusters 2 and 3 during the 17th and the first part of the 18th century. The AD 1624 fire was identified from charred subfossil logs preceding a discontinuity in the temporal trend of innermost tree-ring dates (i.e. several riparian trees established after this fire), while the AD 1674 and 1729 fires were identified from charred subfossil logs and discontinuities in the trend of outermost tree-ring dates (i.e. several riparian trees died during these fires; see the cluster 2 in Fig. 3). All these wildfires were less severe than the AD 1251 fire, as the recruitment of subfossil logs was altered but not interrupted. Despite the fact that a charred log with an outermost tree-ring in 1684 was found at the boundary between clusters 1 and 2, the recruitment of subfossil logs remained high and constant in cluster 1, indicating uninterrupted forest development and negligible fire impact.

Although all clusters at L18 exhibited similar recruitment rates of subfossil logs prior to the AD 1251 fire, cluster 1, which escaped severe fire disturbances during the last millennium, has been subsequently characterized by much higher and constant recruitment rates than clusters 2 and 3 (Fig. 3). This suggests that the density of riparian trees was similar among clusters before AD 1251 and that the fires produced a long-lasting decrease of stem density at clusters 2 and 3. These two clusters seem to have diverged from each other following the fires of the 17th and 18th centuries because cluster 2 has exhibited higher recruitment rates than cluster 3 since the mid 18th century (6.5 vs 2.4 to 2.9 logs per 100 years per 100 meter of shoreline). These higher rates are consistent with the higher present-day density of large-sized trees (≥ 12 cm DBH) in the riparian plots of cluster 2 as compared to cluster 3 (Table 2). At cluster 3B, the low

recruitment rate of the last two centuries can in part be explained by a tree mortality peak, which can also be perceived at cluster 1, and which coincides with the large Tambora volcanic eruption in AD 1815 (Figs 3 and 8).

Fires were less frequent at L20 than at L18, as we detected only two fire events over the last millennium (Fig. 4). The only fire confirmed by charred marks on the logs occurred at AD 1592 and almost completely burned the riparian forest of cluster 2, as based on a severe reduction of subfossil log recruitment. The fire probably stopped near plot 20, at the border between clusters 1 and 2, where we found a charred subfossil log. The remaining plots of cluster 1 escaped the fire, as indicated by the very regular and high recruitment rates of subfossil logs. A peak of tree mortality in cluster 2 most likely indicates a previous mid-severity fire at about AD 1207, even if no charred logs were discovered.

Similarly to L18, dense present-day forest stands with high fir percentages at L20 have escaped stand-replacing fires over the last millennium (over at least the last 1400 years at the cluster 1 of L20). Recruitment rates of subfossil logs have always been higher at cluster 1 than at cluster 2, denoting that stem density has probably been higher at cluster 1 over the entire time period covered by our study (Fig. 4).

The yearly ratios of subfossil log abundance in burned relative to unburned clusters at each lake indicate that each fire triggered a specific trajectory of stem density in the burned riparian clusters with varying postfire density alterations and rates of recovery (Fig. 5). These effects included prompt and complete recovery to pre-fire stem density (e.g. cluster 2 at L20 after the AD 1592 fire), full but progressive recovery over several centuries (e.g. cluster 2 at L20 after the AD 1207 fire), extremely slow and partial recovery (e.g. clusters 2 and 3A at L18 following the two successive AD 1251 and ~14th century fires), persistent shift to low stem densities (e.g. cluster 3B at L18 following the two successive AD 1251 and ~14th century fires), as well as increased

stem densities relative to pre-fire conditions (e.g. cluster 2 at L18 after the three fires between AD 1624 and 1729).

Age-related growth curves of the subfossil logs

The analysis of the average growth curves of the subfossil logs showed important climate- and fire-induced impacts on the riparian forest growth during the last millennium. Fires reduced riparian stem density and, as a consequence, the juvenile growth of trees (i.e. for young cambial ages) was faster in the affected riparian clusters than in the unburned ones (i.e. clusters 1 of both sites) during the subsequent fire-free intervals (see the juvenile growth of the subfossil logs of clusters 2 or 3 in comparison to that of logs of cluster 1 in Figs 6 and 7). Furthermore, the average growth curves showed that, in clusters that escaped severe fire disturbances over the entire time period covered by the study (i.e. clusters 1 of both sites), tree grew faster during medieval times than afterward, suggesting the influence of a warmer climate (Figs S9 and S10).

2.2.5 Discussion

Fire vs. trajectories of forest structure and composition

The long-term perspective, along with the high spatial and temporal resolutions provided by this study, allowed the verification of whether or not variations in the present-day structure and composition of contiguous riparian forest stands in the Eastern Canadian taiga correspond to their respective fire histories during the last millennium. Our multivariate analysis of the current riparian forest vegetation revealed three and two homogeneous sections (i.e. clusters) with different forest compositions and structures at L18 and L20, respectively, even if these riparian forests only face 1170 and 990 m of lake shore (Figs 1 and 2 and Table 2). The dendrochronological analysis of the subfossil logs collected in the littoral zone facing these riparian sections confirmed that these clusters experienced site-specific fire histories over the last millennium that locally

influenced forest composition, tree density and tree growth (Figs 3 to 7), thus shaping the present-day landscape diversity. All the riparian sections that were affected by fire during the last millennium are today characterized by more open forests with less dead wood and lower percentages of balsam fir than the unburned stands (Table 2), even despite the most recent fire occurring about 300 to 400 years ago. Consequently, our results support the hypothesis that fire impacts may persist for several centuries in the Eastern Canadian taiga and that present-day landscapes are the outcome of the progressive fire-induced breakup (i.e. forest cover opening and balsam fir exclusion) of a previously closed-crown spruce-fir vegetation zone (Sirois 1997; Arseneault & Sirois 2004; Ali et al. 2008; de Lafontaine & Payette 2010).

An important result of this study is the large variability in the postfire forest structure trajectories in the riparian environment over the last millennium. Although it is generally assumed that black spruce is a fire-adapted species due to its serotinous cones, our results suggest that the classical model of postfire forest recovery in black spruce forests (i.e. fast recovery to pre-fire stem densities) is over-simplistic because each fire can trigger a specific forest structure trajectory characterized by a different stem density reduction and a different rate of recovery. Despite the fact that an increase in stem density relative to pre-fire conditions occurred at the cluster 2 of L18 following the three low to mid-severity fires between AD 1624 and 1729, all other fires decreased stem densities or maintained the low densities triggered by previous fires and the rates of recovery were extremely variable (Fig. 5). All time periods of fire-induced low stem densities reconstructed from low recruitment rates of subfossil logs (i.e. AD 1207-1592 at cluster 2 of L20 and AD 1251-1994 at clusters 2 and 3 of L18) are confirmed by concomitant faster juvenile growth of spruce trees in burned clusters (Figs 6 and 7). Indeed, black spruce grows faster in open postfire woodlands than in dense postfire or old-growth forests stands due to less intense competition (Fourrier, Pothier & Bouchard 2013).

Although we could not identify the processes that have influenced the variability of the postfire forest trajectories, several circumstances may have contributed to hamper rapid postfire recovery to pre-fire stem densities, especially in the taiga context where severe climate conditions may limit spruce growth and reproduction and may led to significant tree mortality events (Bond-Lamberty et al. 2014). The most important conditions that must be met to permit dense postfire spruce regeneration include a time interval of at least 50 years since the previous fire to allow an adequate seed availability in the spruce stand (Viglas, Brown & Johnstone 2013), an annual heat sum of at least 500 growing degree-days above 5°C in the years prior the fire event to allow seed maturation (Sirois 2000), a fire severity allowing the survival of a sufficient number of seeds (Arseneault 2001), and the occurrence of favourable postfire seedbeds on mineral soil or unburned Sphagnum mosses (Greene et al. 2004; Boiffin & Munson 2013). The failure of any of these requirements may result in a postfire reduction of spruce density relative to pre-fire conditions, causing the development of an open stand (Sirois & Payette 1991; Girard, Payette & Gagnon 2008). For example, high fire severity and a short time interval between the severe AD 1251 fire and the subsequent supposed fire prior to AD 1400 may explain the low stem densities that have characterized the last 750 years in the clusters 2 and 3 of L18 (Fig. 5). Unfavourable conditions for seed maturation during the Little Ice Age may also have contributed to these low postfire tree densities. Once such open stands are initiated due to insufficient postfire regeneration, tree density is likely to remain low until at least the next fire because a continuous lichen mat subsequently develops at the soil surface and inhibits seedling establishment (Morneau & Payette 1989).

Contrary to black spruce, balsam fir does not retain its seeds in serotinous cones and thus must re-establish from fire survivors outside burned areas (Asselin, Fortin & Bergeron 2001). Consequently, balsam fir abundance and dominance increase with decreasing fire recurrence across its distribution range. Paleoecological studies have already suggested that balsam fir migrated northward more than 5000 years ago under

the low-frequency fire regime of the mid-Holocene (Carcaillet & Richard 2000) and that an increased fire frequency subsequently reduced its abundance in the taiga of Eastern Canada (Sirois 1997; Arseneault & Sirois 2004; Boucher, Arseneault & Hétu 2006; Ali et al. 2008; de Lafontaine & Payette 2010). Indeed, subfossil trunks buried in peat and alluvial deposits revealed that balsam fir occurred much more frequently prior to 4000 BP than afterward (Sirois 1997; Arseneault & Sirois 2004; Boucher, Arseneault & Hétu 2006). At both of our study sites, all riparian clusters that experienced at least one severe fire exhibited low fir percentages (0-8%) and all clusters with abundant fir (i.e. more than 20%; Table 2) had escaped fire or were only marginally affected by fire over remarkably long time intervals of more than 1200 years (Figs 3 and 4). This exclusive and systematic high fir abundance in the present-day unburned forest remnants strongly supports the idea that balsam fir is out of phase with the late Holocene fire regime and the associated climate. If balsam fir had been in equilibrium with the fire regime, then the time intervals of 300-400 years since the last fires in the fire-affected clusters of L18 and L20 should have permitted its recovery. Indeed, mature fir individuals disperse abundant seeds each few years and fir seedlings can establish under the spruce canopy as they are very shade tolerant (Frank 1990).

Our results did not allow the reconstruction of past variations in fir abundance from direct field evidence because very few firs were found among the subfossil logs (five firs at L18 and 57 at L20 of which only 16 could be crossdated). This low abundance of firs and their low dating rate are due to the fact that only high dominant trees near the shoreline can generate persistent subfossil samples with a sufficient number of tree-rings for the crossdating procedure (Gennaretti, Arseneault & Bégin 2014), whereas, at our sites, fir trees are smaller and less abundant within the first line of trees along the shoreline compared to spruce. However, most subfossil firs (80% at L18 and 72% at L20) faced plots of the unburned clusters 1, supporting the idea that fir has persisted in unburned refugia.

Climate change impacts

Despite the fact that fire disturbance has been the dominant driver of change in forest stem density and growth over the past millennium, climate variability was also important. Recent climate reconstructions indicate that a well-defined Medieval Climate Anomaly occurred at about AD 900-1250 in the North American taiga and forest tundra, followed by a progressive decrease of summer temperatures down to the coldest period of the last millennium, which occurred during the first half of the 19th century (Viau, Ladd & Gajewski 2012; Pages 2k Consortium 2013). A reconstruction of summer temperatures from tree-ring widths of more than 1700 subfossil logs collected in six lakes of our study area, including L18 and L20 (Gennaretti et al. unpublished data), closely reproduces these trends, also indicating that the cold period of the early 1800's was triggered by the successive AD 1809 (unknown volcano) and AD 1815 (Tambora) volcanic eruptions (see also Fig. 8). Both of these opposed climate anomalies influenced forest dynamics at our study sites. At the unburned clusters (i.e. cluster 1), where age-related growth trends have not been disturbed by fire events and consequent changes in forest density, spruce trees grew faster during the Medieval Anomaly than afterward, reflecting its warmer climate (Figs S9 and S10). This period was also characterized by relatively high stem density at all clusters of both sites (Fig. 5). However, our data do not allow the differentiation of the role of the warmer climate or of the possible absence of previous fire disturbances on these high stem densities for this older period. At the other extreme of the climatic gradient, the precise correspondence between the AD 1809-1815 eruptions, a sharp tree growth reduction, and a peak in riparian tree mortality at our sites (Fig. 8), confirms that volcanoes forced this cold episode and influenced forest dynamics. At L18, this episode of tree mortality was less severe in cluster 2 than in clusters 1 and 3 (Fig. 3), possibly reflecting its more sheltered position along concave lakeshore segments (Fig. 1). At L18, the subsequent decrease of subfossil log recruitment over the 1820-1870 time period also suggests that, at this site, the most

vulnerable riparian trees died rapidly in less than about 10 years after the two eruptions, thus attenuating later mortality (Fig. 8).

Long-term fire imprints on landscape diversity

Our study provides a long-term perspective that helps explain how fire disturbance and time since fire have shaped the present-day landscape diversity in the Eastern Canadian taiga, in the context of the generalized decrease in conifer stem density that has characterized the northern boreal zone over the last 600-900 years (Payette & Gagnon 1985; Sirois & Payette 1991; Payette & Morneau 1993; Lavoie & Sirois 1998; Girard, Payette & Gagnon 2008; Payette, Filion & Delwaide 2008). The high variability in the postfire stem density reduction and in its rate of recovery displayed by our riparian clusters since the first detected fire at about AD 1207 (Fig. 5) suggests that present-day landscapes (see Fig. S1) are mosaics of forest patches representing different times since fire along specific postfire forest structure trajectories. In the taiga, open woodlands would have experienced at least one severe fire since the Medieval Climate Anomaly, often reducing tree densities or maintaining low densities triggered by previous fires and excluding balsam fir from stands where the species was still present. In addition some important implications can be deduced from the fact that present-day forest stands reflect the past fire history even if the last fire occurred at least 300-400 years ago. First, it indicates that several centuries are needed for stem density and forest composition to converge between forest stands that experienced or escaped fire. Second, it shows that only a few fires per millennia are sufficient to maintain open woodlands in the Eastern Canadian taiga. Third, it proves that the taiga contains two types of old-growth forest stands (i.e. some centuries old) on well-drained soils (dense vs open old-growth forest stands) depending on whether or not they burned during the last 800 years. Lastly, our results show that, under the late Holocene climate and its fire regime, balsam fir can persist only in the rare, residual, unburned forest patches.

It has already been observed that the long-term absence of severe disturbances can lead to the decline of forest ecosystems and to the reduction of forest biomass in several biomes (Wardle, Walker & Bardgett 2004). In this study, we observed rather that sites that did not burn during the last 1200 years had higher stem density, tree basal area and tree species diversity than sites that burned 2-5 times over the same time period. Even if these dense stands are relict from previous more favourable climate conditions, they nevertheless indicate that relatively high stem densities can be maintained over at least a millennium in absence of fire. Extrapolating the recent regional burn rate of about 0.2% per year (based on the 1980-2010 fire data; Boulanger et al. 2012) to the last millennium, and assuming that stand age distribution is negative exponential (Johnson 1992), stands older than 1000 years would represent only about 15% of the present-day landscape. We conclude that the forest decline stage linked to the absence of disturbances is uncommon in the northern taiga of Eastern Canada.

The increase in fire occurrence and area burned that is expected for the Eastern Canadian taiga over the 21th century (Boulanger et al. 2013) is likely to impact landscape diversity in our study area. Our data suggest that higher burn rates will accelerate the regression of balsam fir and will increase the abundance of more open woodlands, unless climactic thresholds that once allowed the development of dense spruce-fir stands are surpassed improving the forest regeneration processes (Sirois, Bonan & Shugart 1994). In addition, considering that the jack pine eastern range limit is located only 10 km west of site L18, and that pine has faster juvenile growth, earlier sexual maturity, and higher seed retention in serotinous cones than black spruce (Rudolph & Laidly 1990), jack pine is likely to expand into our study region with an increased fire frequency. If a pine expansion occurs, then open spruce woodlands will be likely shift to denser pine-spruce stands after fire with pine abundance increasing after repeated fires, as observed within the current pine range limit (Lavoie & Sirois 1998; Le Goff & Sirois 2004).

2.2.6 Acknowledgments

The authors wish to thank Julia Autin, Yves Bouthillier, Pierre-Paul Dion, Sébastien Dupuis, Benjamin Dy, Joëlle Marion and Antoine Nicault for field and laboratory assistance, Aurore Catalan for technical assistance and Luc Sirois for its comments on the paper. This research is a contribution of the ARCHIVES project and was financially supported by NSERC, Hydro-Quebec, Ouranos, ArcticNet, the EnviroNorth training program and the Centre for Northern Studies.

2.2.7 Data Accessibility

All data from the manuscript will be archived in "Figshare" (the DOI is still to be obtained).

2.2.8 References

Ali, A. A., Asselin, H., Larouche, A. C., Bergeron, Y., Carcaillet, C. & Richard, P. J. H. (2008) Changes in fire regime explain the Holocene rise and fall of Abies balsamea in the coniferous forests of western Québec, Canada. *Holocene*, **18,** 693-703.

Arseneault, D. (2001) Impact of fire behavior on postfire forest development in a homogeneous boreal landscape. *Canadian Journal of Forest Research*, **31,** 1367-1374.

Arseneault, D., Boucher, E. & Bouchon, E. (2007) Asynchronous forest-stream coupling in a fire-prone boreal landscape: insights from woody debris. *Journal of Ecology*, **95,** 789-801.

Arseneault, D., Dy, B., Gennaretti, F., Autin, J. & Bégin, Y. (2013) Developing millennial tree ring chronologies in the fire-prone North American boreal forest. *Journal of Quaternary Science*, **28,** 283-292.

Arseneault, D. & Sirois, L. (2004) The millennial dynamics of a boreal forest stand from buried trees. *Journal of Ecology*, **92,** 490-504.

Asselin, H., Fortin, M. J. & Bergeron, Y. (2001) Spatial distribution of late-successional coniferous species regeneration following disturbance in southwestern Québec boreal forest. *Forest Ecology and Management*, **140,** 29-37.

Boiffin, J. & Munson, A. D. (2013) Three large fire years threaten resilience of closed crown black spruce forests in eastern Canada. *Ecosphere*, **4,** art56.

Bond-Lamberty, B. & Gower, S. T. (2008) Decomposition and fragmentation of coarse woody debris: Re-visiting a boreal black spruce chronosequence. *Ecosystems*, **11,** 831-840.

Bond-Lamberty, B., Peckham, S. D., Ahl, D. E. & Gower, S. T. (2007) Fire as the dominant driver of central Canadian boreal forest carbon balance. *Nature*, **450,** 89-92.

Bond-Lamberty, B., Rocha, A. V., Calvin, K., Holmes, B., Wang, C. & Goulden, M. L. (2014) Disturbance legacies and climate jointly drive tree growth and mortality in an intensively studied boreal forest. *Global Change Biology*, **20,** 216-227.

Boucher, É., Arseneault, D. & Hétu, B. (2006) Late Holocene development of a floodplain along a small meandering stream, northern Québec, Canada. *Geomorphology*, **80,** 267-281.

Boulanger, Y., Gauthier, S., Burton, P. J. & Vaillancourt, M. A. (2012) An alternative fire regime zonation for Canada. *International Journal of Wildland Fire*, **21,** 1052-1064.

Boulanger, Y., Gauthier, S., Gray, D. R., Le Goff, H., Lefort, P. & Morissette, J. (2013) Fire regime zonation under current and future climate over eastern Canada. *Ecological Applications*, **23,** 904-923.

Brunbjerg, A. K., Borchsenius, F., Eiserhardt, W. L., Ejrnæs, R. & Svenning, J. C. (2012) Disturbance drives phylogenetic community structure in coastal dune vegetation. *Journal of Vegetation Science,* **23,** 1082-1094.

Carcaillet, C. & Richard, P. J. H. (2000) Holocene changes in seasonal precipitation highlighted by fire incidence in eastern Canada. *Climate Dynamics,* **16,** 549-559.

Carcaillet, C., Richard, P. J. H., Bergeron, Y., Fŕchette, B. & Ali, A. A. (2010) Resilience of the boreal forest in response to Holocene fire-frequency changes assessed by pollen diversity and population dynamics. *International Journal of Wildland Fire,* **19,** 1026-1039.

de Lafontaine, G. & Payette, S. (2010) The Origin and Dynamics of Subalpine White Spruce and Balsam Fir Stands in Boreal Eastern North America. *Ecosystems,* **13,** 932-947.

Esper, J., Cook, E. R., Krusic, P. J., Peters, K. & Schweingruber, F. H. (2003) Tests of the RCS method for preserving low-frequency variability in long tree-ring chronologies. *Tree-ring research,* **59,** 81-98.

Folke, C., Carpenter, S., Walker, B., Scheffer, M., Elmqvist, T., Gunderson, L. & Holling, C. S. (2004) Regime shifts, resilience, and biodiversity in ecosystem management. *Annual Review of Ecology, Evolution, and Systematics,* **35,** 557-581.

Fourrier, A., Pothier, D. & Bouchard, M. (2013) A comparative study of long-term stand growth in eastern Canadian boreal forest: Fire versus clear-cut. *Forest Ecology and Management,* **310,** 10-18.

Frank, R. M. (1990) Abies balsamea (L.) Mill. *Silvics of North America: 1. Conifers; 2. Hardwoods. Agriculture Handbook 654.* (eds R. M. Burns & B. H. Honkala), pp. 26-47. U.S. Department of Agriculture, Forest Service, Washington, DC.

Fraterrigo, J. M. & Rusak, J. A. (2008) Disturbance-driven changes in the variability of ecological patterns and processes. *Ecology Letters,* **11,** 756-770.

Gennaretti, F., Arseneault, D. & Bégin, Y. (2014) Millennial stocks and fluxes of large woody debris in lakes of the North American taiga. *Journal of Ecology*, **102**, 367–380.

Girard, F., Payette, S. & Gagnon, R. (2008) Rapid expansion of lichen woodlands within the closed-crown boreal forest zone over the last 50 years caused by stand disturbances in eastern Canada. *Journal of Biogeography,* **35,** 529-537.

Greene, D. F. & Johnson, E. A. (1999) Modelling recruitment of Populus tremuloides, Pinus banksiana, and Picea mariana following fire in the mixedwood boreal forest. *Canadian Journal of Forest Research,* **29,** 462-473.

Greene, D. F., Noël, J., Bergeron, Y., Rousseau, M. & Gauthier, S. (2004) Recruitment of Picea mariana, Pinus banksiana, and Populus tremuloides across a burn severity gradient following wildfire in the southern boreal forest of Quebec. *Canadian Journal of Forest Research,* **34,** 1845-1857.

Harvey, B. J. & Holzman, B. A. (2014) Divergent successional pathways of stand development following fire in a California closed-cone pine forest. *Journal of Vegetation Science*, **25**, 88-99.

He, H. S., Hao, Z., Larsen, D. R., Dai, L., Hu, Y. & Chang, Y. (2002) A simulation study of landscape scale forest succession in northeastern China. *Ecological Modelling*, **156,** 153-166.

Johnson, E. A. (1992) *Fire and vegetation dynamics: studies from the North American boreal forest.* Cambridge University Press; Cambridge Studies in Ecology.

Johnstone, J. F., Hollingsworth, T. N., Chapin, F. S. & Mack, M. C. (2010) Changes in fire regime break the legacy lock on successional trajectories in Alaskan boreal forest. *Global Change Biology*, **16,** 1281-1295.

Lavoie, L. & Sirois, L. (1998) Vegetation Changes Caused by Recent Fires in the Northern Boreal Forest of Eastern Canada. *Journal of Vegetation Science,* **9,** 483-492.

Le Goff, H. & Sirois, L. (2004) Black spruce and jack pine dynamics simulated under varying fire cycles in the northern boreal forest of Quebec, Canada. *Canadian Journal of Forest Research,* **34,** 2399-2409.

Melvin, T. M., Brifffa, K. R., Nicolussi, K. & Grabner, M. (2007) Time-varying-response smoothing. *Dendrochronologia*, **25,** 65-69.

Morneau, C. & Payette, S. (1989) Postfire lichen-spruce woodland recovery at the limit of the boreal forest in northern Quebec. *Canadian Journal of Botany,* **67,** 2770-2782.

Newbery, D. M., Van Der Burgt, X. M., Worbes, M. & Chuyong, G. B. (2013) Transient dominance in a central african rain forest. *Ecological Monographs,* **83,** 339-382.

Pages 2k Consortium (2013) Continental-scale temperature variability during the past two millennia. *Nature Geoscience,* **6,** 339-346.

Payette, S., Delwaide, A., Schaffhauser, A. & Magnan, G. (2012) Calculating long-term fire frequency at the stand scale from charcoal data. *Ecosphere,* **3,** art59.

Payette, S., Filion, L. & Delwaide, A. (2008) Spatially explicit fire-climate history of the boreal forest-tundra (Eastern Canada) over the last 2000 years. *Philosophical Transactions of the Royal Society B: Biological Sciences,* **363,** 2301-2316.

Payette, S. & Gagnon, R. (1985) Late Holocene deforestation and tree regeneration in the forest-tundra of Québec. *Nature,* **313,** 570-572.

Payette, S. & Morneau, C. (1993) Holocene Relict Woodlands at the Eastern Canadian Treeline. *Quaternary Research,* **39,** 84-89.

Rudolph, T. D. & Laidly, P. R. (1990) Pinus banksiana Lamb. *Silvics of North America: 1. Conifers; 2. Hardwoods. Agriculture Handbook 654.* (eds R. M. Burns & B. H. Honkala), pp. 555-586. U.S. Department of Agriculture, Forest Service, Washington, DC.

Saucier, J.-P., Grondin, P., Robitaille, A. & Bergeron, J.-F. (2003) *Zones de végétation et domaines bioclimatiques du Québec.* Gouvernement du Québec, Ministère des Ressources naturelles, de la Faune et des Parcs, Québec.

Senici, D., Lucas, A., Chen, H. Y. H., Bergeron, Y., Larouche, A., Brossier, B., Blarquez, O. & Ali, A. A. (2013) Multi-millennial fire frequency and tree abundance differ between xeric and mesic boreal forests in central Canada. *Journal of Ecology,* **101,** 356-367.

Sirois, L. (1995) Initial phase of postfire forest regeneration in two lichen woodlands of northern Quebec. *Ecoscience,* **2,** 177-183.

Sirois, L. (1997) Distribution and dynamics of balsam fir (Abies balsamea L. Mill.) at its northern limit in the James Bay area. *Ecoscience,* **4,** 340-352.

Sirois, L. (2000) Spatiotemporal variation in black spruce cone and seed crops along a boreal forest - Tree line transect. *Canadian Journal of Forest Research,* **30,** 900-909.

Sirois, L., Bonan, G. B. & Shugart, H. H. (1994) Development of a simulation model of the forest-tundra transition zone of northeastern Canada. *Canadian Journal of Forest Research*, **24**, 697-706.

Sirois, L. & Payette, S. (1991) Reduced postfire tree regeneration along a boreal forest-forest- tundra transect in northern Quebec. *Ecology,* **72,** 619-627.

Stocks, B. J., Mason, J. A., Todd, J. B., Bosch, E. M., Wotton, B. M., Amiro, B. D., Flannigan, M. D., Hirsch, K. G., Logan, K. A., Martell, D. L. & Skinner, W. R. (2003) Large forest fires in Canada, 1959-1997. *Journal of Geophysical Research D: Atmospheres,* **108**.

Vanderwel, M. C., Coomes, D. A. & Purves, D. W. (2013) Quantifying variation in forest disturbance, and its effects on aboveground biomass dynamics, across the eastern United States. *Global Change Biology,* **19,** 1504-1517.

Viau, A. E., Ladd, M. & Gajewski, K. (2012) The climate of North America during the past 2000 years reconstructed from pollen data. *Global and Planetary Change*, **84-85,** 75-83.

Viglas, J. N., Brown, C. D. & Johnstone, J. F. (2013) Age and size effects on seed productivity of northern black spruce. *Canadian Journal of Forest Research*, **43,** 534-543.

Villnäs, A., Norkko, J., Hietanen, S., Josefson, A. B., Lukkari, K. & Norkko, A. (2013) The role of recurrent disturbances for ecosystem multifunctionality. *Ecology*, **94,** 2275-2287.

Wardle, D. A., Walker, L. R. & Bardgett, R. D. (2004) Ecosystem properties and forest decline in contrasting long-term chronosequences. *Science*, **305,** 509-513.

Zwicke, M., Alessio, G. A., Thiery, L., Falcimagne, R., Baumont, R., Rossignol, N., Soussana, J. F. & Picon-Cochard, C. (2013) Lasting effects of climate disturbance on perennial grassland above-ground biomass production under two cutting frequencies. *Global Change Biology*, **19,** 3435-3448.

2.2.9 Tables

Table 2-1. Variables used to describe present-day forest structure and composition in triplets of sampling plots at the sites L18 and L20

Variable ID	Unit	Description
Nliv	No. ha^{-1}	Density of living trees comprising saplings and seedlings
Ntot	No. ha^{-1}	Density of living trees comprising saplings and seedlings plus snags and stumps
Nreg	No. ha^{-1}	Density of saplings and seedlings
Nliv2	No. ha^{-1}	Density of living trees ≥ 2 cm DBH
Nliv6	No. ha^{-1}	Density of living trees ≥ 6 cm DBH
Nliv12	No. ha^{-1}	Density of living trees ≥ 12 cm DBH
Ndead	No. ha^{-1}	Density of snags and stumps
Ncwd	No. ha^{-1}	Density of coarse woody debris pieces on the floor
BAliv	cm^2 ha^{-1}	Basal area of living trees ≥ 2 cm DBH
MeanBAliv	cm^2 $tree^{-1}$	Average basal area per living tree ≥ 2 cm DBH
BAdead	cm^2 ha^{-1}	Basal area of snags and stumps
MeanBAdead	cm^2 $tree^{-1}$	Average basal area per snag or stump
F%reg	%	Percentage of fir in the sapling and seedling
F%	%	Percentage of fir among living trees ≥ 2 cm DBH
T%	%	Percentage of tamarack among living trees ≥ 2 cm DBH
Age	years	Average minimum stand age of the three plots
a	-	Coefficient "a" of the power function model describing the stand size structure of living trees*
b	-	Coefficient "b" of the power function model*

* $y = a * x^{(-b)}$ where y is the number of individuals per hectare and x is the central value of 2-cm size classes (Tables S1 and S2)

Table 2-2. Description of the riparian forest of each cluster at L18 and L20. Distinguishing traits are in bold. Standard deviations (SD) refer to variability among triplets of sampling plots

	L18			L20	
	Cluster 1 (mean ± SD)	Cluster 2 (mean ± SD)	Cluster 3 (mean ± SD)	Cluster 1 (mean ± SD)	Cluster 2 (mean ± SD)
Nliv (No. ha^{-1})	22578 ± 9255	11671 ± 2640	25806 ± 6088	24393 ± 5432	15396 ± 4337
Ntot (No. ha^{-1})	23778 ± 9103	12171 ± 2714	26457 ± 6120	25671 ± 5672	16135 ± 4370
Nreg (No. ha^{-1})	17889 ± 9083	9225 ± 2367	**23500 ± 5931**	**19964 ± 5156**	12608 ± 4197
Nliv2 (No. ha^{-1})	**4689 ± 435**	2445 ± 758	2306 ± 548	**4429 ± 418**	2788 ± 488
Nliv6 (No. ha^{-1})	**2244 ± 271**	1182 ± 262	1237 ± 308	2036 ± 385	1351 ± 250
Nliv12 (No. ha^{-1})	544 ± 19	482 ± 207	**296 ± 142**	421 ± 103	273 ± 123
Ndead (No. ha^{-1})	**1200 ± 219**	500 ± 166	651 ± 95	**1279 ± 379**	739 ± 166
Ncwd (No. ha^{-1})	811 ± 84	757 ± 335	580 ± 254	610 ± 100	590 ± 116
Baliv (cm^2 ha^{-1})	186942 ± 19140	148115 ± 49150	108277 ± 26050	181739 ± 28759	114771 ± 24030
MeanBAliv (cm^2 $tree^{-1}$)	40 ± 1	67 ± 31	49 ± 13	41 ± 5	41 ± 6
Badead (cm^2 ha^{-1})	108140 ± 16916	67733 ± 17550	69507 ± 21521	**104133 ± 24791**	60797 ± 19972
MeanBAdead (cm^2 $tree^{-1}$)	90 ± 2	142 ± 37	109 ± 38	85 ± 20	85 ± 27
F%reg (%)	3 ± 3	0 ± 0	0 ± 0	**42 ± 21**	9 ± 16
F% (%)	**22 ± 4**	1 ± 2	0 ± 0	**28 ± 13**	8 ± 9
T% (%)	0 ± 0	2 ± 2	1 ± 1	1 ± 2	2 ± 1
Age (years)	245 ± 32	226 ± 15	**252 ± 13**	217 ± 15	207 ± 17
a	17871 ± 9090	9220 ± 2367	23497 ± 5932	19949 ± 5159	12597 ± 4201
b	2.0 ± 0.4	2.2 ± 0.5	**3.1 ± 0.5**	2.2 ± 0.2	2.2 ± 0.4

2.2.10 Figures

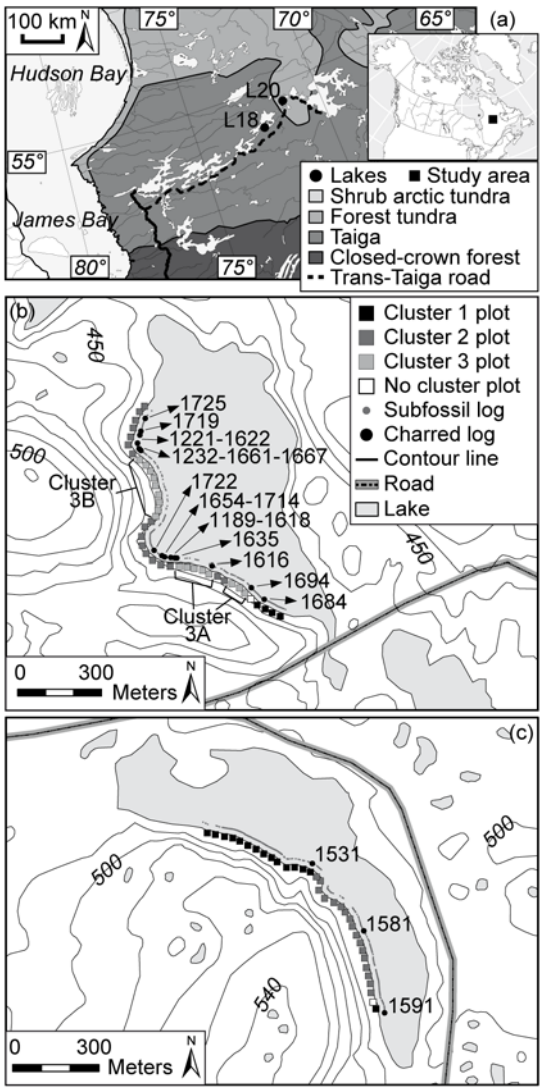

Fig. 2-1. Map of the study area in the northern taiga of Eastern Canada (a) and of lake L18 (b) and L20 (c) with plots assigned to the corresponding cluster. In b and c, the outermost tree-ring dates of charred subfossil logs are also shown. If two or more charred logs are facing the same plot, their outermost tree-ring dates are separated by a minus sign.

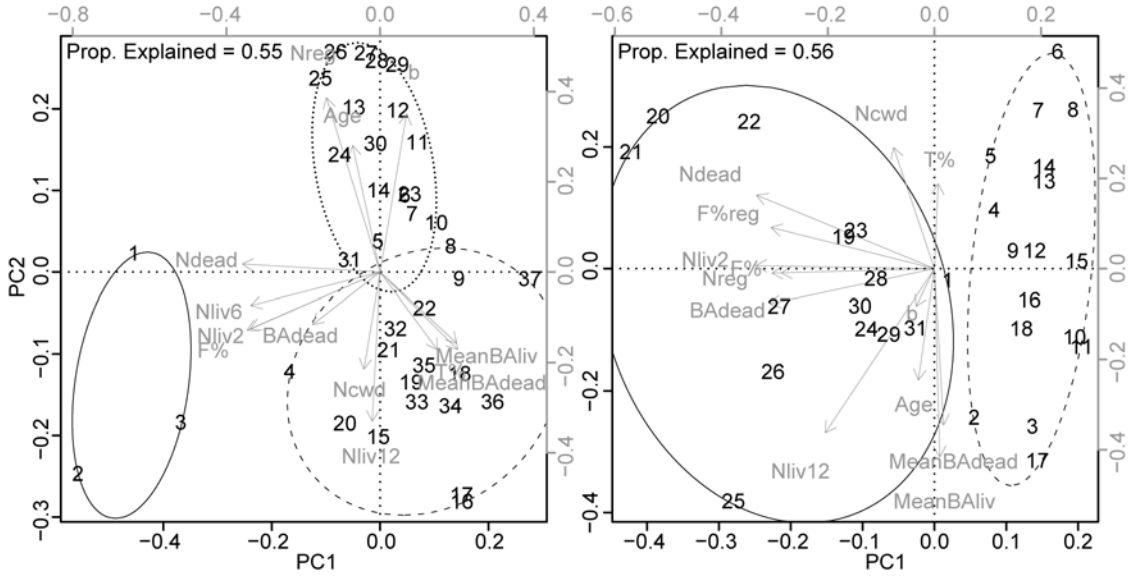

Fig. 2-2. Biplots of the first two principal components of the L18 (left) and L20 (right) PCAs. Variables are in grey and triplets of plots are in black. Triplets belonging to the same cluster are enclosed in minimum spanning ellipses (solid: cluster 1; dashed: cluster 2; dotted: cluster 3).

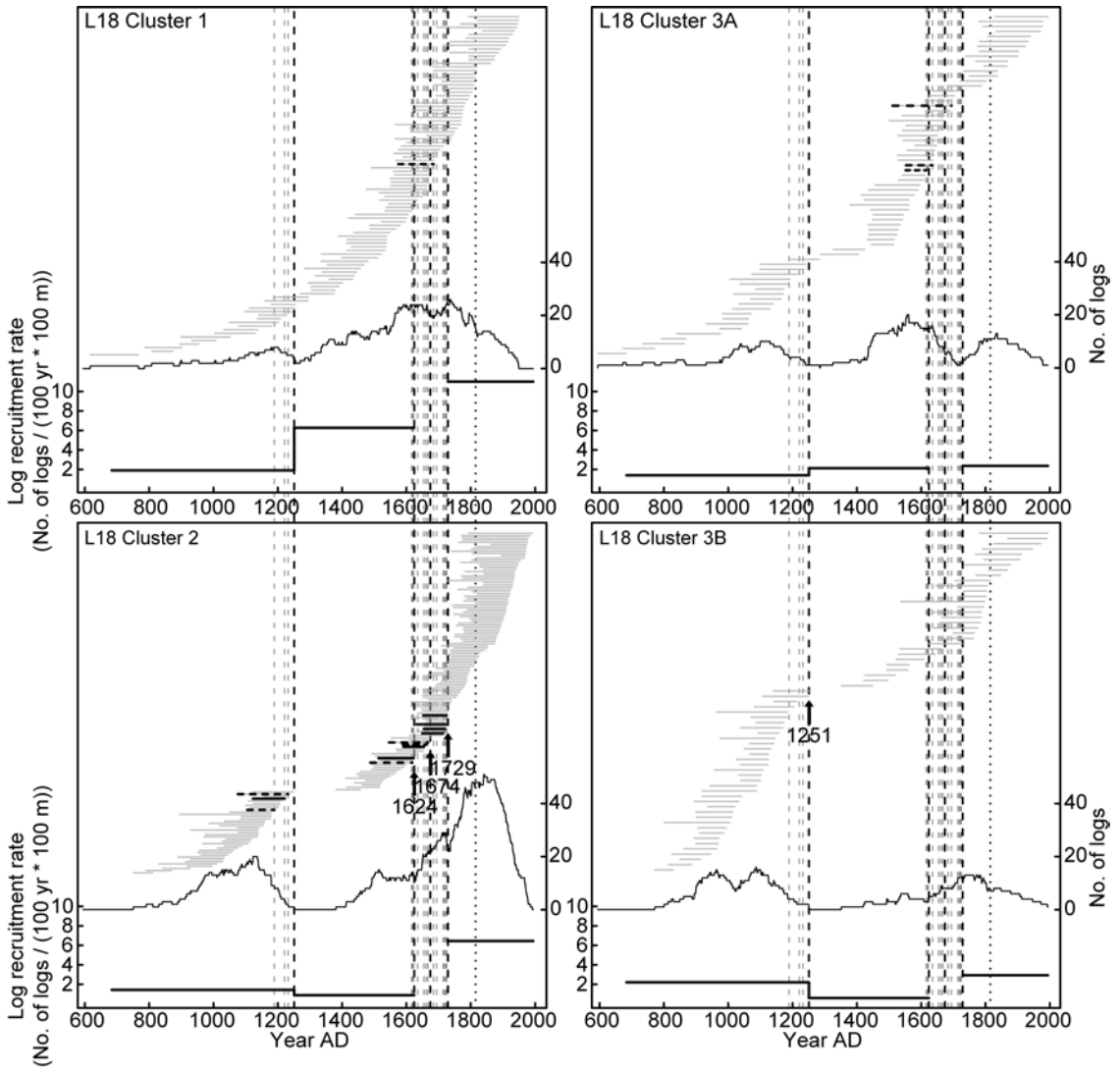

Fig. 2-3. Life spans, abundance and recruitment rate of L18 subfossil logs crossdated to the calendar year and assigned to the corresponding cluster according to their location. Each horizontal grey solid line refers to the life span of one log. Charred logs facing plots at the boundary between two cluster (horizontal black dashed lines) and other charred logs (horizontal black solid lines) are also shown, as well as the recruitment date of all charred logs in the littoral zone (based on their outermost tree-ring date; vertical grey dashed lines), the estimated wildfire dates (vertical black arrows on the most recent fire evidence and vertical black dashed lines) and the date of the Tambora eruption (AD 1815; vertical black dotted line). The thin black line at the middle of each panel shows the number of logs that were living each year. The thick black line at the bottom of each panel shows the average recruitment rate of logs during the identified fire-free interval (number recruited per 100 years per 100 m of shoreline based on the outermost tree-ring dates).

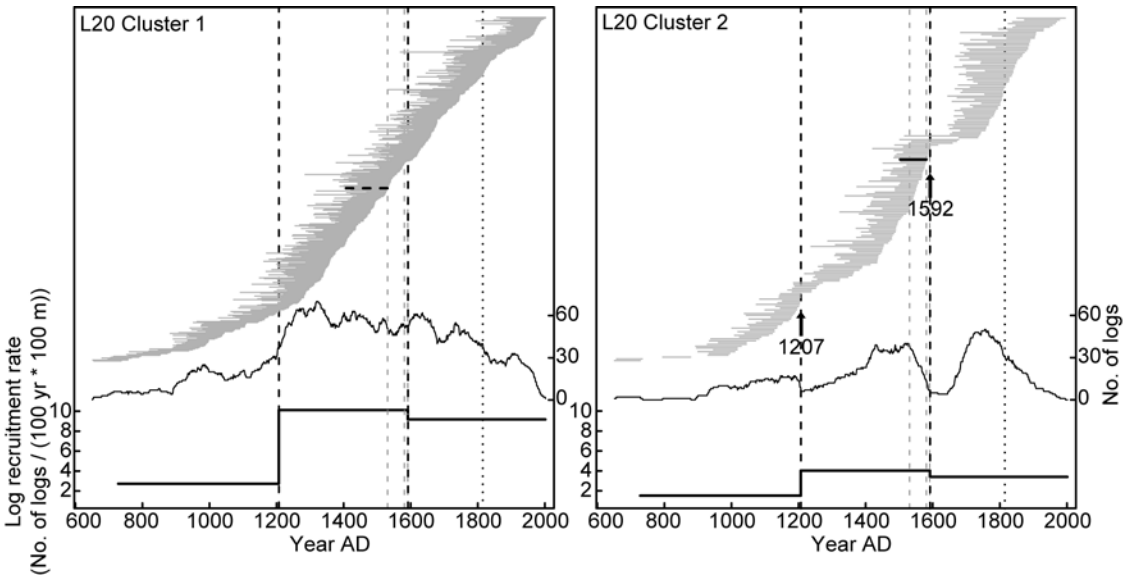

Fig. 2-4. Life spans, abundance and recruitment rate of L20 subfossil logs crossdated to the calendar year and assigned to the corresponding cluster according to their location. All symbols are as in Fig. 3.

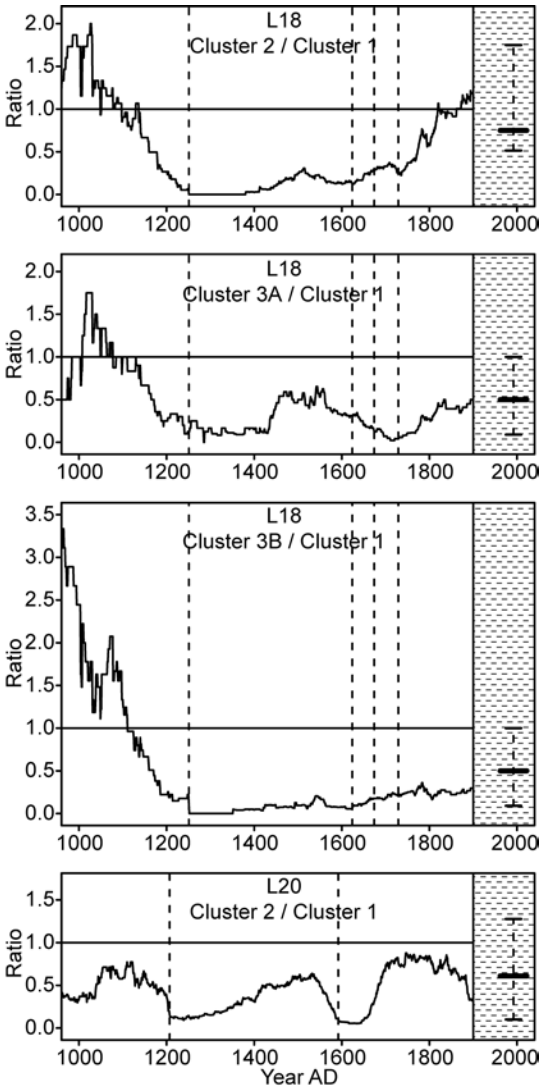

Fig. 2-5. Ratio between the number of subfossil logs that were living each year per 100 m of shoreline in the cluster 2 or 3 and the number of logs in the cluster 1 at L18 (three upper panels) and L20 (bottom panel). Values older than AD 1000 or more recent than AD 1900 are not shown because they are influenced by relevant losses of subfossil logs through decomposition and burial (Gennaretti, Arseneault & Bégin 2014) or by the fact that the recruitment of subfossil logs in the littoral zones is still ongoing, respectively. The estimated wildfire dates at each lake (vertical dashed lines) and the 5^{th}, 50^{th} and 95^{th} percentiles of the ratios between the density of living trees≥ 12 cm DBH (Nliv12) in the triplets of sampling plots belonging to the corresponding clusters (bold horizontal line and whiskers) are shown.

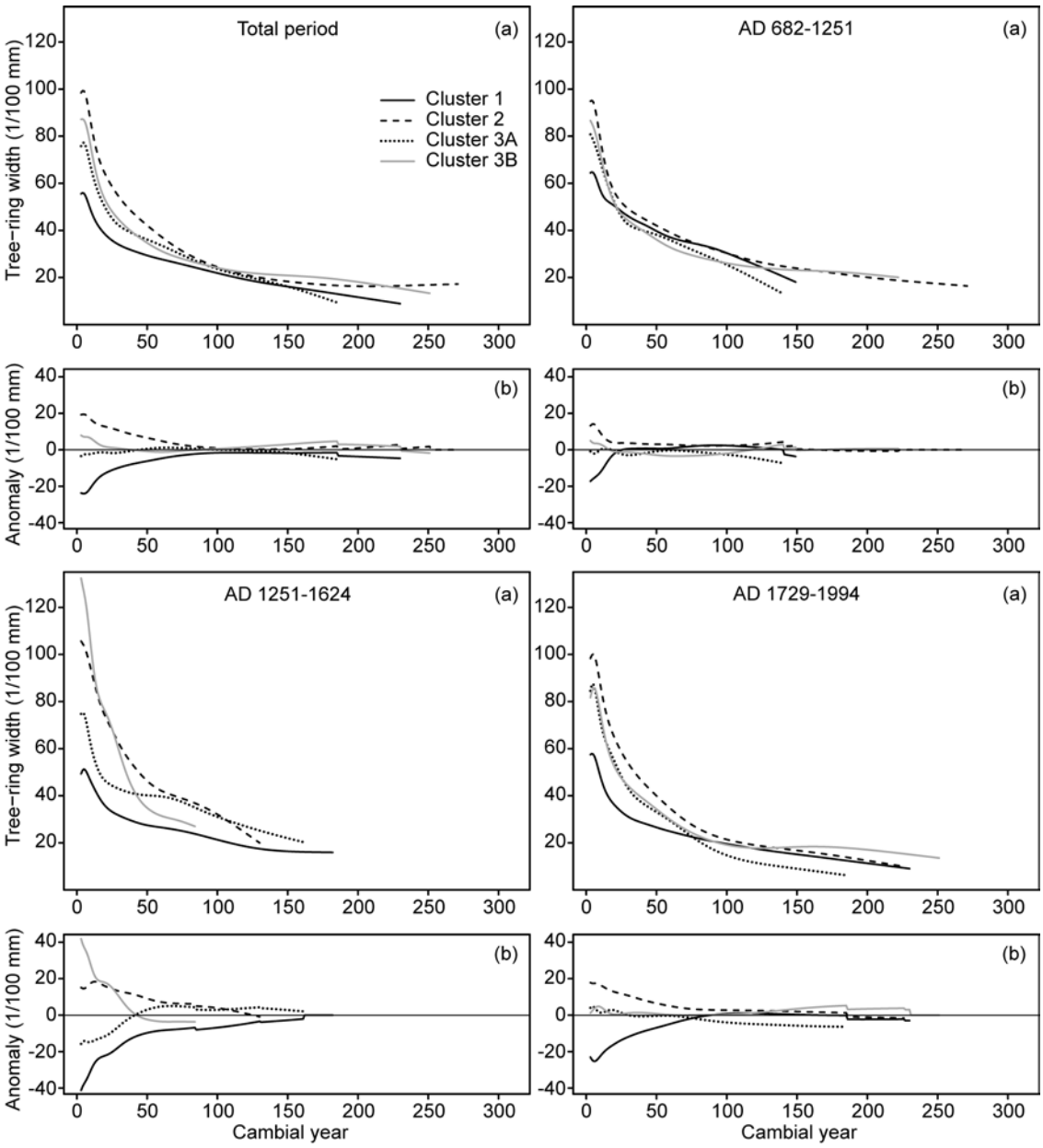

Fig. 2-6. Comparison among all clusters at L18 of the smoothed average growth curves for the subfossil logs recruited during different fire-free intervals. The "a" plots show the smoothed average growth curves, while "b" plots show the growth anomalies calculated with a subtraction against the average of the four curves with each corresponding to a cluster or a cluster section. The legend in the first "a" plot refers to the other plots as well.

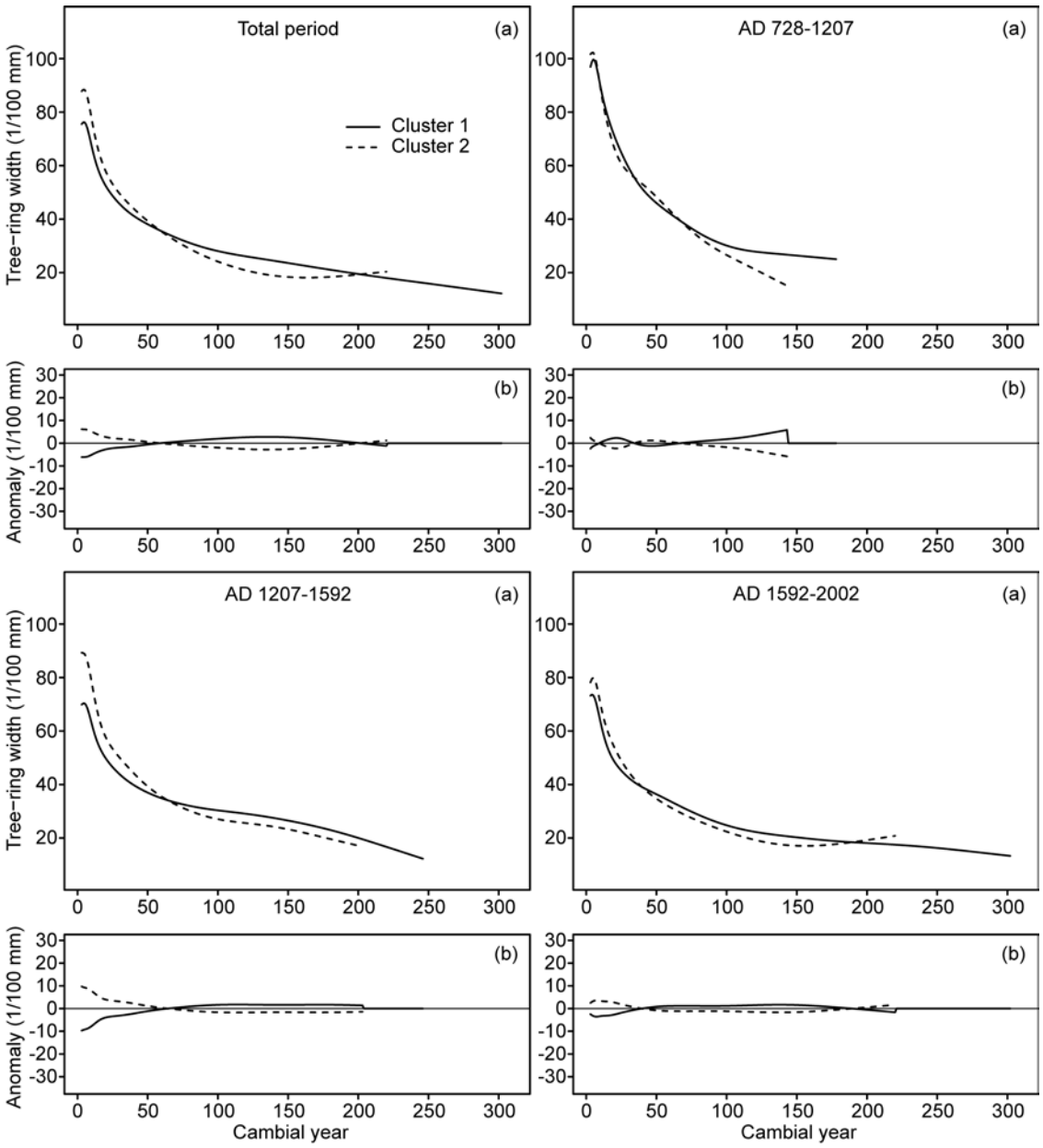

Fig. 2-7. Comparison between the two clusters at L20 of the smoothed average growth curves for the subfossil logs recruited during different fire-free intervals. The legend and plots "a" and "b" are as in Fig. 6.

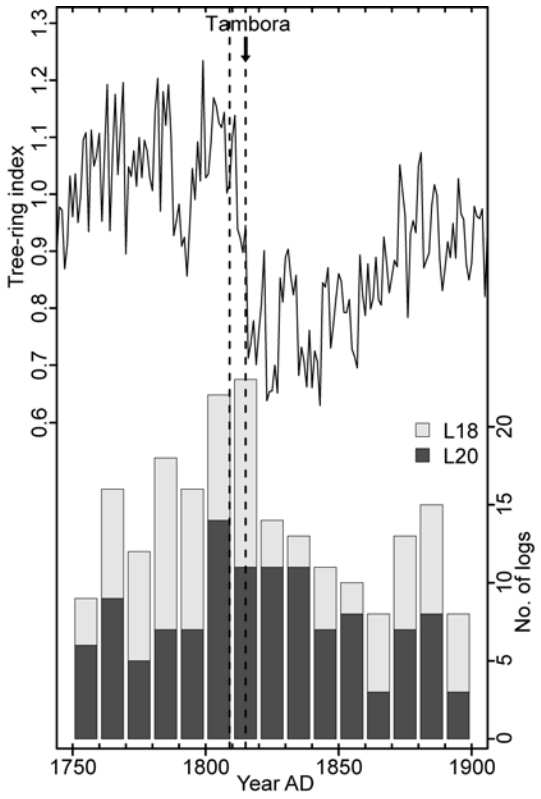

Fig. 2-8. Effect of the Tambora eruption on tree-growth and mortality at L18 and L20. The plot shows the average of the two local tree-ring chronologies (RCS-standardized; Esper et al. 2003) developed with the ring-width series of the L18 and L20 subfossil logs (black solid line), as well as the dates of the Tambora and of the former AD 1809 eruptions (vertical dashed lines), and the number of subfossil logs recruited at L18 and L20 (based on their outermost tree-ring dates) per each 10-year class over the analyzed period.

2.2.11 Supporting information

Supporting Tables

Table 2-S1. Parameters, their *P*-values and the standard error (SE) of the residuals of the power function models describing the stand size structure of living trees of triplets of plots at L18 (i.e. $y = a * x^{(-b)}$ where y is the number of individuals per hectare and x is the central value of 2-cm size classes)

Triplet	N. of observations	a	P-value of a	b	P-value of b	d.f.	Residual SE
1	9	28322.88	1.03e-11	2.40	4.98e-07	7	344.42
2	9	13475.05	2.17e-10	1.72	1.99e-07	7	253.54
3	9	11813.09	1.31e-10	1.74	1.43e-07	7	206.75
4	10	10986.20	3.22e-11	2.07	7.65e-07	8	223.33
5	10	17995.34	3.01e-13	2.67	3.83e-07	8	203.72
6	10	19498.32	8.45e-15	3.06	1.41e-07	8	141.18
7	9	15164.34	7.05e-13	2.59	9.96e-08	7	125.59
8	8	10998.35	2.98e-10	2.50	5.00e-06	6	140.92
9	9	8330.99	3.88e-11	2.18	5.07e-07	7	122.40
10	9	13664.72	7.05e-12	2.84	4.07e-06	7	157.29
11	8	21165.56	4.78e-11	3.40	6.49e-05	6	199.89
12	8	28164.90	3.36e-11	3.30	2.88e-05	6	250.74
13	10	31164.94	1.04e-14	3.33	1.00e-06	8	231.59
14	13	24997.38	3.35e-19	2.97	1.30e-09	11	179.84
15	14	15329.75	3.73e-18	2.79	1.40e-08	12	176.93
16	13	8826.76	2.05e-15	2.23	8.53e-09	11	140.48
17	12	7992.93	1.54e-14	2.05	4.08e-09	10	121.05
18	11	10663.17	9.22e-15	2.30	4.52e-09	9	113.97
19	10	9989.49	2.41e-12	1.96	2.99e-08	8	146.78
20	10	8659.61	4.93e-13	1.53	3.52e-10	8	104.47
21	10	9506.17	1.29e-13	1.56	1.12e-10	8	96.96
22	10	9338.89	1.07e-13	1.63	1.45e-10	8	93.00
23	9	16994.87	2.34e-12	2.43	1.33e-07	7	167.12
24	8	21491.93	2.03e-09	2.61	5.33e-05	6	379.32
25	8	29662.34	2.67e-10	2.97	4,19e-05	6	373.08
26	7	29994.88	1.13e-08	2.87	1.61e-04	5	428.72
27	8	27831.15	1.45e-10	3.18	6.32e-05	6	316.31
28	9	30499.06	1.62e-12	3.66	9.29e-05	7	284.47
29	8	26999.66	3.24e-11	4.38	4.47e-03	6	238.95
30	9	27166.01	1.80e-12	3.57	6.45e-05	7	257.24
31	11	16996.07	7.28e-14	2.72	6.66e-07	9	228.58
32	11	11657.64	3.25e-13	2.13	4.39e-08	9	185.21
33	11	6818.80	1.61e-12	1.73	1.09e-08	9	129.61
34	10	5490.41	1.62e-11	1.70	3.47e-08	8	102.49
35	10	7826.32	6.03e-11	2.26	4.50e-06	8	172.07
36	13	5663.52	1.12e-14	2.43	2.44e-07	11	105.25
37	12	8666.29	1.17e-15	3.59	5.13e-05	10	101.35
Composite*	365	16481.54	2.52e-127	2.55	8.04e-12	363	2664.62

* The model for composite is fitted to the data of all triplets

Table 2-S2. Parameters, their *P*-values and the standard error (SE) of the residuals of the power function models describing the stand size structure of living trees of triplets of plots at L20 (i.e. $y = a * x^{(-b)}$ where y is the number of individuals per hectare and x is the central value of 2-cm size classes)

Triplet	N. of observations	a	*P*-value of a	b	*P*-value of b	d.f.	Residual SE
1	10	16320.15	1.62e-11	2.22	9.77e-07	8	304.26
2	10	10983.37	1.81e-11	1.94	1.80e-07	8	207.76
3	10	18492.19	2.84e-12	2.55	1.52e-06	8	277.22
4	9	19491.19	2.19e-10	2.59	2.72e-05	7	366.73
5	9	19821.31	1.33e-10	2.38	5.37e-06	7	347.51
6	9	10483.03	3.72e-10	1.85	7.44e-07	7	212.93
7	9	8811.68	1.92e-09	1.72	1.76e-06	7	226.60
8	7	11320.36	4.07e-07	2.17	3.31e-04	5	331.91
9	8	18327.75	1.94e-09	2.71	8.18e-05	6	321.14
10	9	15330.47	2.59e-11	2.87	1.64e-05	7	212.51
11	9	12830.39	9.85e-12	2.60	1.43e-06	7	154.93
12	9	10825.81	9.29e-11	2.12	8.60e-07	7	180.24
13	8	12661.53	9.54e-11	2.12	2.48e-07	6	134.20
14	9	11992.67	8.80e-12	2.11	8.12e-08	7	142.53
15	9	7823.69	4.27e-11	1.86	9.30e-08	7	116.60
16	9	8152.50	8.59e-10	1.93	2.60e-06	7	186.68
17	9	7144.64	8.90e-09	1.77	1.00e-05	7	228.91
18	9	9652.86	4.59e-10	1.98	1.89e-06	7	202.01
19	10	14812.54	4.26e-11	1.98	5.39e-07	8	311.92
20	12	23649.11	1.07e-14	2.23	1.17e-08	10	345.18
21	11	27484.74	1.08e-13	2.35	7.32e-08	9	386.08
22	11	22651.10	3.17e-14	2.16	5.34e-09	9	277.81
23	9	19982.56	1.05e-10	2.14	1.09e-06	7	338.57
24	10	16640.94	6.73e-11	1.98	8.37e-07	8	371.05
25	11	27490.81	2.38e-13	2.64	1.22e-06	9	421.75
26	11	24823.34	3.35e-14	2.42	3.77e-08	9	306.28
27	11	25489.10	4.18e-15	2.26	1.57e-09	9	249.49
28	10	15820.45	3.71e-13	1.94	4.00e-09	8	183.94
29	10	13483.55	8.10e-13	1.81	3.63e-09	8	172.88
30	9	16819.08	1.18e-10	2.17	1.45e-06	7	289.84
31	10	13810.54	4.74e-11	1.94	4.63e-07	8	294.70
Composite*	296	15917.36	1.23e-137	2.19	1.80e-26	294	1904.85

* The model for composite is fitted to the data of all triplets

Table 2-S3. Correlation matrix of the variables used to characterize the riparian forest structure and composition of the L18 triplets of plots. Correlations higher than 0.8 are in bold

	Nliv	Ntot	Nreg	Nliv2	Nliv6	Nliv12	Ndead	Ncwd	BAliv	MeanBAliv	BAdead	MeanBAdead	F%reg	F%	T%	Age	a
Ntot	**1.00**																
Nreg	**0.99**	**0.99**															
Nliv2	0.16	0.17	0.05														
Nliv6	0.34	0.36	0.26	0.78													
Nliv12	-0.40	-0.40	-0.42	0.16	0.36												
Ndead	0.39	0.41	0.33	0.57	0.70	0.04											
Ncwd	-0.25	-0.25	-0.27	0.15	-0.02	0.37	0.12										
BAliv	-0.25	-0.24	-0.29	0.36	0.60	**0.89**	0.19	0.30									
MeanBAliv	-0.38	-0.39	-0.33	-0.52	-0.16	0.51	-0.30	0.03	0.52								
BAdead	-0.02	0.00	-0.04	0.25	0.28	0.23	0.55	0.26	0.29	0.12							
MeanBAdead	-0.50	-0.51	-0.47	-0.30	-0.45	0.18	-0.53	0.15	0.12	0.45	0.38						
F%reg	0.11	0.13	0.05	0.61	0.64	0.18	0.65	0.13	0.33	-0.15	0.44	-0.19					
F%	0.10	0.12	0.02	0.72	0.73	0.22	**0.81**	0.18	0.36	-0.21	0.52	-0.28	**0.83**				
T%	-0.37	-0.38	-0.35	-0.25	-0.08	0.50	-0.30	0.13	0.35	0.33	-0.38	-0.08	-0.16	-0.24			
Age	0.66	0.66	0.68	-0.06	0.05	-0.16	0.14	-0.01	-0.24	-0.23	0.11	-0.14	0.05	0.01	-0.14		
a	**0.99**	**0.99**	**1.00**	0.05	0.26	-0.42	0.33	-0.27	-0.29	-0.33	-0.04	-0.47	0.05	0.02	-0.35	0.68	
b	0.65	0.65	0.72	-0.56	-0.17	-0.32	0.03	-0.29	-0.30	0.24	0.00	-0.12	-0.21	-0.29	-0.18	0.57	0.72

Table 2-S4. Correlation matrix of the variables used to characterize the riparian forest structure and composition of the L20 triplets of plots. Correlations higher than 0.8 are in bold

	Nliv	Ntot	Nreg	Nliv2	Nliv6	Nliv12	Ndead	Ncwd	BAliv	MeanBAliv	BAdead	MeanBAdead	F%reg	F%	T%	Age	a
Ntot	**1.00**																
Nreg	**0.99**	**0.99**															
Nliv2	0.78	0.79	0.71														
Nliv6	0.71	0.70	0.65	**0.87**													
Nliv12	0.48	0.48	0.45	0.57	0.72												
Ndead	0.72	0.75	0.69	0.76	0.46	0.24											
Ncwd	0.27	0.28	0.28	0.09	-0.11	-0.34	0.43										
BAliv	0.74	0.74	0.68	**0.90**	**0.95**	**0.84**	0.56	-0.11									
MeanBAliv	0.03	0.01	0.04	-0.09	0.27	0.71	-0.30	-0.39	0.35								
BAdead	0.59	0.60	0.55	0.64	0.46	0.49	0.73	0.19	0.62	0.01							
MeanBAdead	-0.16	-0.18	-0.16	-0.13	-0.02	0.40	-0.32	-0.30	0.11	0.47	0.38						
F%reg	0.67	0.68	0.64	0.73	0.57	0.26	0.71	0.01	0.60	-0.17	0.53	-0.23					
F%	0.42	0.44	0.37	0.59	0.38	0.41	0.65	0.02	0.52	-0.01	0.68	0.12	0.66				
T%	-0.15	-0.14	-0.16	-0.01	-0.08	-0.25	0.00	0.07	-0.09	-0.13	-0.19	-0.21	0.18	0.30			
Age	0.08	0.07	0.07	0.09	0.16	0.30	-0.10	-0.13	0.20	0.36	0.01	0.20	0.01	0.11	-0.19		
a	**0.99**	**0.99**	**1.00**	0.71	0.65	0.45	0.69	0.28	0.68	0.04	0.55	-0.16	0.63	0.37	-0.17	0.07	
b	0.51	0.49	0.59	-0.11	0.06	0.08	0.02	0.21	0.03	0.30	-0.02	-0.09	0.00	-0.21	-0.21	0.16	0.59

Supporting Figures

Fig. 2-S1. Photo from a helicopter of a typical area of the taiga zone in Eastern Canada showing a mosaic of spruce-lichen woodlands of various postfire ages, along with numerous lakes and peatlands.

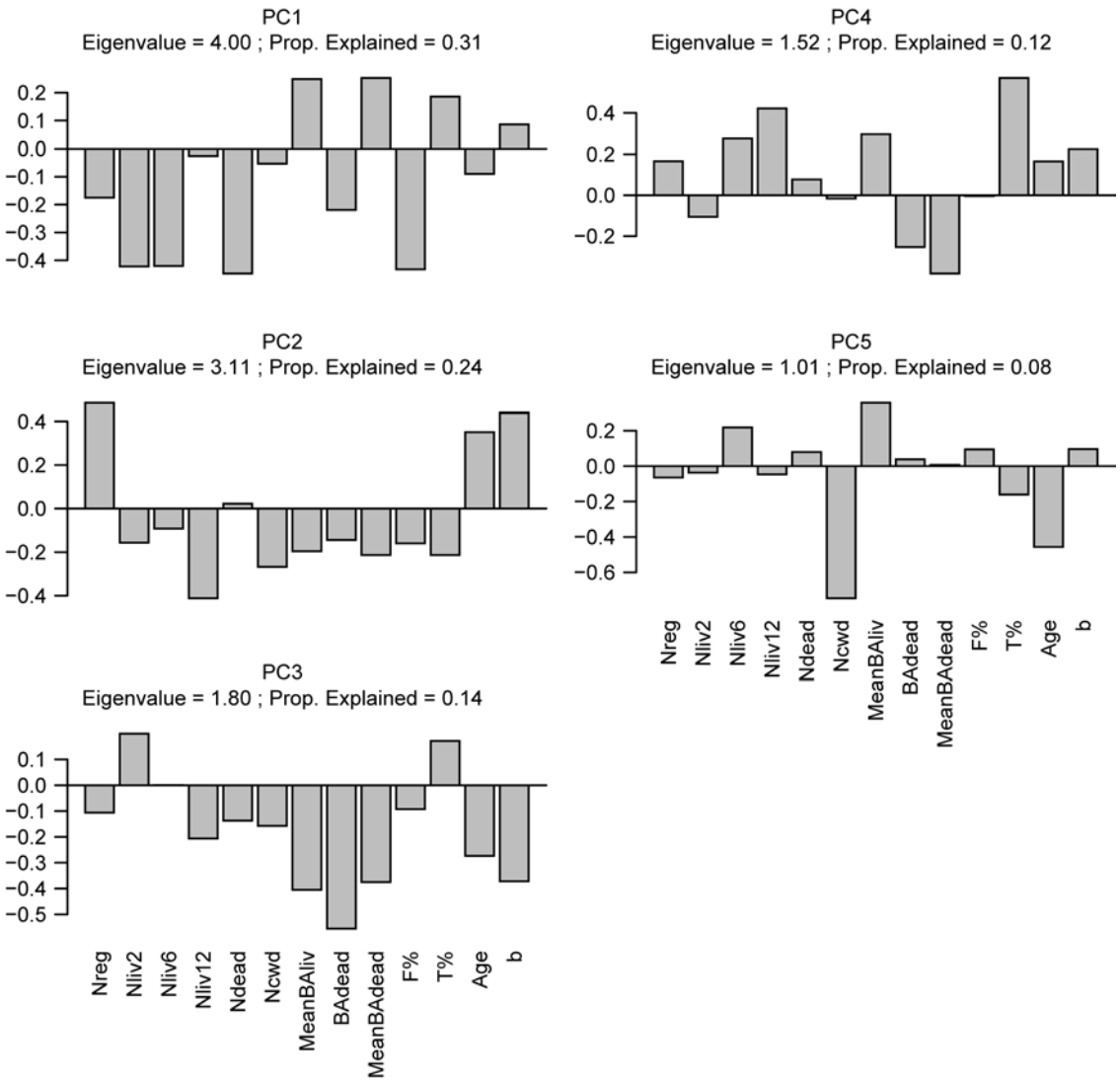

Fig. 2-S2. Loadings of components with eigenvalues larger than one for L18 PCA.

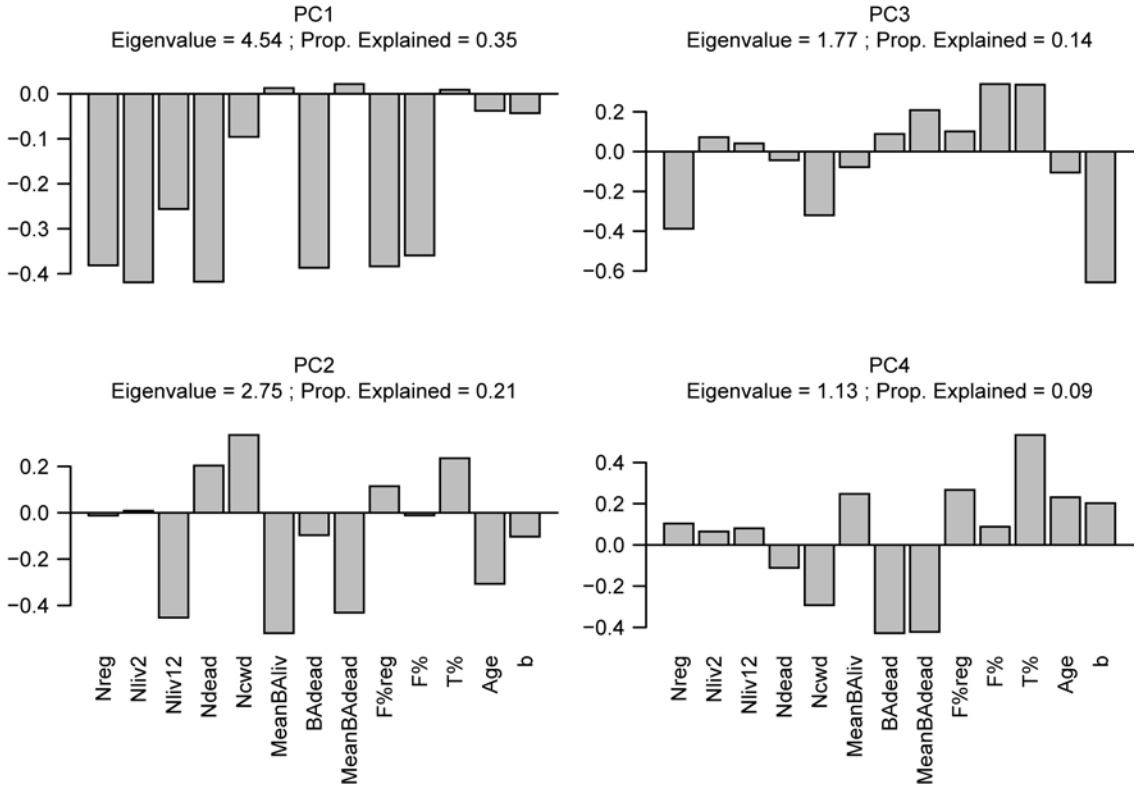

Fig. 2-S3. Loadings of components with eigenvalues larger than one for L20 PCA.

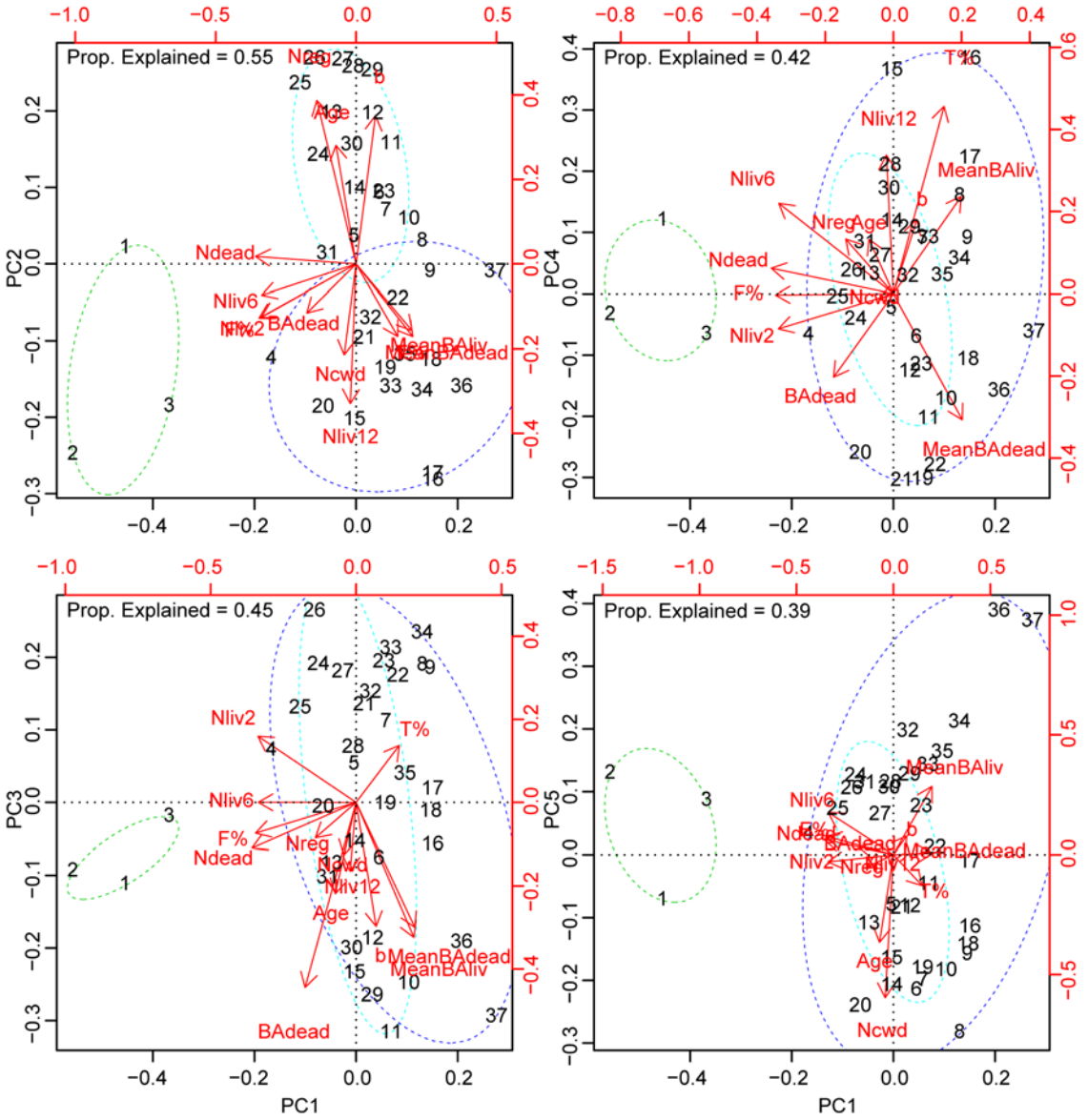

Fig. 2-S4. L18 PCA biplots. Variables are in red and triplets of plots are in black. Triplets belonging to the same cluster (see Fig. S6) are enclosed in minimum spanning ellipses (green: cluster 1; blue: cluster 2; light blue: cluster 3).

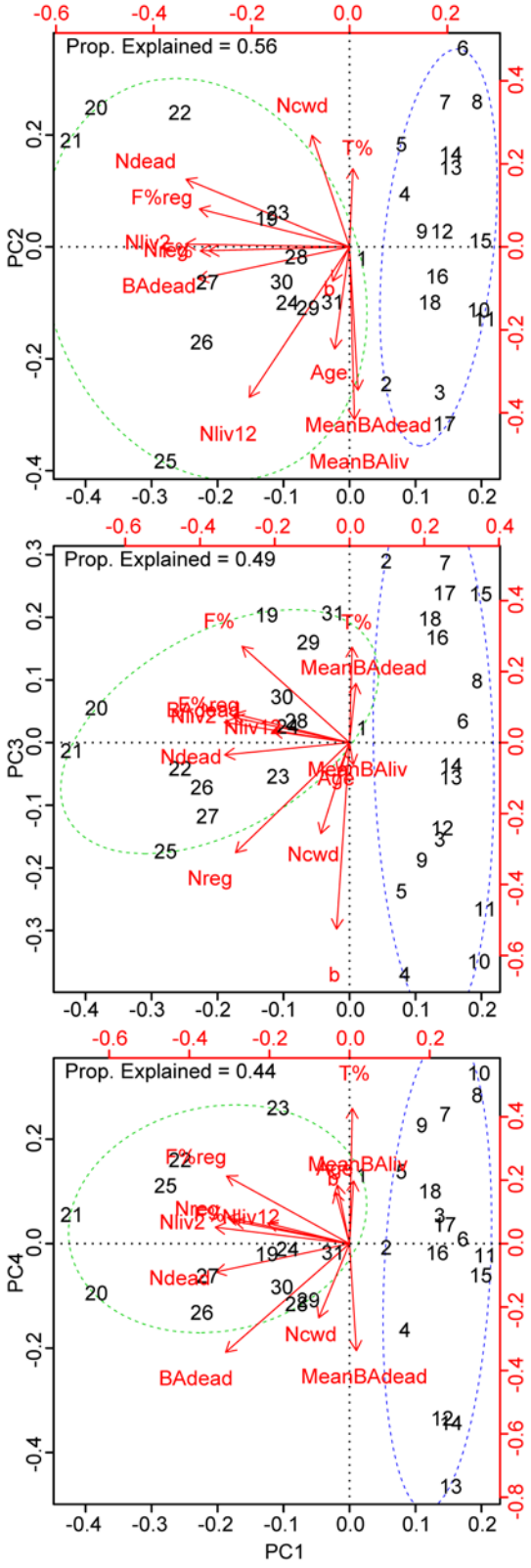
Prop. Explained = 0.56
PC2
Ncwd
T%
Ndead
F%reg
Nliv2
Nreg
BAdead
Age
Nliv12
MeanBAdead
MeanBAliv
Prop. Explained = 0.49
PC3
F%
T%
MeanBAdead
Ncwd
Nreg
b
Prop. Explained = 0.44
PC4
T%
Ndead
Ncwd
BAdead
MeanBAdead
PC1

Fig. 2-S5. L20 PCA biplots. Variables are in red and triplets of plots are in black. Triplets belonging to the same cluster (see Fig. S7) are enclosed in minimum spanning ellipses (green: cluster 1; blue: cluster 2).

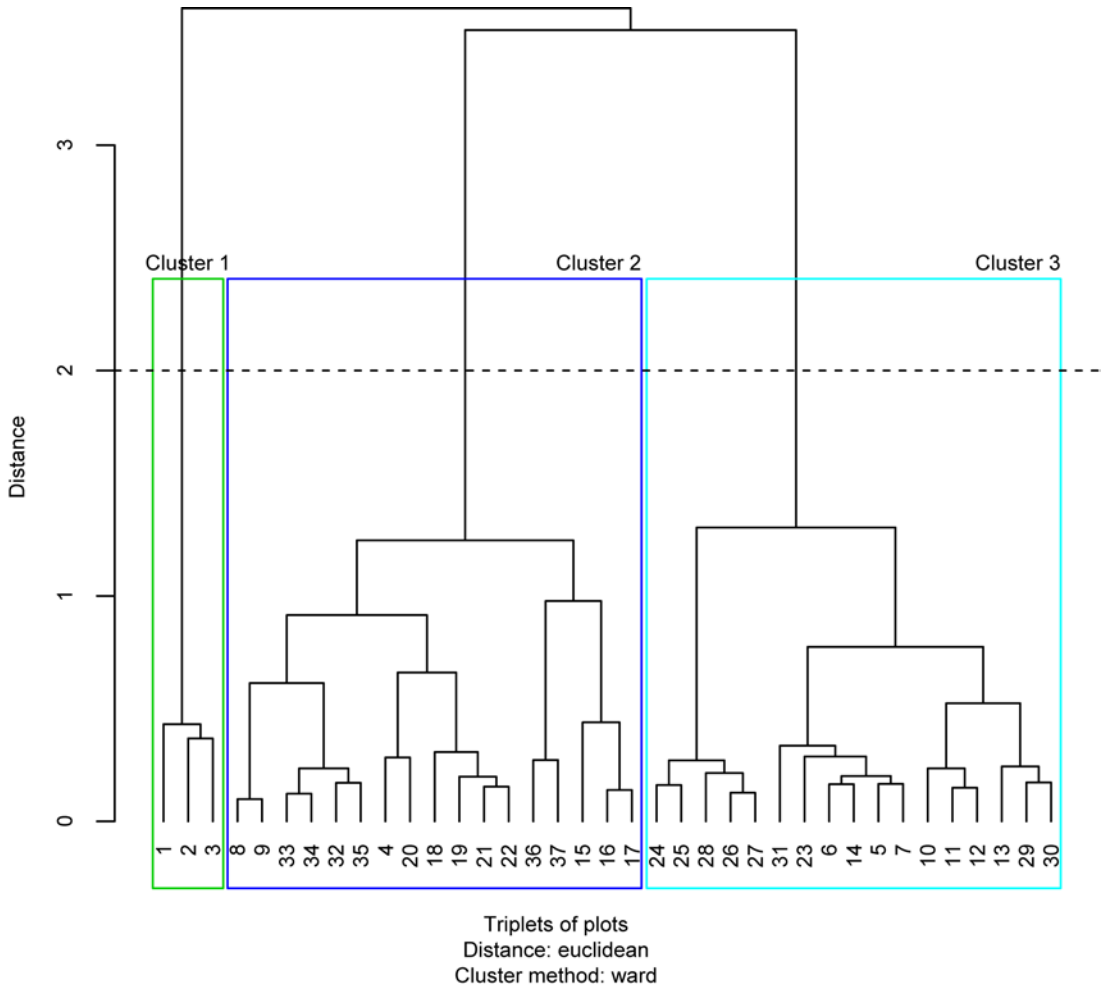

Fig. 2-S6. Cluster dendrogram for L18 triplets of plots. The horizontal dashed line shows the threshold used to define homogeneous clusters.

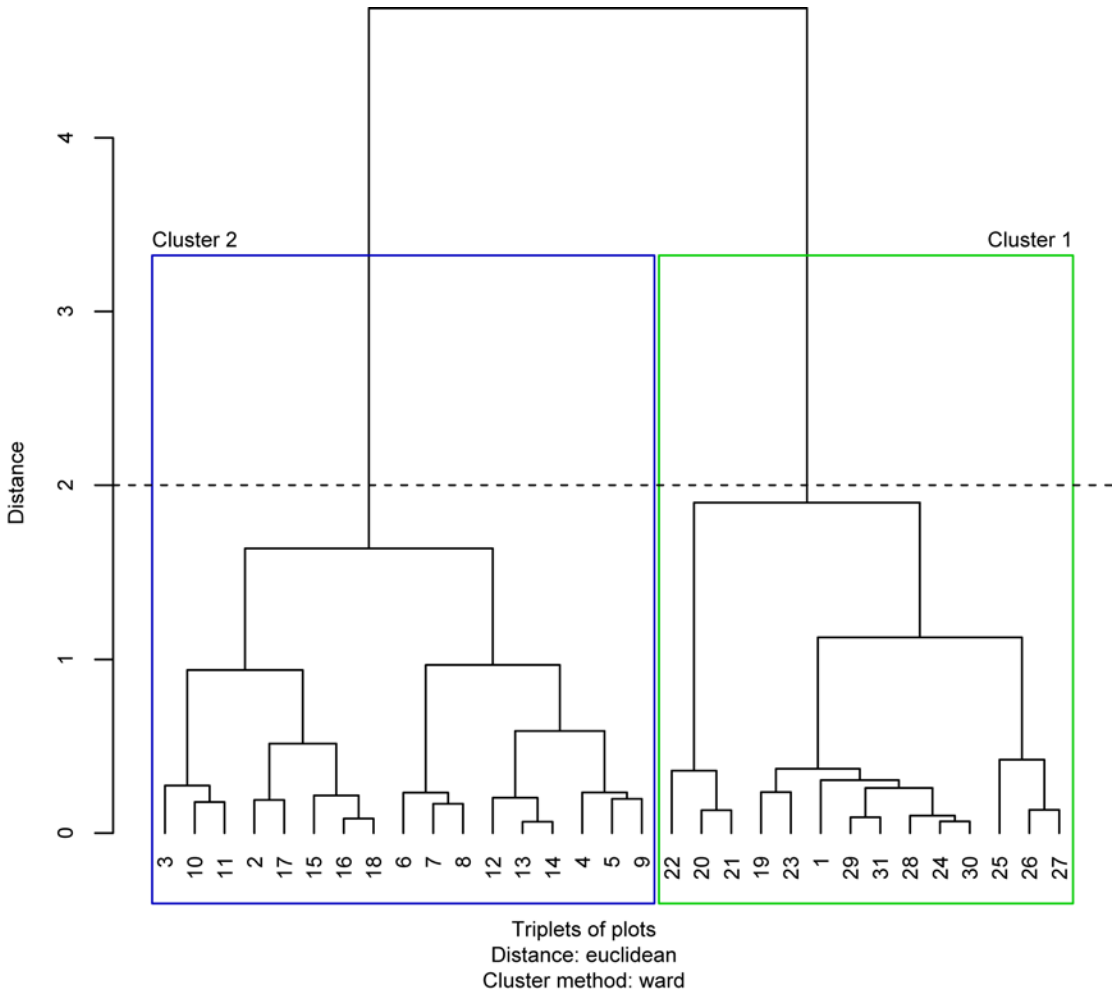

Fig. 2-S7. Cluster dendrogram for L20 triplets of plots. The horizontal dashed line shows the threshold used to define homogeneous clusters.

Fig. 2-S8. Examples of charred subfossil logs. On the left, a log with charred branch tips. This kind of charred mark indicates that the riparian tree died during the fire event and that, in absence of erosion, the outermost tree-ring date of the log coincides with the fire year or with the previous year. On the right, a log with charred trunk. This kind of mark indicates that the riparian tree was already dead when the fire took place. At our sites 19 charred subfossil logs could be crossdated to the calendar year and 15 out of them were of the kind on the left.

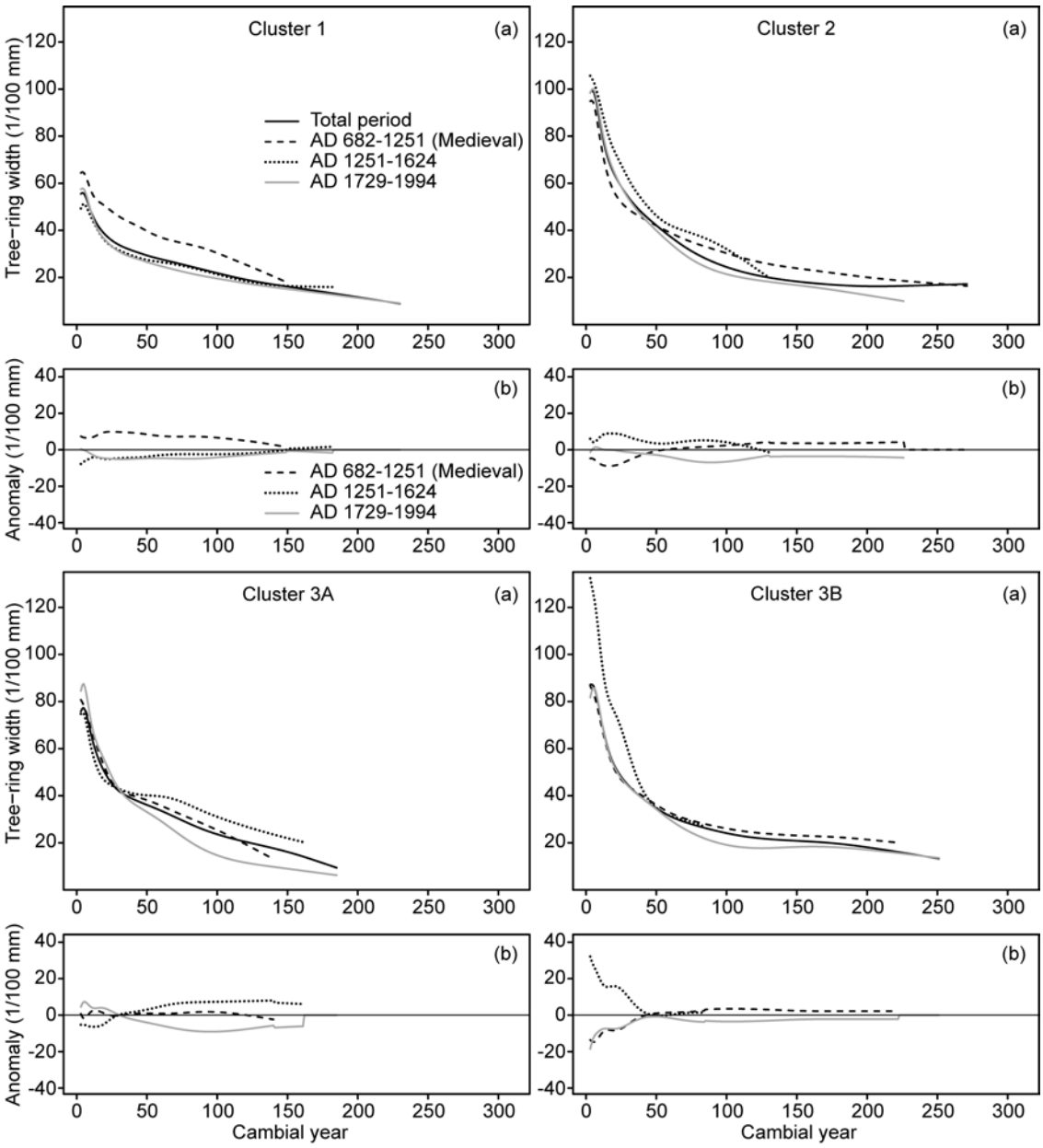

Fig. 2-S9. Comparison among fire-free intervals of the smoothed average growth curves of the subfossil logs for each cluster at L18. The "a" plots show the smoothed average growth curves, while the "b" plots show the growth anomalies calculated with a subtraction against the average of the three curves (curves for the periods 682-1251, 1251-1624 and 1729-1994). The legends in the plots of the first cluster also refer to the other plots.

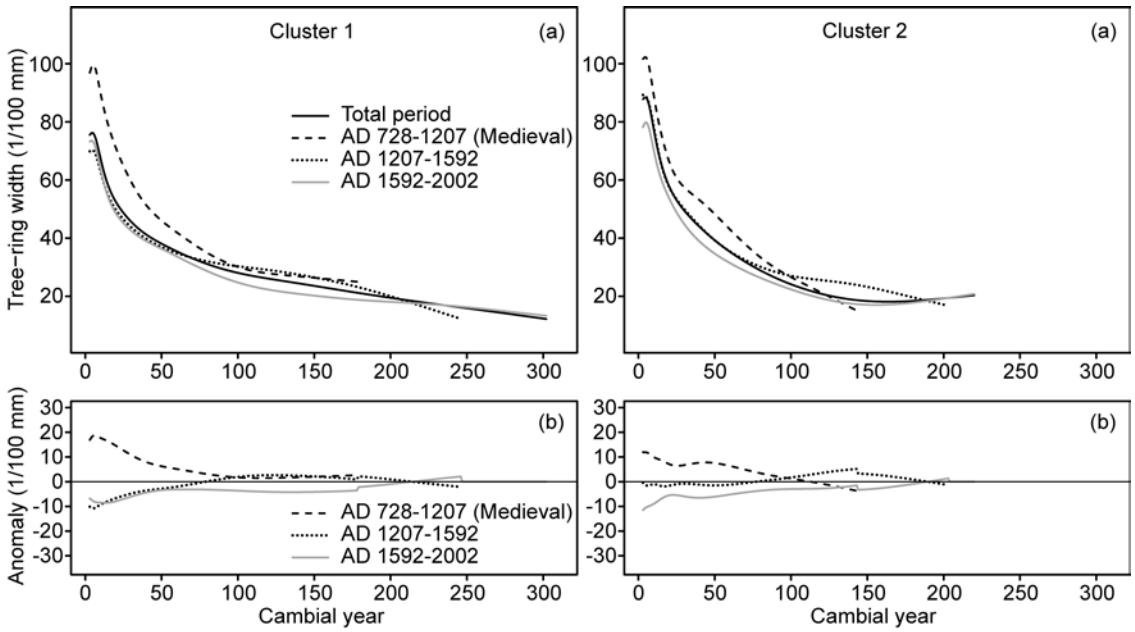

Fig. 2-S10. Comparison among fire-free intervals of the smoothed average growth curves of the subfossil logs for each cluster at L20. The "a" plots show the smoothed average growth curves, while the "b" plots show the growth anomalies calculated with a subtraction against the average of the three curves (curves for the periods 728-1207, 1207-1592 and 1592-2002). The legends in the plots of the first cluster also refer to the other plots.

CHAPITRE 3.
RECONSTITUTION DENDROCHRONOLOGIQUE DES TEMPÉRATURES ESTIVALES DU DERNIER MILLÉNAIRE DANS LA TAÏGA DE L'EST DE L'AMÉRIQUE DU NORD

3.1 RÉSUMÉ EN FRANÇAIS DU TROISIÈME ARTICLE

Le troisième article de ma thèse, intitulé « *Volcano-induced regime shifts in millennial tree-ring chronologies from Northeastern North America* », a bénéficié de la collaboration de cinq membre du projet ARCHIVES (projet CRSNG-RDC avec Hydro-Québec): moi-même, mon directeur de recherche Dominique Arseneault (UQAR), Antoine Nicault (ECCOREV), Luc Perreault (IREQ) et mon co-directeur Yves Bégin (INRS-ETE). Cet article a été soumis pour la publication aux éditeurs de la revue *Proceedings of the National Academy of Sciences of the United States of America* en janvier 2014. Tous les auteurs ont participé aux travaux de terrain et à la discussion des résultats et des implications de l'article à travers toutes les étapes de sa réalisation. L'analyse des échantillons, le choix des méthodes statistiques et la rédaction ont principalement été prises en charge par moi-même et mon directeur Dominique Arseneault. Je remercie spécialement Luc Perreault pour avoir permis, avec ses connaissances en statistique bayésienne, l'application d'une méthode capable de détecter formellement les changements de régimes dans la reconstitution des températures effectuée.

Des datations récentes des périodes d'expansion des calottes glacières dans l'arctique canadien ont suggéré que le Petit Âge glaciaire a débuté de manière abrupte

entre 1275 et 1300 apr. J.-C. suite à une série de fortes éruptions volcaniques. Malgré que cette idée soit supportée par les résultats de simulations effectuées avec des modèles climatiques, des confirmations supplémentaires basées sur des données de terrain sont inexistantes. En particulier, le réseau nord hémisphérique de séries dendrochronologiques millénaires sensibles aux températures, qui regroupe principalement des sites euro-asiatiques, semble montrer que les éruptions les plus fortes du dernier millénaire ont seulement causé des baisses de température qui ont duré moins de 10 ans.

Dans ce contexte, notre article présente un nouveau réseau de séries dendrochronologiques millénaires dans la taïga du Nord-Est de l'Amérique du Nord, qui comble une lacune importante dans le réseau nord hémisphérique de séries dendrochronologiques disponibles pour des reconstitutions des températures. Notre réseau supporte l'hypothèse de l'influence volcanique que ce soit sur le commencement ou sur le début de la période la plus froide du Petit Âge glaciaire. En effet, suite à l'Optimum climatique médiéval (approximativement 910-1257 apr. J.-C.), qui comprend les décennies les plus chaudes du dernier millénaire, notre reconstitution des températures montre un changement abrupt de régime vers des températures estivales plus basses. Ce changement de régime coïncide précisément avec une série d'éruptions volcaniques centrée aux alentours de l'éruption du Samalas en 1257 et précède l'expansion des calottes glacières dans l'arctique canadien. De plus, les deux éruptions volcaniques successives de 1809 (volcan inconnu) et 1815 (Tambora) ont provoqué dans notre région d'étude un autre baisse significative des températures et le début de la période de 40 ans la plus froide des 1100 dernières années.

Ces résultats appuient l'hypothèse que des séries de fortes éruptions volcaniques peuvent entrainer des changements de régime des températures qui, selon la région considérée, peuvent être très significatifs et persistants et que le climat du Nord-Est de l'Amérique du Nord est particulièrement sensible au forçage volcanique.

3.2 VOLCANO-INDUCED REGIME SHIFTS IN MILLENNIAL TREE-RING CHRONOLOGIES FROM NORTHEASTERN NORTH AMERICA

3.2.1 Abstract

Dated records of ice-cap growth from Arctic Canada recently suggested that a succession of strong volcanic eruptions forced an abrupt onset of the Little Ice Age between A.D. 1275 and 1300 (Miller et al. 2012). Although this idea is supported by simulation experiments with general circulation models, additional support from field data is limited. In particular, the Northern Hemisphere network of temperature-sensitive millennial tree-ring chronologies, which principally comprises Eurasian sites, suggests that the strongest eruptions only caused cooling episodes lasting less than about 10 years. Here we present a new network of millennial tree-ring chronologies from the taiga of Northeastern North America, which fills a wide gap in the network of the Northern Hemisphere's chronologies suitable for temperature reconstructions, and supports the hypothesis that volcanoes triggered both the onset and the coldest episode of the Little Ice Age. Following the well-expressed Medieval Climate Anomaly (approximately A.D. 910-1257), which comprised the warmest decades of the last millennium, our tree-ring-based temperature reconstruction displays an abrupt regime shift towards lower average summer temperatures precisely coinciding with a series of 13th century eruptions centered around the 1257 Samalas event and closely preceding ice-cap expansion in Arctic Canada. Furthermore, the successive 1809 (unknown volcano) and 1815 (Tambora) eruptions triggered a subsequent shift to the coldest 40-year period of the last 1100 years. These results confirm that series of large eruptions may cause region-specific regime shifts in the climate system and that the climate of Northeastern North America is especially sensitive to volcanic forcing.

3.2.2 Significance Statement

The cooling effect on the Earth's climate system of sulfate aerosols injected into the stratosphere by large volcanic eruptions has been under debate during the last years. While some simulation and field data shows that these effects are short-lasting (less than about 10 years), other evidences suggest that large and successive eruptions can lead to the onset of cooling episodes that can persist over several decades sustained by consequent sea-ice/ocean feedbacks. Here, we present a new network of millennial tree-ring chronologies suitable for temperature reconstructions from Northeastern North America where no similar records are available, and we show that during the last millennium persistent shifts towards lower average temperatures in this region are coincident to series of large eruptions.

3.2.3 Introduction

Tree-ring chronologies are the type of proxy record most used to develop climate reconstructions covering the last millennium (1). These chronologies have been integrated into large-scale networks, often with additional proxies, to document the amplitude, duration, and forcing mechanisms of the Medieval Climate Anomaly, the Little Ice Age, and the recent warming trend. However, the spatial coverage of long tree-ring records must be improved to allow a better understanding of regional variations in past climate (1, 2). For example, in Eastern North America millennial climate reconstructions have been performed from tree species and sites sensitive to drought and precipitation (3), whereas temperatures were inferred solely from low-resolution proxies, such as pollen data (4, 5). Furthermore, only tree-ring based climate reconstructions shorter than a millennium or using chronologies poorly replicated prior to A.D. 1500 have been published for the entire North American boreal forest (6, 7), whereas several millennial, highly replicated, temperature-sensitive tree-ring records have been developed across the Eurasian boreal zone. This lack of data is an important issue that

causes the poor representation of North America in long-term, large-scale temperature reconstructions (1, 4).

The feasibility of reconstructing volcanic forcing from tree-ring data has been debated, especially in regards to large and successive eruptions. Two of the largest eruptions of the last millennium, the A.D. 1257 Samalas and A.D. 1815 Tambora events, were both closely followed and preceded by additional large eruptions in 1227, 1275, 1284, 1809, and 1835 (8-11). Whereas general circulation model experiments suggest that the impacts of large and successive eruptions might have influenced climate systems for periods ranging from 20 years, several decades, or even centuries (12-16), Northern Hemisphere tree-ring based temperature reconstructions only display negative temperature anomalies lasting between 2-10 years (17-20). Region-specific responses of the climate system to volcanic forcing may in part explain this discrepancy (17). For example, large and successive eruptions may have had stronger impacts on summer temperatures in Northeastern North America (hereafter NENA) than elsewhere. An extensive Northern Hemisphere network of tree-ring-density chronologies supports this idea, showing that the coldest 1816 temperature anomalies occurred over the Quebec-Labrador Peninsula (21), where they may have persisted for several decades (7). The idea is also supported by the abrupt acceleration of ice-cap growth in the Eastern Canadian Arctic during A.D. 1275-1300, at the onset of the Little Ice Age, as a consequence of a series of eruptions (22). However, the lack of millennial, well-replicated, and temperature-sensitive tree-ring chronologies in the NENA sector precludes the examination of the volcano-temperature relationship in a long-term context with an annual resolution.

In this study, we have built a network of six highly replicated millennial tree-ring chronologies from large stocks of black spruce (*Picea mariana* (Mill.) B.S.P.) subfossil trees preserved in lakes of the NENA taiga from which we developed a millennial reconstruction (A.D. 910-2011) of regional July-August temperatures. For this purpose, we selected homogeneous sites with infrequent and well-documented ecological

disturbances (23), and sampled homogeneous subfossil and living samples in order to maximize the robustness of our reconstruction. We then used a Bayesian mixture of probability distributions with dependence (also referred to as hidden Markov models or Markov switching models, see 24 and 25) to detect possible regime shifts in summer temperatures triggered by series of large eruptions and to provide new insights concerning the climate history of NENA during the last 1100 years.

3.2.4 Results and Discussion

Our summer temperature reconstruction for Eastern Canada (hereafter STREC) closely reproduces the warming trend of July-August temperatures over the study area during the last century (Fig. 1a), even when the region experienced one of the strongest increases in summer temperatures worldwide according to the gridded temperature dataset CRU TS3.20 (26). The correlation between STREC and the gridded July-August temperature data (1905-2011; CRU TS3.20) is highly significant (0.61, $p<0.001$), even when the instrumental period is split into two subsets (1905-1957 and 1958-2011; Fig. 1a). The skill of the reconstruction in reproducing temperature data is indicated by the positive values of the reduction-of-error statistics computed with different calibration periods and on unsmoothed and smoothed datasets (Table S1). Cross-calibration verification confirms that STREC is robust and better predicts low frequencies than high frequencies (Table S1). In our study, the ring-width series of the subfossil and living tree samples were homogenized in order to remove the bias caused by varying sampling heights (see Methods) and avoid divergence between temperatures and standardized tree growth (Figs. S1 and S2). Spatial correlations show that STREC is mostly valid over the central Quebec-Labrador Peninsula within the NENA sector (Fig. 2).

Volcanism has been the primary factor forcing changes in summer temperatures on the decadal time scale in Eastern Canada during the last millennium. Numerous cooling episodes in STREC are synchronous with episodes already reported in

hemispheric temperature reconstructions (6, 27-30) and simulations (31-33) in response to strong volcanic eruptions (Fig. S3). The agreement between peaks in the global stratospheric volcanic sulfate aerosol injections (9) and cold anomalies inferred by STREC is also striking (Fig. 4a). A Superimposed Epoch Analysis (SI Methods) demonstrates that the 10 strongest volcanic eruptions of the last millennium produced highly significant cooling episodes in Eastern Canada lasting for about two decades, while less intense volcanic eruptions had a shorter influence (Fig. 3). The 20 post-event summers were significantly colder than the preceding ones for 8 out of the 10 largest eruptions ($p<0.1$; Table S2). For example, temperature anomalies ranged from -1.3 to -3.0°C in response to the three strongest tropical eruptions of the last millennium (A.D. 1257, 1452/1453, and 1815). With about two cooling episodes per century lasting for 10 to 20 years with a consequent reduction in tree growth, the volcanic signature in the NENA taiga is comparable to the epidemic signal of the eastern spruce budworm (*Choristoneura fumiferana*), which is the most destructive insect in the commercial forest of Eastern Canada south of our study area (34). Therefore, volcanic forcing during the last millennium has clearly impacted net primary production and the carbon balance in the NENA forests, at least over the Quebec-Labrador taiga.

Volcanism also strongly influenced century-scale temperature variability in NENA, as shown by our Bayesian analysis of regime shifts in STREC (SI Methods). Two of the strongest eruptions of the last 1100 years, the A.D. 1257 Samalas and A.D. 1815 Tambora events, which were followed and preceded by other eruptions, coincide exactly with the two most persistent regime shifts detected in STREC. According to the Schwarz criterion (35), STREC is best modeled with a four-state normal Bayesian hidden Markov model, with the two warmer and the two colder regimes largely dominating the A.D. 910-1257 and A.D. 1816-2011 time periods, respectively (Figs. 4b and S4). Consequently the strong overall cooling trend obtained by fitting a linear regression model to STREC (-1.60 ± 0.11°C per 1000 years; estimate ± SE; $p<0.001$) can be mostly attributed to the A.D. 1257 and A.D. 1815 shifts. Some proxy-based

evidences have shown that a long-term cooling trend due to orbital changes has characterized the climate of the last 2000 years in many regions of the world (4, 36, 37), including NENA (38). However, this cooling trend has been estimated at about -0.3 to -0.5°C per 1000 years (4, 37, 38) and is much weaker than the one of STREC. This fact, in addition to the absence of any negative trends in STREC over the A.D. 1257-1815 time period (Fig. S5), highlights the importance of volcanic-induced temperature regime shifts in NENA. Along with volcanism and orbital forcing, additional factors may have contributed to the strong negative trend of STREC and the associated transition from warm to cold regimes (Figs. 4b, S4 and S5), including solar forcing (19), and the specific regional domain of STREC.

A well-expressed Medieval Climate Anomaly (A.D. 910-1257) occurred in NENA prior to the A.D. 1257 Samalas event. The warmest decades reconstructed by STREC occurred between A.D. 1141 and 1170 (positive anomalies ranging from 0.89 to 1.80°C with respect to the last decade) and between A.D. 1061 and 1095 (0.87 to 1.19°C; Table S3). The confidence intervals of STREC for these two periods were almost all higher than the mean temperatures of the last decade (Fig. 1b). The amplitude and timing of the Medieval Climate Anomaly reconstructed by STREC also resemble the results of a pollen-based temperature reconstruction for the North American forest tundra (5), and closely correspond to a period of ice-cap melting in the Eastern Canadian Arctic (22; Fig. 4a). Collectively, these complementary data sources demonstrate that a major and prolonged climatic shift occurred over the NENA sector after a series of 13th century volcanic eruptions centered around the A.D. 1257 Samalas event. This shift marked the end of the Medieval Climate Anomaly and the beginning of the Little Ice Age in this sector.

Similarly, the series of eruptions centered around the A.D. 1815 Tambora event shifted summer temperatures to the coldest 40-year period of the last 1100 years in NENA. The A.D. 1815-1857 episode was extremely cold in Eastern Canada, with decadal anomalies reconstructed by STREC ranging from -2.76 to -3.58°C relative to the

last decade (Table S3). Low solar activity during this period, that started during the Dalton Minimum, could have concurred to cause the cooling episode (39). However, the regime shift observed in STREC coincides with the A.D. 1815 Tambora eruption (Figs. 4b and S4). The same climate shift has already been observed in a 263-year tree-ring based summer temperature reconstruction whose sampling sites are 400 km eastward from our study sites (7), whereas a pollen-based temperature reconstruction suggests that this period was the coldest of the last 2000 years in the North American boreal forest and forest-tundra (5). This climate shift was probably limited to the NENA sector as STREC diverges from the ensemble of Northern Hemisphere reconstructions and simulations after A.D. 1816 (Fig. S3c,d).

Although the last century reconstructed by STREC was warmer than the early 19th century, it was colder than the Medieval Climate Anomaly (the difference between the average summer temperature of the 12th century and of the last 100 years is 1.66°C, $p<0.001$ according to the one-tailed Wilcoxon rank-sum test). In fact, STREC shows that the NENA sector experienced relatively cold conditions until late into the 20th century. This persistence of cold conditions over NENA is also suggested by the strong warming trend of the last 100 years denoting a colder starting point (Fig. 1a,b), as well as by permafrost growth during the mid 20th century on the southern shore of Hudson Strait (40) and by the lack of post-fire forest recovery over the last 900 years at the northern Quebec treeline in contrast to what occurred during the Medieval Climate Anomaly (41, 42). The warming trend in our study area has accelerated over the last 30 years (+0.7°C per decade according to the dataset CRU TS3.20). If this trend continues, then summer temperatures will be similar to the maximum of the last 750 years during the next decade and to the maximum of the last 1100 years during the following one (based on STREC and the data of Table S3).

Several hypothesis have been suggested to explain why post-eruption temperature anomalies reconstructed from tree-ring data generally express higher values than expected, including regional variations in response to volcanic events, autocorrelation in

ring-width series (17, 18), failure of growth rings to form during volcano-induced cold summers (20), and increased tree growth caused by volcano-induced diffuse radiation (43). In this study we observed a strong response of ring-width data to volcanic activity, with the amplitudes and duration of negative anomalies (including persistent regime shifts) similar to model predictions. Diagnostic light rings are frequent in black spruce trees of our study area (44), thus allowing for a rigorous control of ring dating and for indentifying the occurrence of missing rings. In addition, although autocorrelation in ring-width chronologies of black spruce is high (Table 1), the results of a simple model show that its effects on the amplitude and duration of reconstructed negative temperature anomalies after volcanic events are low (Fig. S6). Instead, our results suggest that the climatic impacts of eruptions vary amongst regions of the Northern Hemisphere and that the NENA sector is especially sensitive to these impacts as compared to Eurasia, where the majority of temperature-sensitive tree-ring chronologies have been previously developed. This idea is also supported by recent simulation experiments (12-16, 22), which show that large and successive eruptions may trigger cold episodes whose duration may be sustained by complex and variable sea-ice-ocean feedbacks in the North Atlantic and that the resultant northward heat transport would tend to be more severely attenuated in the NENA than in the Eurasian sectors.

3.2.5 Methods

Our sampling area is situated in the Eastern Canadian taiga between latitudes 53.8 and 54.6 N and longitudes 70.2 and 72.5 W (Table 1). According to the gridded temperature dataset CRU TS3.20 (26), this region has experienced one of the fastest temperature increases on Earth during the last century. The mean July-August temperature, which is the object of our reconstruction, has increased by an average of 0.68 ± 0.15°C and 0.19 ± 0.02°C (estimate ± SE) each 10 years during the last 30 and the last 110 years, respectively.

To implement our network of tree-ring chronologies, 1782 black spruce (*Picea mariana* (Mill.) B.S.P.) subfossil trees were sampled from six lakes of the study area and crossdated to the calendar year. Particular care was taken in selecting and replicating sites and trees in order to construct a dataset suitable for Regional Curve Standardization (RCS). The RCS method preserves long-term climate trends in tree-ring chronologies built with short-lived species, but requires high replication of trees belonging to a homogeneous population not disturbed by external factors (45). The selected sites were all characterized by an old-growth riparian forest on the leeward side of the lake, an abrupt forest-lake transition, large stocks of subfossil trees in the littoral zone, and a well-documented low fire recurrence (23, 46). This allowed the development of an exceptional network of climate-sensitive tree-ring data comprising six local chronologies in the same region (one per lake), each composed from 75 to 586 subfossil trees and spanning from 1238 to 1440 years (Table 1). The living trees extending the chronologies to the present-day (25 trees per site) were sampled at the same sites as the subfossil samples and issues related to tree selection and sampling height were also considered (see below).

To produce the six local chronologies (Fig. S3), two radii were measured at a precision of 1/100 mm and then averaged for each tree. A spline with a 50% frequency cut-off and a time-varying response (starting from 10 years and increasing of one each year; 47) was used as smoothing algorithm to generate the local growth curves needed for RCS standardization. All specimens had well-preserved piths, and pith offset could easily be accounted for in the chronology development.

To guarantee homogeneity between subfossil and living samples, the 25 living trees at each site were selected among those growing near the lakeshore, as they would be the most likely to have generated subfossil stems (37). Furthermore, we considered that the growth trends of subfossil and living samples can diverge depending on the sampling height of the living trees (48), thus generating biases in the RCS chronologies. To reduce these biases, we sampled all living trees at four meters above the soil surface

(i.e. the sampling height that minimized the differences between the growth trends of living and subfossil trees) and we corrected all ring-width series before standardization by subtracting the difference between the local growth curves of the living and subfossil trees (see Figs. S1 and S2).

All the non-robust time intervals of the local RCS chronologies were discarded, with the resulting gaps being reconstructed using the analogue method (49). Most of these intervals were asynchronous amongst the lakes and were caused by wildfires that temporarily reduced the inputs of tree remains into the littoral zone (23, 46). We identified the non-robust time intervals using the Rbar statistic (mean correlation between pairs of individual series) over 31-year moving windows and discarded all intervals with negative or non-computable Rbar values due to low replication. At lake L16, the 1978-2011 period was also discarded as the construction of a road raised the lake water level and disturbed the riparian trees. Over the 1102 years retained for STREC (see below), we discarded 114, 70, 52, 19, 0, and 31 years for lakes L1, L12, L16, L18, L20, and L22, respectively. The analogue method employed to reconstruct these gaps is commonly used in paleoclimatology to infill proxy-climate matrices containing missing values. The procedure is based on the identification, for each year where no value exists, of the most similar years in the calibration period, i.e., all other years where values exist, that are weighted according to their similarity and used to reconstruct the gaps (49). The measure of similarity is based on the Euclidian distance.

We used the CRU TS3.20 climate dataset (26) to calibrate our reconstruction. The first four years (1901-1904) were excluded because of a poor fit with the tree-ring indexes due to the lack of operating weather stations at the beginning of the last century near the study area. The climate reconstruction method was based on a linear scaling procedure. Each local RCS chronology was rescaled so that its mean and standard deviation matched those of the July-August mean temperature in the calibration period (1905-2011). The final STREC was then obtained by computing the median of the six local reconstructions. This approach attenuated the influence of local non-climatic

disturbances, as the median of the six reconstructions is not sensitive to outliers. It also obtained better cross-calibration-verification results (1905-1957 vs 1958-2011) than a reconstruction based on a partial least squares regression, especially when considering low frequencies (i.e. smoothed datasets; Table S1). Only reconstructed values subsequent to A.D. 910 were retained to limit the analyzed period to the statistically reliable interval (overall replication >53 individual series and Expressed Population Signal >0.85; Fig. 1c,e). Due to the fast temperature increase in the study area during the 20th century, the reconstructed values in the calibration encompassed a range of 4.3°C (from 9.6 to 14.0°C), and 86% of the total STREC reconstructed values are inside this range.

We generated realistic time-varying confidence intervals considering two kinds of errors (Fig. 1a,b). The first one depends on the non-perfect fit between observed and reconstructed values over the verification periods and was computed as the mean root-mean-square error between the two datasets. The second one is due to the variation over time of the strength of the common climate signal for each of the six local chronologies and was computed each year as the interval among the four central reconstructed values from the six chronologies. The consideration of this error produces a time-varying 60% confidence interval.

The volcanic signature in STREC was analyzed using Superimposed Epoch Analysis (SEA) and Bayesian hidden Markov models. We employed SEA to test the agreement between the strongest volcanic eruptions of the last millennium and corresponding cooling episodes in STREC. Our SEA was performed in the R environment as described in the SI Methods. We used Bayesian hidden Markov models to identify sudden changes in the STREC time series. Such models provide an explicit mechanism to represent transitions between different states and allowed the data to be classified into distinct regimes. The Schwarz criterion is used to identify the number of states and the probability distribution that best fits the data. This approach is briefly described in the SI Methods.

All tree-ring and temperature data are included in the Database S1 and will be available from the World Data Center for Paleoclimatology (http://www.ncdc.noaa.gov/paleo/paleo.html).

3.2.6 Acknowledgments

The authors wish to thank Julia Autin, Yves Bouthillier, Pierre-Paul Dion, Sébastien Dupuis, Benjamin Dy, and Joëlle Marion for field and laboratory assistance, Aurore Catalan for technical assistance and Joel Guiot for its comments on the paper. This research is a contribution from the ARCHIVES project and was financially supported by NSERC, Hydro-Quebec, Ouranos, ArcticNet, the EnviroNorth training program, and the Centre for Northern Studies.

3.2.7 References

1. Jansen E, et al. (2007) Palaeoclimate. In: Climate Change 2007: The Physical Science Basis. Contribution of Working Group I to the Fourth Assessment Report of the Intergovernmental Panel on Climate Change, eds Solomon S, Qin D, Manning M, Chen Z, Marquis M, Averyt KB, Tignor M, Miller HL (Cambridge University Press, Cambridge and New York), pp 433-497.

2. Jones PD, et al. (2009) High-resolution palaeoclimatology of the last millennium: a review of current status and future prospects. Holocene 19(1):3-49.

3. Stahle DW, et al. (2012) Tree-ring analysis of ancient baldcypress trees and subfossil wood. Quat Sci Rev 34:1-15.

4. Pages 2k Consortium (2013) Continental-scale temperature variability during the past two millennia. Nat Geosci 6:339-346.

5. Viau AE, Ladd M, Gajewski K (2012) The climate of North America during the past 2000 years reconstructed from pollen data. Glob Planet Change 84-85:75-83.

6. D'Arrigo R, Wilson R, Jacoby G (2006) On the long-term context for late twentieth century warming. J Geophys Res Atmos 111(D3):D03103

7. Jacoby GC, Ivanciu IS, Ulan LD (1988) A 263-year record of summer temperature for northern Quebec reconstructed from tree-ring data and evidence of a major climatic shift in the early 1800's. Palaeogeogr Palaeoclimatol Palaeoecol 64(1-2):69-78.

8. Lavigne F, et al. (2013) Source of the great A.D. 1257 mystery eruption unveiled, Samalas volcano, Rinjani Volcanic Complex, Indonesia. Proc Natl Acad Sci USA 110(42):16742-16747.

9. Gao C, Robock A, Ammann C (2008) Volcanic forcing of climate over the past 1500 years: An improved ice core-based index for climate models. J Geophys Res Atmos 113(23):D23111.

10. Crowley TJ (2000) Causes of Climate Change Over the Past 1000 Years. Science 289(5477):270-277.

11. Cole-Dai J, et al. (2009) Cold decade (AD 1810-1819) caused by Tambora (1815) and another (1809) stratospheric volcanic eruption. Geophys Res Lett 36(22):L22703.

12. Schleussner CF, Feulner G (2013) A volcanically triggered regime shift in the subpolar North Atlantic Ocean as a possible origin of the Little Ice Age. Climate of the Past 9(3):1321-1330.

13. Zhong Y, et al. (2011) Centennial-scale climate change from decadally-paced explosive volcanism: A coupled sea ice-ocean mechanism. Climate Dynamics 37(11-12):2373-2387.

14. Zanchettin D, et al. (2012) Bi-decadal variability excited in the coupled ocean-atmosphere system by strong tropical volcanic eruptions. Climate Dynamics 39(1-2):419-444.

15. Stenchikov G, et al. (2009) Volcanic signals in oceans. J Geophys Res Atmos 114(D16):D16104.

16. Otterå OH, Bentsen M, Drange H, Suo L (2010) External forcing as a metronome for Atlantic multidecadal variability. Nat Geosci 3(10):688-694.

17. D'Arrigo R, Wilson R, Anchukaitis KJ (2013) Volcanic cooling signal in tree ring temperature records for the past millennium. J Geophys Res Atmos 118(16):9000-9010.

18. Esper J, et al. (2013) European summer temperature response to annually dated volcanic eruptions over the past nine centuries. Bulletin of Volcanology 75(7):1-14.

19. Breitenmoser P, et al. (2012) Solar and volcanic fingerprints in tree-ring chronologies over the past 2000years. Palaeogeogr Palaeoclimatol Palaeoecol 313-314:127-139.

20. Mann ME, Fuentes JD, Rutherford S (2012) Underestimation of volcanic cooling in tree-ring-based reconstructions of hemispheric temperatures. Nat Geosci 5(3):202-205.

21. Briffa KR, Jones PD, Schweingruber FH, Osborn TJ (1998) Influence of volcanic eruptions on Northern Hemisphere summer temperature over the past 600 years. Nature 393(6684):450-455.

22. Miller GH, et al. (2012) Abrupt onset of the Little Ice Age triggered by volcanism and sustained by sea-ice/ocean feedbacks. Geophys Res Lett 39(2):L02708.

23. Gennaretti F, Arseneault D, Bégin Y (2013) Millennial stocks and fluxes of large woody debris in lakes of the North American taiga. J Ecol Article in press.

24. Évin G, Merleau J, Perreault L (2011) Two-component mixtures of normal, gamma, and Gumbel distributions for hydrological applications. Water Resour Res 47(8):W08525.

25. Perreault L, Garçon R, Gaudet J (2007) Analyse de séquences de variables aléatoires hydrologiques à l'aide de modèles de changement de régime exploitant des variables atmosphériques. Modelling hydrologic time series using regime switching models and measures of atmospheric circulation (Translated from French) Houille Blanche (6):111-123 (in French).

26. Mitchell TD, Jones PD (2005) An improved method of constructing a database of monthly climate observations and associated high-resolution grids. International journal of climatology 25(6):693-712.

27. Moberg A, Sonechkin DM, Holmgren K, Datsenko MH, Karlén W (2005) Highly variable Northern Hemisphere temperatures reconstructed from low- and high-resolution proxy data. Nature 433(7026):613-617.

28. Mann ME, Bradley RS, Hughes MK (1999) Northern hemisphere temperatures during the past millennium: Inferences, uncertainties, and limitations. Geophys Res Lett 26(6):759-762.

29. Cook ER, Esper J, D'Arrigo RD (2004) Extra-tropical Northern Hemisphere land temperature variability over the past 1000 years. Quat Sci Rev 23(20-22):2063-2074.

30. Jones PD, Briffa KR, Barnett TP, Tett SFB (1998) High-resolution palaeoclimatic records for the last millennium: Interpretation, integration and comparison with General Circulation Model control-run temperatures. Holocene 8(4):455-471.

31. Plattner GK, Joos F, Stocker TF, Marchal O (2001) Feedback mechanisms and sensitivities of ocean carbon uptake under global warming. Tellus B Chem Phys Meteorol 53(5):564-592.

32. Petoukhov V, et al. (2000) CLIMBER-2: A climate system model of intermediate complexity. Part I: Model description and performance for present climate. Climate Dynamics 16(1):1-17.

33. Montoya M, et al. (2005) The earth system model of intermediate complexity CLIMBER-3α. Part I: Description and performance for present-day conditions. Climate Dynamics 25(2-3):237-263.

34. Boulanger Y, et al. (2012) Dendrochronological reconstruction of spruce budworm (Choristoneura fumiferana) outbreaks in southern Quebec for the last 400 years. Can J For Res 42(7):1264-1276.

35. Schwarz G (1978) Estimating the Dimension of a Model. Ann Stat 6(2):461-464.

36. Kaufman DS, et al. (2009) Recent warming reverses long-term arctic cooling. Science 325(5945):1236-1239.

37. Esper J, et al. (2012) Orbital forcing of tree-ring data. Nat Clim Chang 2(12):862-866.

38. Miller GH, Lehman SJ, Refsnider KA, Southon JR, Zhong Y (2013) Unprecedented recent summer warmth in Arctic Canada. Geophys Res Lett 40(21):5745-5751.

39. Wagner S, Zorita E (2005) The influence of volcanic, solar and CO2 forcing on the temperatures in the Dalton Minimum (1790-1830): A model study. Climate Dynamics 25(2-3):205-218.

40. Kasper JN, Allard M (2001) Late-Holocene climatic changes as detected by the growth and decay of ice wedges on the southern shore of Hudson Strait, northern Québec, Canada. Holocene 11(5):563-577.

41. Payette S, Morneau C (1993) Holocene Relict Woodlands at the Eastern Canadian Treeline. Quaternary Research 39(1):84-89.

42. Payette S, Filion L, Delwaide A (2008) Spatially explicit fire-climate history of the boreal forest-tundra (Eastern Canada) over the last 2000 years. Philos Trans R Soc Lond B Biol Sci 363(1501):2301-2316.

43. Robock A (2005) Cooling following large volcanic eruptions corrected for the effect of diffuse radiation on tree rings. Geophys Res Lett 32(6):1-4.

44. Filion L, Payette S, Gauthier L, Boutin Y (1986) Light rings in subarctic conifers as a dendrochronological tool. Quaternary Research 26(2):272-279.

45. Esper J, Cook ER, Krusic PJ, Peters K, Schweingruber FH (2003) Tests of the RCS method for preserving low-frequency variability in long tree-ring chronologies. Tree-ring research 59(2):81-98.

46. Arseneault D, Dy B, Gennaretti F, Autin J, Bégin Y (2013) Developing millennial tree ring chronologies in the fire-prone North American boreal forest. Journal of quaternary science 28(3):283-292.

47. Melvin TM, Brifffa KR, Nicolussi K, Grabner M (2007) Time-varying-response smoothing. Dendrochronologia 25(1):65-69.

48. Clyde MA, Titus SJ (1987) Radial and longitudinal variation in stem diameter increment of lodgepole pine, white spruce, and black spruce: species and crown class differences. Can J For Res 17(10):1223-1227.

49. Guiot J, et al. (2005) Last-millennium summer-temperature variations in western Europe based on proxy data. Holocene 15(4):489-500.

3.2.8 Tables

Table 3-1. Sampling sites and tree-ring chronologies used for STREC.

Site	Latitude (°)	Longitude (°)	Number of trees (subfossil / living)	Length (A.D.)	MSL (years ± SD)	Mean ring width (1/100 mm ± SD)	Mean correlation (mean ± SD)	Lag1 AC	AR order
L1	+53.86	-72.41	190/25	642-2011	106±32	39±24	0.43±0.25	0.84	4
L12	+54.46	-70.39	220/25	572-2011	101±32	42±23	0.45±0.23	0.78	9
L16	+54.10	-71.63	75/25	774-2011	112±36	37±20	0.46±0.25	0.75	10
L18	+54.25	-72.38	419/25	596-2011	105±38	38±26	0.40±0.27	0.76	4
L20	+54.56	-71.24	586/25	653-2011	102±36	40±24	0.41±0.23	0.72	9
L22	+54.15	-70.29	292/25	650-2011	104±38	39±25	0.42±0.25	0.73	6

"MSL" is mean segment length. "Mean correlation" is average correlation between standardized individual series and their respective local RCS chronology. "Lag1 AC" is lag 1 autocorrelation of the RCS chronology. "AR order" is the order selected by the Akaike Information Criterion of the autoregressive model fitted to the RCS chronology. "Lag1 AC" and "AR order" are computed over the time period retained for STREC (A.D. 910-2011).

3.2.9 Figures

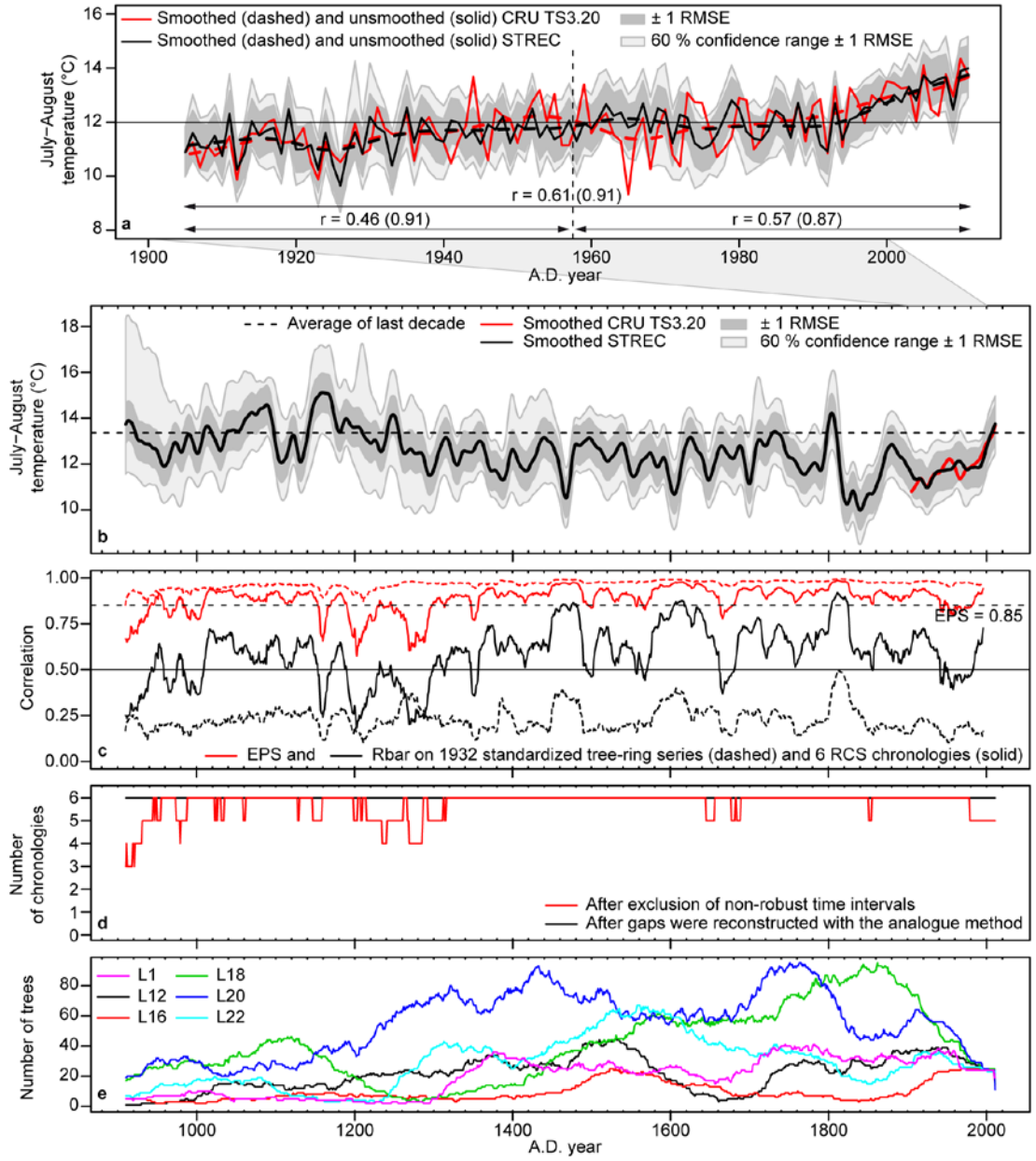

Fig. 3-1. STREC reconstructed values and robustness. Observed (15 cells of the CRU TS3.20 dataset covering our sampling sites) and reconstructed (STREC) July-August temperatures in the taiga of Eastern Canada during the last century (**a**) and the last 1100 years (**b**). Smoothed values are 20-year splines. In **a**, correlations between brackets refer

to smoothed values. Expressed Population Signal (EPS) and Rbar statistics computed over 31-year moving windows are also shown (**c**), as well as replication among (**d**) and within (**e**) chronologies.

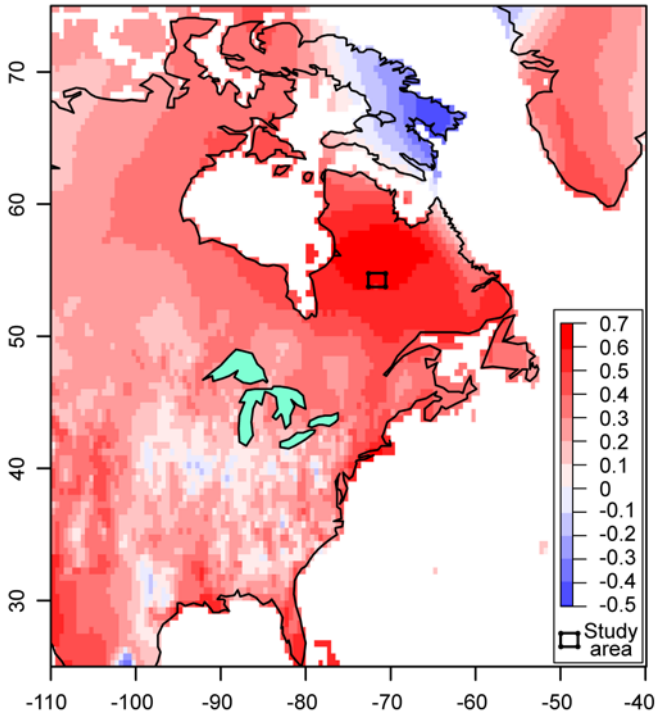

Fig. 3-2. STREC spatial domain. Spatial variation of the correlation between observed (CRU TS3.20) and reconstructed (STREC) July-August temperatures over the 1905-2011 period.

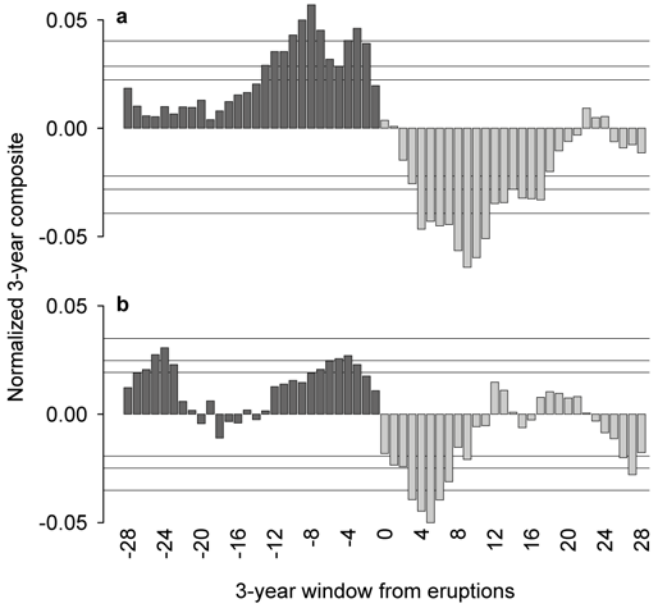

Fig. 3-3. STREC responses to volcanic eruptions. Dimensionless normalized 3-year composites which are the result of the Superimposed Epoch Analysis showing summer temperature responses in Eastern Canada to the 10 strongest (**a**) and 10 strong (**b**) volcanic eruptions of the last millennium deduced by ref. 9 (see SI Methods). Each 3-year composite is labeled with the year nearest to the eruption year (e.g. 0 stands for the 3-year composite composed of years 0, 1, and 2 from eruption). Confidence ranges (90%, 95%, 99%) are indicated by horizontal lines. Black and grey columns mark pre and post eruption composites.

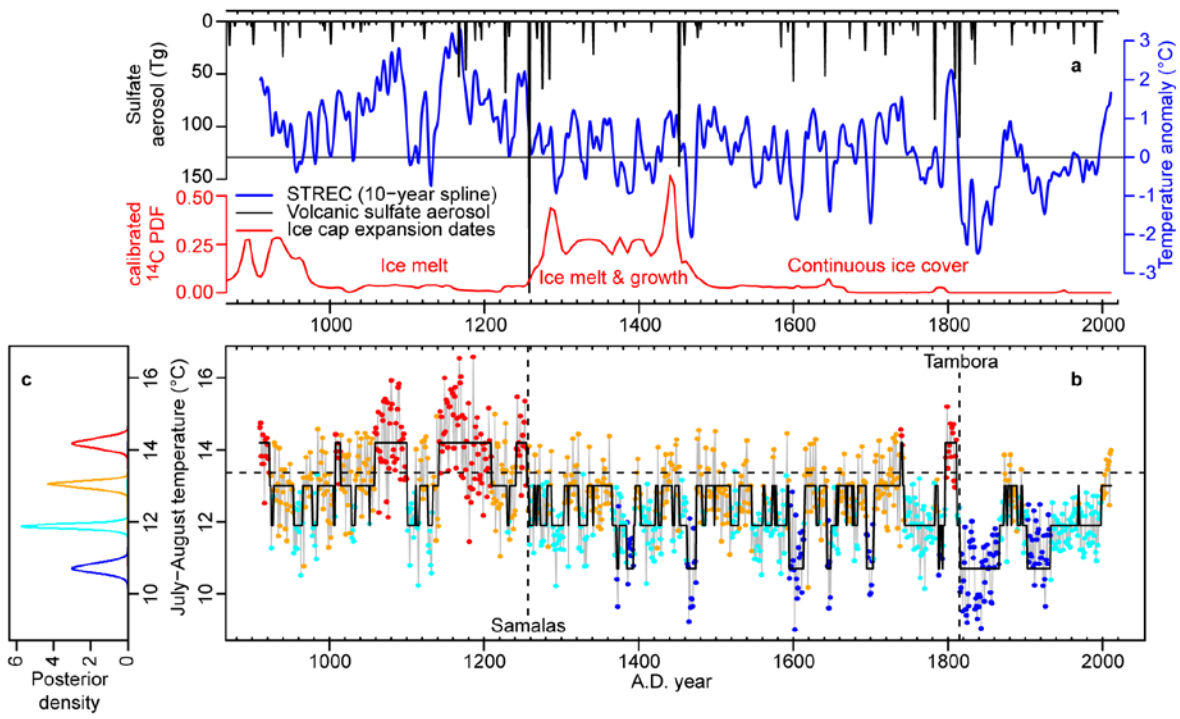

Fig. 3-4. Volcano-induced regime shifts in STREC. Comparison (**a**) between STREC, a reconstruction of global stratospheric volcanic sulfate aerosol injections (9) and a reconstruction of ice-cap expansion dates from Arctic Canada (22). Detected regime shifts in STREC based on a four-component Bayesian hidden Markov model with normal probability distributions (SI Methods) are also shown (**b**), as well as the posterior probability density functions of the mean temperature of each regime (**c**). in **b**, each reconstructed value is assigned to the most likely regime (color dots) and the mean temperature of the last decade is shown (horizontal dashed lines), as well as the dates of the A.D. 1257 Samalas and A.D. 1815 Tambora eruptions (vertical dashed lines).

3.2.10 Supporting information

SI Methods - Superimposed Epoch Analysis.

The Superimposed Epoch Analysis (SEA) is a statistical method that can be used to verify the presence and the significance of systematic responses in a dataset related to particular events occurring during key dates. We employed SEA to test the striking agreement between the occurrence of the major volcanic eruptions of the last millennium and some cooling episodes inferred by STREC (summer temperature reconstruction for Eastern Canada). Our analysis was implemented as proposed by ref. 1, which employed SEA to study connections between explosive volcanic eruptions and subsequent El Niño climate episodes. Our SEA was performed in the R environment according to the following steps:

First, two subsets of key volcanic dates from the last millennium were selected using the reconstruction of the global stratospheric volcanic sulfate aerosol injections of ref. 2. The 10 years with the highest sulfate aerosol loadings and the 10 years with loading values just below the preceding ones were considered as key dates corresponding to the 10 strongest and the 10 next strongest volcanic eruptions, respectively.

Second, the key volcanic dates were then used to generate two "eruption matrices" with the number of rows equal to the number of eruptions. In each row, we stacked the 30 STREC reconstructed values for each pre and post eruption date. In this way, two matrices were created with each composed of 10 rows and 61 columns. The values in the matrices were then normalized to attenuate the influence of large anomalies that could have occurred before or after a particular key volcanic date. To do so, the values in each row were divided by the maximum value of the row and, subsequently, the overall mean of the values in each matrix was subtracted from all values.

Third, dimensionless normalized composites, which represent the mean response of summer temperatures in Eastern Canada to each subset of volcanic eruptions, were obtained by averaging the values of each column for each matrix. To evaluate the significance of the obtained composites, we used a Monte Carlo randomization procedure that reshuffles blocks of two values in each row of an eruption matrix, thus creating 10000 randomly generated eruption matrices. These matrices can then be used to generate 10000 sets of composites and, subsequently, a random composite distribution for any specific year from a volcanic eruption (in our case 61 distributions). We used these distributions to test the significance of the obtained composites at the 90%, 95%, and 99% confidence levels. The Monte Carlo randomization procedure is based on reshuffling blocks of two values rather than individual values because this allows randomly generated eruption matrices to be obtained with first-order autocorrelations similar to the original ones.

Fourth, to smooth out annual variations in the results of the SEA, we generated 3-year mean composites from the obtained composites and random 3-year mean composite distributions from the 10000 randomly generated sets of composites. The final results are illustrated in Fig. 3 and show that the 10 major volcanic eruptions of the last millennium have produced highly significant cooling episodes in Eastern Canada that lasted for about two decades, while less intense volcanic eruptions had a shorter influence. For this reason, we decided also to test, if the 20 or 10 post-event summers were significantly colder than the preceding ones, for each of the 10 strongest and each of the 10 next strongest volcanic eruptions, respectively. The statistical test used was a one-tailed Wilcoxon rank-sum test (Table S2).

SI Methods - Bayesian analysis of regime shifts.

Regime shifts in the STREC time series were analyzed using a mixture of probability distributions to which a persistence structure was added. Such probabilistic models are often called hidden Markov models (HMM). Here, they provided an explicit

and formal mechanism to detect shifts in the STREC time series and the length of "warm" and "cold" sequences (i.e. the regimes).

Hidden Markov models are useful when it is suspected that observations in time exhibit persistence in several regimes with occasional transitions between them. While the observations come from distinct populations, it is not possible to identify exactly when the changes took place. Hidden Markov models are typically specified through a hierarchical structure. In the first level, the way in which the transitions from one state to another occur is formalized. This is done by assuming that the "hidden" states follow a Markov process. The shifts and the persistence of each regime are governed by state transition probabilities. The second level represents the process which generates the data, given the current regime. For a given year, the data is generated from a statistical distribution whose parameters depend upon the current regime. In this study, two statistical probability distributions have been considered: a normal distribution and a lognormal distribution.

The parameters of the models (means, standard deviations, transition probabilities) are estimated using a Bayesian approach, as presented in details in ref. 3. The estimation process involves Monte Carlo Markov Chain simulations (MCMC), since no explicit algebraic solutions are available for the parameter estimates of such models. More specifically we used Gibbs sampling.

Twelve configurations were considered to model the STREC time series. Bayesian HMM with one to six regimes and two probability distributions were applied (normal and lognormal). In this paper, we chose to compute the Schwarz information criterion (4) in order to select the best representation of the STREC time series between the competing models. The Schwarz criterion was calculated for each of the 12 configurations and allowed us to formally identify both the number of regimes and which probability distribution best fits the STREC time series. It is important to mention that this criterion takes into account both the statistical goodness of fit and the number of

parameters that have to be estimated to achieve this particular degree of fit by imposing a penalty for increasing the number of parameters. We recall that we gave preference to the model that maximized the Schwarz criterion.

The estimation of the twelve HMM and the computation of their respective Schwarz criterion were performed in the MATLAB environment using codes developed by ref. 3. The first step in Bayesian analysis is to set up a full probability model. That is, in addition to modeling the observable quantities (i.e. the STREC data) using a HMM, we must represent the prior degree of belief concerning all the unknowns (i.e. the parameters of the model: means, standard deviations, and transition probabilities). Here we considered non-informative prior distributions for each parameter and let the data talk for itself. In our case, the Schwarz criterion reported evidence in favour of a 4-state Bayesian HMM with normal distributions. This result, which states that a normal distribution is more suitable than a lognormal distribution for our data, is not surprising. In fact, in most meteorological and climatological studies, temperatures are assumed to be normally distributed.

In the Bayesian framework, all statistical inferences about the unknown parameters are based on the posterior distribution. Just as the prior distribution reflects beliefs about the parameters of the HMM prior to experimentation, the posterior distribution reflects the updated beliefs after observing the sample data. Fig. 4c represents the posterior distributions of the mean temperature of each regime. These distributions do not superimpose, which indicates significant differences between the average temperatures of the four regimes. Furthermore, the bottom panels of Fig. S4 show the posterior distributions of the transition probability p_{kk} of each regime and indicate a strong persistence with a probability to stay in a given regime k greater than 0.8 for all regimes.

Finally, the posterior probabilities of each observation to belong to a given regime can be evaluated. These are presented in Fig. S4 for each regime. These graphs can be

used to locate sudden changes from one regime to another and identify historical sequences of warm or cold temperatures that may have occurred.

Supporting References

1. Adams JB, Mann ME, Ammann CM (2003) Proxy evidence for an El Niño-like response to volcanic forcing. *Nature* 426(6964):274-278.

2. Gao C, Robock A, Ammann C (2008) Volcanic forcing of climate over the past 1500 years: An improved ice core-based index for climate models. *J Geophys Res Atmos* 113(23):D23111.

3. Évin G, Merleau J, Perreault L (2011) Two-component mixtures of normal, gamma, and Gumbel distributions for hydrological applications. *Water Resour Res* 47(8):W08525.

4. Schwarz G (1978) Estimating the Dimension of a Model. *Ann Stat* 6(2):461-464.

5. Jansen E, et al. (2007) *Palaeoclimate. In: Climate Change 2007: The Physical Science Basis. Contribution of Working Group I to the Fourth Assessment Report of the Intergovernmental Panel on Climate Change*, eds Solomon S, Qin D, Manning M, Chen Z, Marquis M, Averyt KB, Tignor M, Miller HL (Cambridge University Press, Cambridge and New York), pp 433-497.

6. Moberg A, Sonechkin DM, Holmgren K, Datsenko MH, Karlén W (2005) Highly variable Northern Hemisphere temperatures reconstructed from low- and high-resolution proxy data. *Nature* 433(7026):613-617.

7. Mann ME, Bradley RS, Hughes MK (1999) Northern hemisphere temperatures during the past millennium: Inferences, uncertainties, and limitations. *Geophys Res Lett* 26(6):759-762.

8. Cook ER, Esper J, D'Arrigo RD (2004) Extra-tropical Northern Hemisphere land temperature variability over the past 1000 years. *Quat Sci Rev* 23(20-22):2063-2074.

9. Jones PD, Briffa KR, Barnett TP, Tett SFB (1998) High-resolution palaeoclimatic records for the last millennium: Interpretation, integration and comparison with General Circulation Model control-run temperatures. *Holocene* 8(4):455-471.

10. D'Arrigo R, Wilson R, Jacoby G (2006) On the long-term context for late twentieth century warming. *J Geophys Res Atmos* 111(D3):D03103

11. Montoya M, et al. (2005) The earth system model of intermediate complexity CLIMBER-3α. Part I: Description and performance for present-day conditions. *Climate Dynamics* 25(2-3):237-263.

12. Petoukhov V, et al. (2000) CLIMBER-2: A climate system model of intermediate complexity. Part I: Model description and performance for present climate. *Climate Dynamics* 16(1):1-17.

13. Plattner GK, Joos F, Stocker TF, Marchal O (2001) Feedback mechanisms and sensitivities of ocean carbon uptake under global warming. *Tellus B Chem Phys Meteorol* 53(5):564-592.

14. Mitchell TD, Jones PD (2005) An improved method of constructing a database of monthly climate observations and associated high-resolution grids. *International journal of climatology* 25(6):693-712.

15. Cook ER, Kairiukstis LA (1990) *Methods of Dendrochronology: Applications in the Environmental Sciences*, (Kluwer Academic Publishers, Dordrecht), pp xii+394.

16. Fritts HC (1976) *Tree Rings and Climate*, (Academic Press, London, New York and San Francisco), pp xiii+567.

17. Briffa KR, Jones PD, Pilcher JR, Hughes MK (1988) Reconstructing summer temperatures in northern Fennoscandinavia back to AD 1700 using tree-ring data from Scots pine. *Arctic and Alpine Research* 20(4):385-394.

Supporting Tables

Table 3-S1. Summary of the cross-calibration verification results for the reconstruction of July-August temperatures using two different reconstruction methods, a linear scaling procedure as in STREC and a reconstruction based on a partial least squares regression (PLS-R). 15 cells of the CRU TS3.20 dataset (14) covering our sampling sites are used as climate reference.

Statistics	Calibration over 1905-1957 (STREC / PLS-R)	Calibration over 1958-2011 (STREC / PLS-R)	Calibration over 1905-2011 (STREC / PLS-R)
Mean temp. of the 1905-2011 period (°C ± SD)	11.9±0.8 / 11.7±0.5	11.8±1.0 / 11.7±0.8	11.9±0.8 / 11.9±0.7
Correlation over verification period	0.55 / 0.51	0.50 / 0.40	
Correlation over calibration period	0.44 / 0.53	0.55 / 0.68	
Correlation over total period	0.60 / 0.60	0.61 / 0.65	0.61 / 0.68
RMSE over verification period (°C)	0.88 / 0.93	0.81 / 0.79	
RMSE over calibration period (°C)	0.77 / 0.66	0.92 / 0.77	
RMSE over total period (°C)	0.83 / 0.81	0.87 / 0.78	0.81 / 0.73
Significance of FDST over verification	1.00 / 1.00	0.76 / 0.99	
Significance of FDST over calibration	0.96 / 0.96	0.99 / 1.00	
Significance of FDST over total	1.00 / 1.00	0.98 / 1.00	1.00 / 1.00
RE	0.52 / 0.47	0.44 / 0.46	0.34 / 0.46*
CE	0.28 / 0.19	-0.07 / -0.02	
RE on smoothed datasets (20-year spline)	0.85 / 0.73	0.90 / 0.70	0.83 / 0.90*
CE on smoothed datasets (20-year spline)	0.66 / 0.40	0.58 / -0.17	

"FDST" is first difference sign test (15), "RE" is reduction of error (16), and "CE" is coefficient of efficiency (17).
* Computed over the total period and using the corresponding mean temperature as a reference.

Table 3-S2. Results of the Wilcoxon rank-sum test (one-tailed) used to verify if the 20 or 10 post-event summers inferred by STREC were significantly colder than the preceding ones, for each of the 10 strongest and each of the 10 next strongest volcanic eruptions of the last millennium (deduced by ref. 2), respectively.

Year of sulfate peak	Sulfate aerosol (Tg)	10 or 20 year pre-event mean (A; °C)	10 or 20 year post-event mean (B; °C)	B - A (°C)	P-value
10 strongest volcanic eruptions					
1167†	52.11	14.89	14.07	-0.83	0.02
1227†	67.52	13.06	13.18	0.12	0.54
1258†	257.91	13.70	12.43	-1.26	0.00
1275†	63.72	12.69	12.16	-0.53	0.06
1284†	54.70	12.47	11.90	-0.57	0.03
1452†	137.50	13.03	11.32	-1.71	0.00
1600†	56.59	11.97	11.44	-0.52	0.09
1783†	92.96	11.77	12.61	0.84	0.98
1809†	53.74	13.11	11.06	-2.05	0.00
1815†	109.72	13.55	10.58	-2.98	0.00
Composite†	NA	0.03*	-0.03*	-0.06*	0.00
10 next strongest volcanic eruptions					
1001‡	21.01	12.93	13.07	0.15	0.60
1176‡	45.76	14.84	13.49	-1.35	0.02
1341‡	31.14	12.46	12.46	0.00	0.43
1459‡	21.92	12.56	10.80	-1.76	0.00
1584‡	24.23	12.32	12.47	0.15	0.63
1641‡	51.59	12.47	11.37	-1.09	0.02
1693‡	27.10	12.85	11.07	-1.78	0.00
1719‡	31.48	12.99	13.08	0.09	0.76
1835‡	40.16	10.91	9.90	-1.01	0.01
1883‡	21.86	12.92	12.35	-0.57	0.02
Composite‡	NA	0.02*	-0.03*	-0.05*	0.00

"Composite" is the average result of 10 eruptions as obtained by the SEA.
* Dimensionless normalized units. † shows that 20 years pre and post the volcanic eruption are considered.
‡ shows that 10 years pre and post the volcanic eruption are considered.

Table 3-S3. Extreme decades and temperature increases reconstructed by STREC. Overlapping decades or periods are excluded from the analysis.

10 warmest decades			10 coldest decades			10 strongest temperature increases on a 30-year period		
Rank	Decade	Anomaly relative to 2002-2011 (°C)	Rank	Decade	Anomaly relative to 2002-2011 (°C)	Rank	Period	Increase (°C/10 years ± SE)
1/90	1161-1170	1.80	1/90	1835-1844	-3.58	1/26	1128-1157	1.48±0.20
2/90	1151-1160	1.68	2/90	1818-1827	-3.21	2/26	1600-1629	1.25±0.21
3/90	1086-1095	1.19	3/90	1465-1474	-2.94	3/26	1462-1491	1.15±0.23
4/90	1072-1081	1.00	4/90	1848-1857	-2.76	4/26	1778-1807	1.06±0.20
5/90	1141-1150	0.89	5/90	1602-1611	-2.69	5/26	1852-1881	1.06±0.15
6/90	1798-1807	0.87	6/90	1920-1929	-2.52	6/26	1697-1726	0.84±0.20
7/90	1061-1070	0.87	7/90	1695-1704	-2.41	7/26	1293-1322	0.83±0.15
8/90	1243-1252	0.83	8/90	1384-1393	-2.17	**8/26**	**1982-2011**	**0.78±0.11**
9/90	1184-1193	0.73	9/90	1905-1914	-2.14	9/26	1414-1443	0.74±0.15
10/90	910-919	0.61	10/90	1644-1653	-2.12	10/26	1229-1258	0.69±0.20
19/90	**2002-2011**	**0.00**	**78/90**	**2002-2011**	**0.00**			

Intervals ending in 2011 are in bold.

Supporting Figures

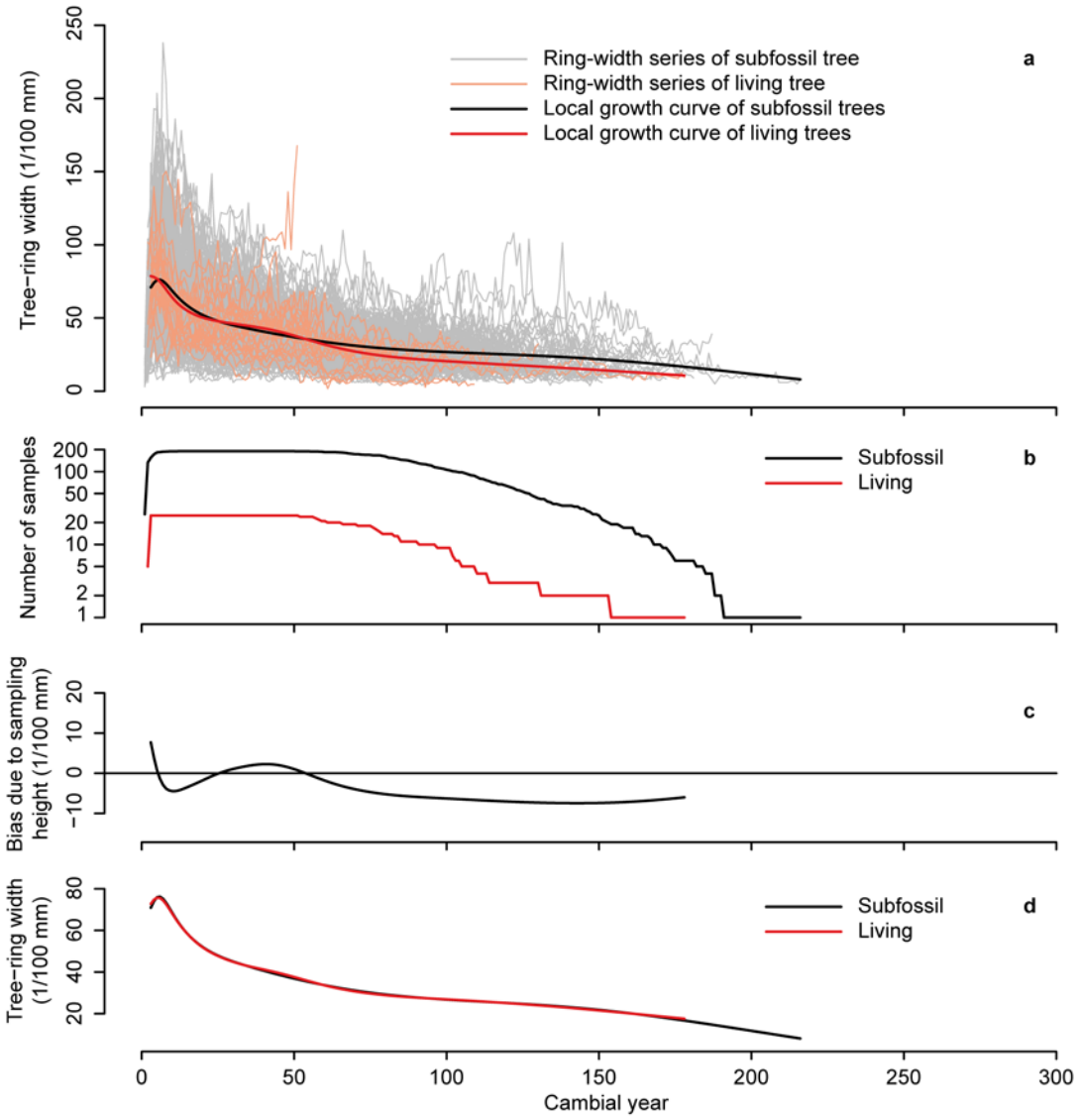

Fig. 3-S1. Local growth curves and homogenisation of subfossil and living tree materials. **a** shows the local growth curves of the subfossil and living trees at L1 (site chosen as example), **b** their sample replication (logarithmic y-axis), **c** the bias due to sampling height (i.e. difference between local growth curves of living and subfossil trees) and **d** the local growth curves after the bias is removed from all ring-width series of living trees.

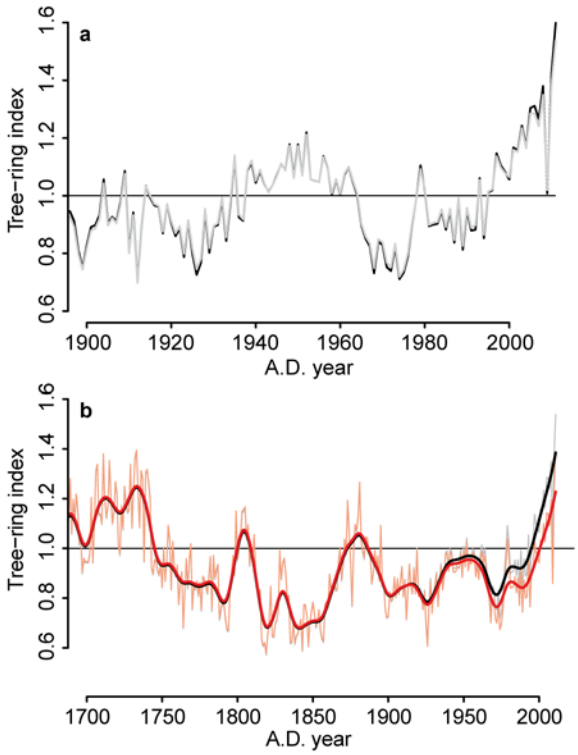

Fig. 3-S2. Effects of removing the sampling height bias from the tree-ring series of living trees. **a** shows the RCS chronologies of L1 (site chosen as example) derived from only living trees over the last century. The local RCS chronology from uncorrected ring-width series of living trees is in black, while the same chronology from corrected series (i.e. the bias due to sampling height is removed from all ring-width series and the local growth curve of subfossil trees is used for standardization) is in grey. a shows that the correction of the sampling height bias is not affecting the RCS standardization results (i.e. sampling height bias can be removed and the local RCS chronology remains unchanged). The corrected ring-width series of living trees can subsequently be used together with those of subfossil samples to develop an unbiased RCS chronology (black line in **b**). The local RCS chronologies of L1 without correction of sampling height bias on the tree-ring series of living trees is shown for comparison (red line in **b**). In **b**, 20-year splines were used to smooth the values.

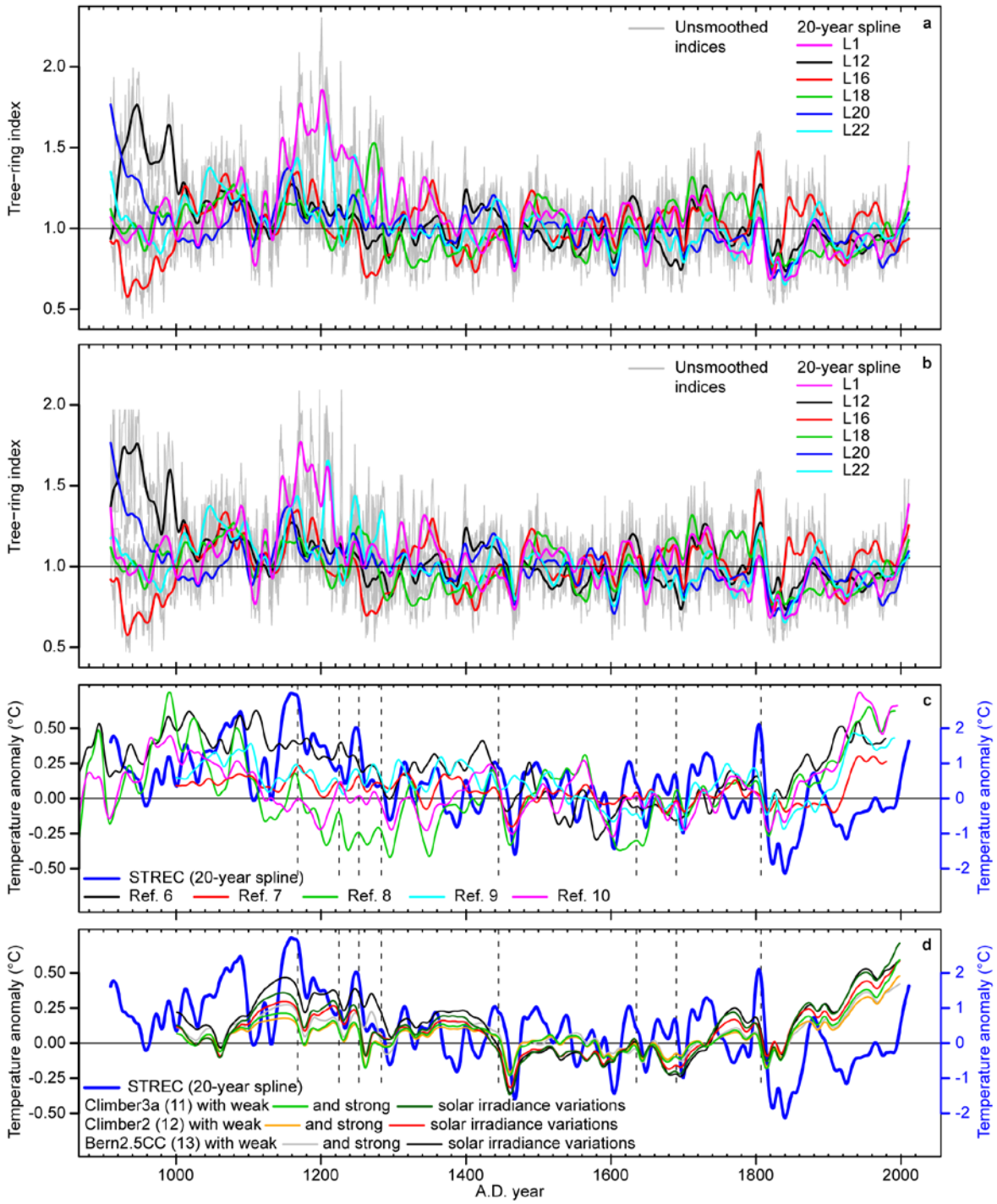

Fig. 3-S3. The network of millennial-long tree-ring chronologies and comparison between STREC and Northern Hemisphere records used in the IPCC-AR4. The two top panels show the six local RCS chronologies (one per lake and composed of living and subfossil trees) over the 1102 years retained for STREC before (**a**) and after (**b**) the

reconstruction of the non-robust time intervals (i.e. intervals for each local chronology where the Rbar statistic calculated over the 31-year moving windows is lower or equal to zero or non-computable because of low replication) using the analogue method. The two bottom panels show the comparison between STREC and five Northern Hemisphere temperature reconstructions (smoothed as plotted in Fig. 6.10 of ref. 5; **c**) and six Northern Hemisphere temperature simulations (three models running twice with weak and strong solar irradiance variations and smoothed as plotted in Fig. 6.14 of ref. 5; **d**). All records in the two bottom panels are expressed as anomalies from their 1500-1899 means. STREC has a larger variability than all other records due to its regional domain, so it is scaled on the *y*-axis to improve the comparison (see blue labels). Vertical dashed lines highlight the beginning of synchronous cooling episodes in most records.

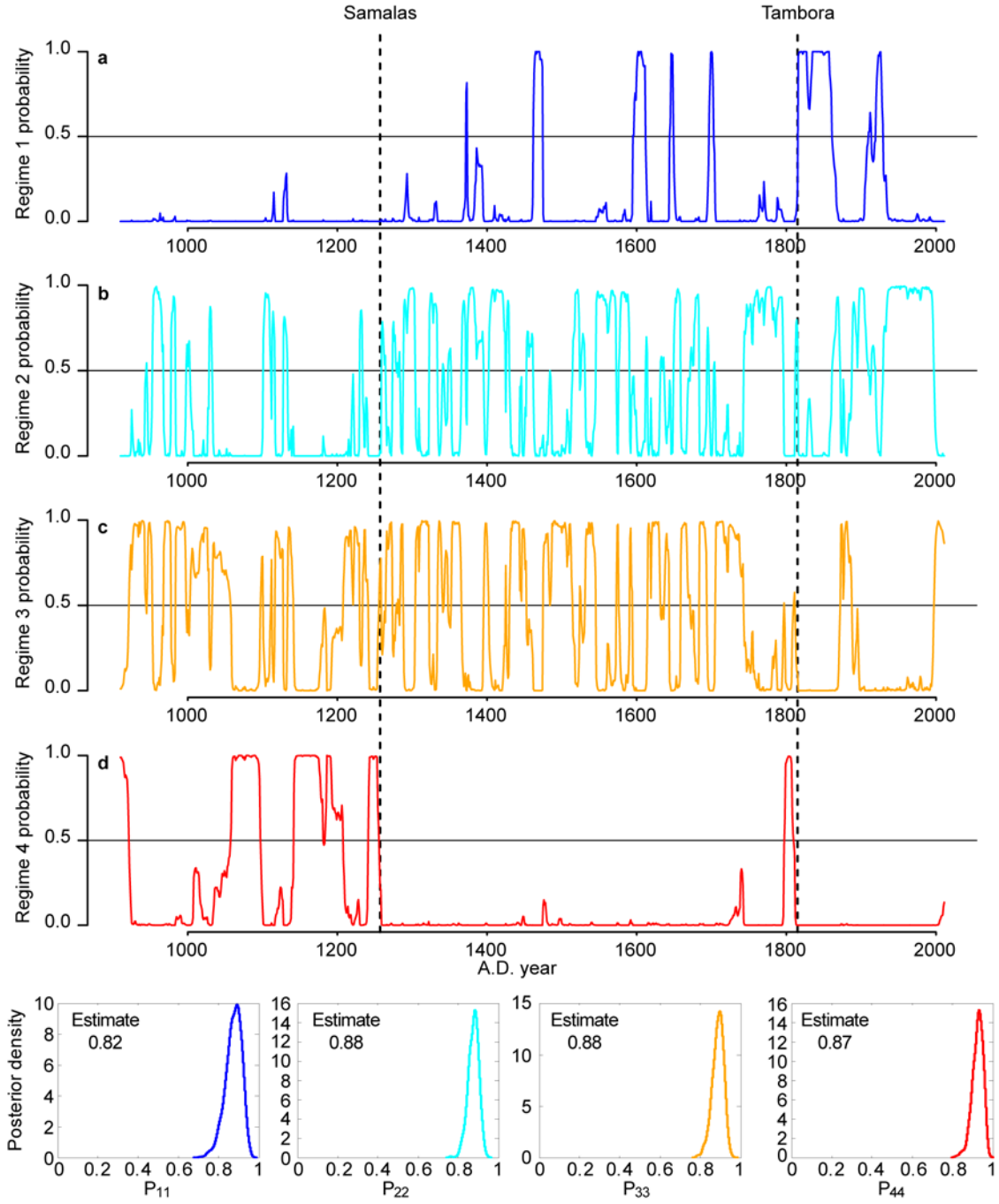

Fig. 3-S4. Regime likelihood. Probability of STREC reconstructed temperature values to belong to any given regime of the four-component Bayesian hidden Markov model with normal distributions. Regimes are ordered from the coldest (**a**) to the warmest (**d**). The bottom panels show the posterior probability density functions of the transition

probability p_{kk} of each regime. Regimes are ordered from the coldest (left) to the warmest (right).

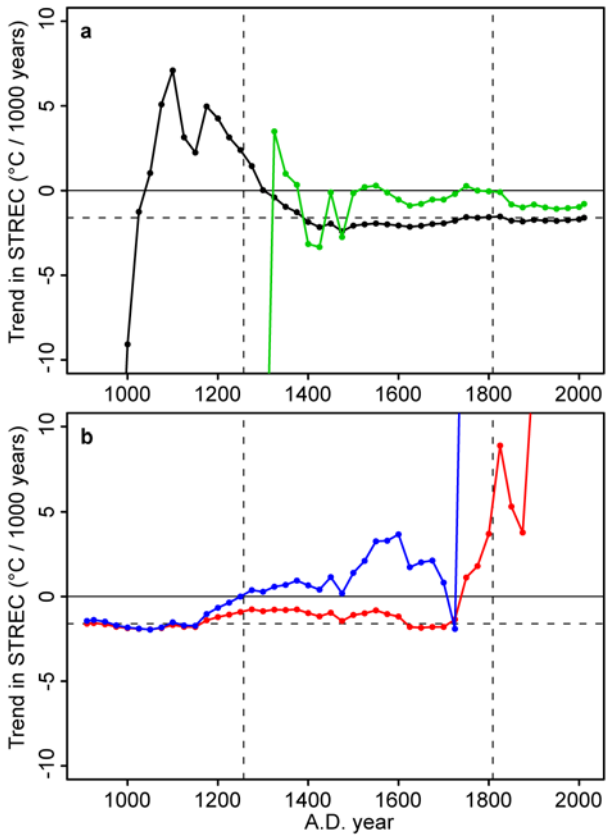

Fig. 3-S5. Trends in STREC. In **a**, linear regression coefficients are obtained considering time periods starting from A.D. 910 (black) or A.D. 1257 (green) and increased by successive 25-year time steps (e.g. 910-950 with dot in 950, 910-975 with dot in 975...). In **b**, linear regression coefficients are obtained considering time periods starting from A.D. 2011 (red) or A.D. 1809 (blue) and lengthened backward by 25-year time steps (e.g. 1975-2011 with dot in 1975, 1950-2011 with dot in 1950...). The vertical dashed lines show the dates of the A.D. 1257 Samalas and A.D. 1809 (the event preceding the Tambora) eruptions, while the horizontal dashed line shows the trend over the entire time period covered by STREC (A.D. 910-2011; -1.6°C per 1000 years).

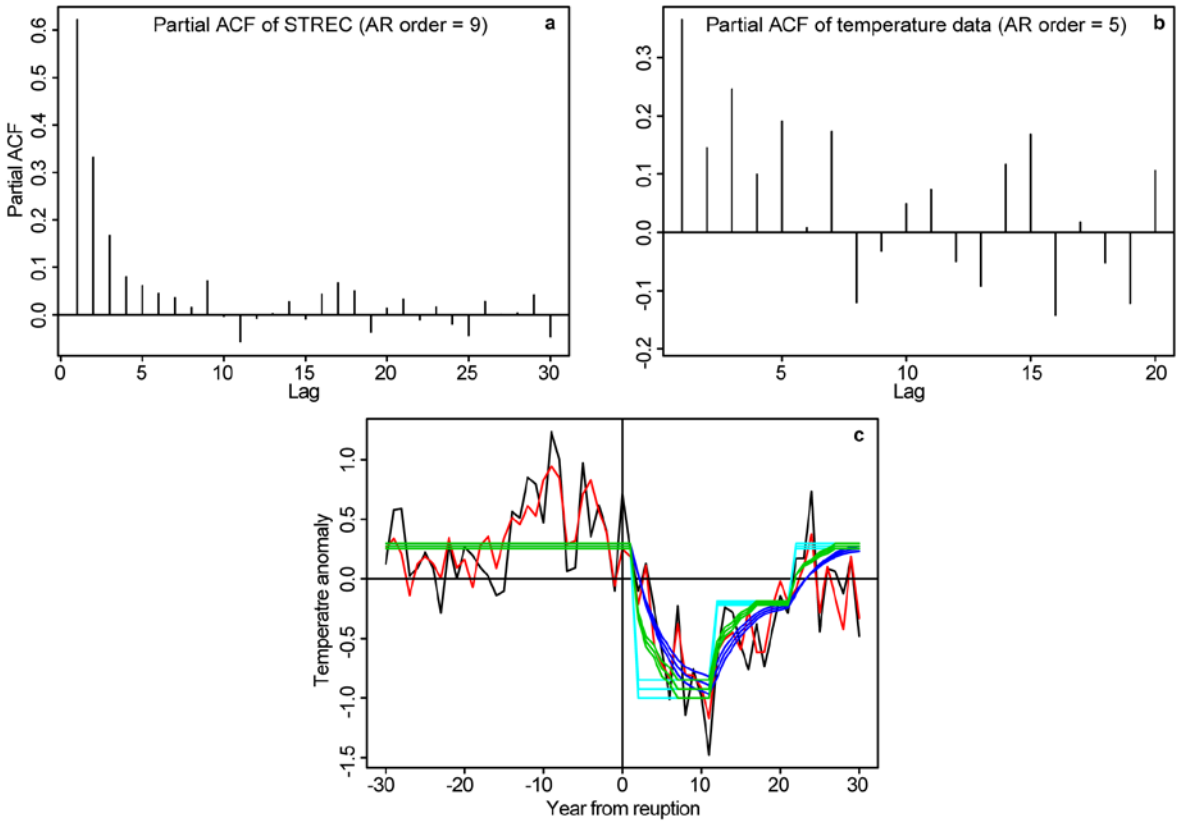

Fig. 3-S6. Effect of autocorrelation on temperature anomalies after volcanic eruptions. The two top panels show the estimates of the partial autocorrelation functions (partial ACF) fitted to STREC (**a**) and fitted to the July-August temperature data over the study area (**b**; 15 cells of the CRU TS3.20 dataset). The orders of the autoregressive model (AR order) selected by the Akaike Information Criterion are 9 and 5 for STREC and the temperature data, respectively. **c** shows the real mean (red) and median (black) responses of STREC to the 10 strongest volcanic eruptions of the last 1100 years deduced by ref. 2, along with simulated temperature data (green) and simulated STREC (dark blue) after applying three different climate inputs (light blue) chosen to reduce the mean squared error between observed (red) and simulated (dark blue) STREC. Simulated temperature data were obtained with the formula:

$$\mathrm{SimT_i} = \frac{\sum_{k=0}^{n} \mathrm{Input_{(i-k)}AC_k}}{\sum_{k=0}^{n} \mathrm{AC_k}}$$

where $SimT_i$ is the simulated temperature in the year i, n is the order of the autoregressive model fitted to the July-August temperature data over the study area, k is the lag of the partial autocorrelation function, $Input_{(i-k)}$ is the climate input in the year $(i-k)$ and AC_k is the estimate of lag k for the partial autocorrelation function fitted to the

July-August temperature data over the study area (note that AC_o=1). Here, we chose a 2-step climate input composed of a constant reduction over 10 years starting from year 2 from eruptions (constant values were -1.1, -1.2 and -1.3°C) followed by another constant reduction over 10 years (40% of the first reduction). Once the simulated temperatures were obtained, simulated STREC data were obtained with the formula:

$$\mathrm{SimSTREC_i} = \frac{\sum_{k=0}^{n\_STREC} \mathrm{SimT_{(i-k)}AC\_STREC_k}}{\sum_{k=0}^{n\_STREC} \mathrm{AC\_STREC_k}}$$

The effect of autocorrelation of tree-ring data on STREC can be considered as the difference between the simulated temperatures (green) and the simulated STREC (dark blue).

CONCLUSION

Durant mon doctorat, j'ai développé un réseau de séries dendrochronologiques millénaires en utilisant des restes d'arbres subfossiles d'épinette noire récupérés dans la zone littorale de six lacs de la forêt boréale nordique du Québec. L'analyse dendroécologique et dendroclimatique de ces bois subfossiles a permis de toucher, dans les trois chapitres de ma thèse, des aspects différents mais qui sont importants pour la compréhension de l'évolution de la taïga au cours des deux derniers millénaires. Tout d'abord, nous avons montré comment les interactions entre écosystèmes terrestres et aquatiques dans la région boréale nordique sont influencées par les incendies et comment les incendies du passé ont déterminé la diversité du paysage actuel de la taïga. Ensuite, nous avons documenté les changements climatiques des 1100 dernières années dans notre région d'étude. Notre réseau de séries dendrochronologiques a permis de produire la première reconstitution de résolution annuelle des températures du dernier millénaire dans l'Est de l'Amérique du Nord, comblant ainsi une lacune importante dans le réseau de reconstitutions paléoclimatiques de l'hémisphère nord.

L'originalité de cette thèse a été de découvrir et montrer le potentiel exceptionnel des gisements de bois subfossiles littoraux de lacs de la taïga pour effectuer des analyses paléoécologiques et paléoclimatiques. L'utilisation de ces archives naturelles nous a permis de documenter des changements climatiques et des processus écologiques durant les 1500 dernières années avec une résolution spatiale et temporelle extrêmement fine. Auparavant, dans la taïga du Québec la compréhension des impacts à long terme des incendies et de la variabilité climatique avait été limitée par la rareté de données paléoécologiques ayant une résolution temporelle et spatiale assez précise. Des données dendrochronologiques peuvent être utilisées pour la reconstitution des dynamiques

forestières au niveau d'un peuplement et avec une résolution annuelle (Arseneault et Payette, 1997b; Auger et Payette, 2010). Cependant, dans la majorité des cas, ces reconstitutions ne dépassent pas quelques siècles à cause de la dégradation rapide du bois à la surface des sols (Bond-Lamberty et Gower, 2008). Les pollens et les macrorestes végétaux permettent la reconstitution à long terme des changements de végétation et de l'histoire des feux (Carcaillet *et al.*, 2010; Payette *et al.*, 2012; Senici *et al.*, 2013), mais elles ne fournissent aucune information directe sur la densité passée des arbres ou sur leur croissance, et la datation des perturbations, qui dans ce cas s'appuie sur le radiocarbone, est moins précise qu'avec la dendrochronologie. De plus, contrairement aux impacts des incendies, les données polliniques ne sont pas spécifiques pour un peuplement en raison de la mobilité du pollen. Pour toutes ces raisons, les gisements de bois subfossiles littoraux que nous avons utilisé fournissent des informations paléoécologiques et paléoclimatiques uniques de résolution annuelle qui couvrent facilement le dernier millénaire et qui sont spécifiques à la portion de forêt riveraine qui a généré les bois (Gennaretti, Arseneault et Bégin, 2014). Dans ce projet doctoral, nous avons pu développer un jeu de données impressionnant composé de plus de 1800 bois subfossiles, échantillonnés dans six lacs, interdatés à l'année près sur les 1400 dernières années. Nous avons aussi développé plusieurs séries dendrochronologiques flottantes vielles jusqu'à cinq millénaires qui ont été datées par le radiocarbone (83 spécimens interdatés dans 7 séries).

Dans le premier chapitre de cette thèse, nous avons analysé les stocks actuels de bois dans des gisements littoraux de lacs de la taïga et les flux de bois à travers l'interface forêt-lac au cours des 1400 dernières années en considérant l'influence des incendies passés. Ces gisements sont importants car ils structurent les écosystèmes littoraux (Collins *et al.*, 2012), ils représentent l'habitat idéal pour plusieurs communautés d'organismes aquatiques (Everett et Ruiz, 1993; Lester, Wright et Jones-Lennon, 2007) et peuvent représenter d'importants puits de carbone (Guyette, Dey et Stambaugh, 2008). Malgré que les stocks et les taux de recrutement du bois dans des

écosystèmes littoraux avaient déjà été décrits ailleurs (Guyette et Cole, 1999; Guyette *et al.*, 2002; Chen, Wei et Scherer, 2005; Marburg, Turner et Kratz, 2006; Guyette, Dey et Stambaugh, 2008), une analyse quantitative à long terme sur la base d'un échantillonnage exhaustif comme le notre, couplé à la reconstruction de l'histoire des perturbations passées au niveau du site, n'avait jamais été faite. Nos résultats ont permis d'évaluer la persistance des stocks de bois dans les lacs boréaux, d'estimer la quantité de carbone séquestré dans ces stocks et d'analyser le rôle des incendies dans l'atténuation des stocks et flux de bois dans les lacs de la taïga. Les interactions entre les écosystèmes terrestres et aquatiques sont complexes et abondantes (Naiman et Décamps, 1997), et notre travail a démontré que, dans la forêt boréale nord-américaine, les perturbations touchant les habitats terrestres peuvent être des moteurs de changement fondamentaux pour les zones littorales.

Des aspects supplémentaires rendent le premier chapitre de ma thèse particulièrement intéressant pour une vaste audience scientifique:

1 - Il se situe à la limite entre une étude d'écologie terrestre et une étude d'écologie aquatique et analyse les interactions forêt-lac à travers l'étude des transferts de bois qui sont un exemple de ce que l'on appelle an anglais *cross-boundary subsidy*. C'est-à-dire des éléments qui traversent les frontières entre deux écosystèmes spatialement définis (ex. forêt riveraine vs lac) et apportent dans le milieu de réception un support essentiel pour le réseau trophique.

2 - Des études avaient suggéré que les gisements de bois subfossile peuvent représenter d'importants puits de carbone en raison de la lente décomposition du bois dans l'eau (Guyette *et al.*, 2002; Guyette, Dey et Stambaugh, 2008). Nos résultats ont permis de préciser cette idée. Malgré que le temps de résidence des bois dans les lacs de la taïga soit très long et que les lacs de la taïga soient extrêmement nombreux, les gisements de bois de ces lacs représentent une part négligeable du stock de carbone boréal.

3 - Environ 8% des bois subfossiles enfouis ont passé plus de 1500 ans et jusqu'à 5000 ans dans les sédiments superficiels de nos lacs. Notre étude confirme donc que ces bois forment d'importants gisements qui peuvent être utilisés pour le développement de séries dendrochronologiques millénaires. Ces chronologies sont très utiles pour la reconstitution des changements climatiques (voir par exemple le dernier rapport du GIEC; Stocker *et al.*, 2013) et des dynamiques forestières à long terme.

4 - Des études empiriques ou basées sur des simulations ont montré que les perturbations naturelles des forêts, telles que les incendies et les épidémies d'insectes, peuvent déclencher le recrutement massif de bois dans les écosystèmes aquatiques adjacents (Bragg, 2000; Chen, Wei et Scherer, 2005). Au contraire, la perspective millénaire fournie par notre étude indique que le résultat ultime des perturbations dans les forêts riveraines est de réduire les recrutements et les stocks de bois dans les zones littorales par rapport aux valeurs mesurées en leur absence. Si l'on compare nos résultats au patron régional de fréquence des incendies (Boulanger *et al.*, 2012a), nous pouvons conclure que les incendies représentent le facteur le plus important qui limite l'accumulation des bois dans les zones littorales à l'échelle régionale, surtout vers la côte de la baie James où les incendies sont plus fréquents. De même, l'augmentation prévue de la fréquence des incendies dans la forêt boréale de l'est canadien durant le XXI^{e} siècle (Boulanger *et al.*, 2013) impliquerait une diminution progressive et de grande échelle des gisements de bois dans les lacs boréaux.

Dans le deuxième chapitre de cette thèse, nous avons combiné un inventaire détaillé de la forêt riveraine actuelle située le long du rivage de deux lacs de la taïga du Québec avec la datation dendrochronologique des bois subfossiles qui se sont accumulés dans les zones littorales correspondantes. Notre objectif a été de vérifier si les variations de structure et composition de la forêt riveraine actuelle au sein d'un site pouvaient être attribuées à différentes histoires des feux au cours du dernier millénaire et de montrer les impacts des incendies passés sur la mortalité des arbres, leur densité et leur croissance.

Cette étude est attrayante pour un vaste lectorat parce que des implications importantes peuvent être déduites de nos résultats:

1 - Dans la taïga de l'est canadien plusieurs siècles peuvent être nécessaires pour la convergence de la densité des arbres et de la composition de la forêt entre des peuplements forestiers qui ont connu ou ont échappé au feu. En effet, seulement un ou quelques incendies par millénaire sont suffisants pour maintenir des forêts ouvertes dans cette région. Nos résultats appuient donc l'hypothèse de l'ouverture progressive du couvert forestier de la forêt boréale de l'est canadien comme conséquence du climat plus froids et des incendies du denier millénaire (Payette et Gagnon, 1985; Payette et Morneau, 1993; Payette, Filion et Delwaide, 2008).

2 - La taïga contient deux types de peuplements forestiers anciens (c'est-à-dire vieux de quelques siècles) sur des sols bien drainés (vieilles forêts ouvertes vs vieilles forêts denses) en fonction du fait qu'ils ont brûlé ou non au cours des 800 dernières années.

3 - Les incendies peuvent déclencher dans la taïga des trajectoires spécifiques de structure de la forêt après feu avec une réduction de la densité des arbres et un taux de rétablissement après-feu très variables d'un feu à l'autre.

4 - Sous le climat et le régime de feux de l'Holocène supérieur, le sapin baumier peut, dans la taïga, persister seulement dans les rares peuplements forestiers qui n'ont pas brûlé depuis au moins un millénaire. Nos résultats appuient donc l'hypothèse de la régression vers le sud induite par les incendies de l'aire de répartition du sapin durant les derniers millénaires (Sirois, 1997; Arseneault et Sirois, 2004; Boucher, Arseneault et Hétu, 2006; Ali *et al.*, 2008; de Lafontaine et Payette, 2010).

5 - Une densité élevée des arbres et un couvert forestier plurispécifique peuvent être maintenus pendant au moins un millénaire en l'absence de feu. Ce résultat indique que l'occurrence de la phase de déclin des écosystèmes forestiers liée à l'absence de

perturbations sur de longues périodes, qui a été observée ailleurs dans plusieurs biomes (Wardle, Walker et Bardgett, 2004), est rare dans la taïga de l'est canadien, compte tenu de la récurrence des incendies dans cette région.

6 - Les plus importantes fluctuations climatiques du dernier millénaire dans la taïga de l'est canadien, c'est-à-dire l'Optimum climatique médiéval et la période froide déclenchée par les deux éruptions successives de 1809 et 1815, ont aussi influencé la croissance des arbres et leur mortalité.

7 - Nos données suggèrent que la fréquence accrue des incendies qui est prévue pour le XXI^{e} siècle (Boulanger *et al.*, 2013) pourrait accélérer la régression du sapin baumier vers le sud et pourrait augmenter l'abondance des forêts plus ouvertes, à moins que des seuils climatiques qui ont déjà permis dans le passé le développement de peuplements forestiers denses soient dépassés, améliorant ainsi les processus de régénération de la forêt. De plus, en considérant que la limite de l'aire de répartition du pin gris se situe à seulement une dizaine de kilomètres à l'ouest de notre aire d'étude et que cet arbre est très bien adapté aux feux, une fréquence accrue des incendies dans la région pourrait faciliter son expansion vers l'est.

Dans le troisième chapitre de cette thèse, nous avons utilisé notre réseau de séries dendrochronologiques millénaires hautement répliquées pour développer une reconstitution régionale des températures de juillet-août des 1100 dernières années dans le Nord-Est de l'Amérique du Nord. Ce dernier chapitre de ma thèse présente des avancées scientifiques importantes pour les raisons suivantes:

1 - Tout d'abord, il fournit un réseau très attendu de séries dendrochronologiques millénaires qui peut être utilisé pour des reconstitutions des températures dans l'Est de l'Amérique du Nord où les indicateurs des températures du dernier millénaire de résolution annuelle sont inexistants (voir le dernier rapport du GIEC et Pages 2k Consortium, 2013). Nos résultats et nos données auront donc des implications importantes pour les scientifiques qui tentent de comprendre le rôle des forçages

climatiques au niveau régional ou hémisphérique et d'étudier et prévoir les impacts des changements climatiques, ainsi que pour les modélisateurs du climat passé et futur. Notre jeu de données complet sera mis à la disposition de la communauté scientifique.

2 - Ensuite, la région boréale de l'Est de l'Amérique du Nord est l'une des régions qui a connu les augmentations de température les plus fortes au cours du dernier siècle (basé sur les données du Climatic Reasearch Unit; Mitchell et Jones, 2005). Malgré cela, notre reconstitution indique que, dans cette région, certaines décennies durant l'Optimum climatique médiéval ont été significativement plus chaudes que les dernières années. La possibilité de vérifier si les températures très chaudes des dernières années sont sans précédent par rapport aux fluctuations naturelles du climat des derniers siècles est très intéressante pour un vaste public (Sidorova *et al.*, 2013; Tingley et Huybers, 2013).

3 - Enfin, notre reconstitution clarifie le rôle du forçage volcanique sur la variabilité climatique régionale durant le dernier millénaire dans le Nord-Est de l'Amérique du Nord. Les effets du volcanisme sur le climat global et régional ont été très récemment sous l'attention des scientifiques et des medias. En effet, le réchauffement observé au cours des 15 dernières années à été moins fort par rapport aux prévisions des modèles climatiques (Schmidt, Shindell et Tsigaridis, 2014). Cet écart entre les observations et les simulations climatiques peut être réduit significativement (jusqu'à 15%) en prenant mieux en compte dans les modèles les éruptions volcaniques du XXI^{e} siècle (Santer *et al.*, 2014). De plus, les effets du volcanisme sur le climat du passé ne sont pas encore très clairs. Bien que certaines données dendroclimatiques montrent que les effets des plus grandes éruptions ont été de courte durée (moins de 10 ans; Breitenmoser *et al.*, 2012; D'Arrigo, Wilson et Anchukaitis, 2013; Esper *et al.*, 2013), d'autres données de terrain (Miller *et al.*, 2012; Margreth *et al.*, Sous presse) et des modélisations climatiques (Stenchikov *et al.*, 2009; Otterå *et al.*, 2010; Zhong *et al.*, 2011; Zanchettin *et al.*, 2012; Schleussner et Feulner, 2013) suggèrent que de grandes éruptions successives peuvent déclencher le commencement de périodes froides

beaucoup plus persistantes. Notre reconstitution appuie cette deuxième hypothèse et la sensibilité élevée du Nord-Est de l'Amérique du Nord au volcanisme.

Ma thèse de doctorat s'est insérée dans le projet ARCHIVES (projet CRSNG-RDC avec Hydro-Québec; http://archives.ete.inrs.ca/) qui a eu comme objectif de reconstituer le climat passé pour calibrer les projections climatiques futures dans le Québec boréal et fournir des outils nécessaires pour une meilleure gestion des immenses réservoirs hydroélectriques de cette région. Le projet ARCHIVES m'a permis de collaborer avec une équipe très dynamique est multidisciplinaire de chercheurs de plusieurs universités et instituts de recherche. Mes données et mes résultats auront donc des retombées appliquées car, par exemple, des climatologues d'OURANOS (Consortium sur la climatologie régionale et l'adaptation aux changements climatiques) pourront les utiliser pour valider et calibrer les simulations climatiques produites au moyen du Modèle Régional Climatique Canadien.

En conclusion, les données et les résultats de mon doctorat ont permis la compréhension de processus écologiques qui déterminent la diversité du paysage de la taïga et l'analyse de la variabilité climatique de cette région au cours du dernier millénaire. Mon doctorat a démontré que la taïga du Québec est particulièrement sensible aux changements climatiques et aux facteurs de perturbation. J'espère donc avoir contribué, grâce à ma recherche doctorale, à fournir des outils importants pour une meilleure gestion d'une région stratégique du Québec (la taïga) qui aideront à faire face aux grands enjeux que ce territoire traverse. En effet, la taïga est de plus en plus soumise à des pressions de développement importantes.

RÉFÉRENCES BIBLIOGRAPHIQUES

ALI, A. A., H. ASSELIN, A. C. LAROUCHE, Y. BERGERON, C. CARCAILLET et P. J. H. RICHARD. 2008. « Changes in fire regime explain the Holocene rise and fall of Abies balsamea in the coniferous forests of western Québec, Canada ». *Holocene*, volume 18, numéro 5, pp. 693-703.

AMIRO, B. D., B. J. STOCKS, M. E. ALEXANDER, M. D. FLANNIGAN et B. M. WOTTON. 2001. « Fire, climate change, carbon and fuel management in the Canadian boreal forest ». *International Journal of Wildland Fire*, volume 10, numéro 3-4, pp. 405-413.

ARSENEAULT, D. et S. PAYETTE. 1992. « A postfire shift from lichen-spruce to lichen-tundra vegetation at the tree line. ». *Ecology*, volume 73, numéro 3, pp. 1067-1081.

ARSENEAULT, D. et S. PAYETTE. 1997a. « Landscape change following deforestation at the Arctic tree line in Quebec, Canada ». *Ecology*, volume 78, numéro 3, pp. 693-706.

ARSENEAULT, D. et S. PAYETTE. 1997b. « Reconstruction of millennial forest dynamics from tree remains in a subarctic tree line peatland ». *Ecology*, volume 78, numéro 6, pp. 1873-1883.

ARSENEAULT, D. et S. PAYETTE. 1998. « Chronologie des cernes pâles de l'épinette noire (Picea mariana [Mill.] BSP.) au Québec subarctique : de 706 à 1675 ap. J.-C. ». *Géographie physique et Quaternaire*, volume 52, numéro 2, pp. 219-226.

ARSENEAULT, D. 2001. « Impact of fire behavior on postfire forest development in a homogeneous boreal landscape ». *Canadian Journal of Forest Research*, volume 31, numéro 8, pp. 1367-1374.

ARSENEAULT, D. et L. SIROIS. 2004. « The millennial dynamics of a boreal forest stand from buried trees ». *Journal of Ecology*, volume 92, numéro 3, pp. 490-504.

ARSENEAULT, D., B. DY, F. GENNARETTI, J. AUTIN et Y. BÉGIN. 2013. « Developing millennial tree ring chronologies in the fire-prone North American boreal forest ». *Journal of Quaternary Science*, volume 28, numéro 3, pp. 283-292.

AUGER, S. et S. PAYETTE. 2010. « Four millennia of woodland structure and dynamics at the Arctic treeline of eastern Canada ». *Ecology*, volume 91, numéro 5, pp. 1367-1379.

BERGERON, Y., S. GAUTHIER, V. KAFKA, P. LEFORT et D. LESIEUR. 2001. « Natural fire frequency for the eastern Canadian boreal forest: Consequences for sustainable forestry ». *Canadian Journal of Forest Research*, volume 31, numéro 3, pp. 384-391.

BLACK, R. A. et L. C. BLISS. 1980. « Reproductive Ecology of Picea Mariana (Mill.) BSP., at Tree Line Near Inuvik, Northwest Territories, Canada ». *Ecological Monographs*, volume 50, numéro 3, pp. 331-354.

BOND-LAMBERTY, B. et S. T. GOWER. 2008. « Decomposition and fragmentation of coarse woody debris: Re-visiting a boreal black spruce chronosequence ». *Ecosystems*, volume 11, numéro 6, pp. 831-840.

BOUCHER, É., D. ARSENEAULT et B. HÉTU. 2006. « Late Holocene development of a floodplain along a small meandering stream, northern Québec, Canada ». *Geomorphology*, volume 80, numéro 3-4, pp. 267-281.

BOUCHER, Y., D. ARSENEAULT et L. SIROIS. 2009. « La forêt préindustrielle du Bas-Saint-Laurent et sa transformation (1820-2000) : implications pour l'aménagement écosystémique ». *Le naturaliste canadien*, volume 133, numéro 2, pp. 60-69.

BOULANGER, Y., S. GAUTHIER, P. J. BURTON et M. A. VAILLANCOURT. 2012a. « An alternative fire regime zonation for Canada ». *International Journal of Wildland Fire*, volume 21, numéro 8, pp. 1052-1064.

BOULANGER, Y., D. ARSENEAULT, H. MORIN, Y. JARDON, P. BERTRAND et C. DAGNEAU. 2012b. « Dendrochronological reconstruction of spruce budworm (Choristoneura fumiferana) outbreaks in southern Quebec for the last 400 years ». *Canadian Journal of Forest Research*, volume 42, numéro 7, pp. 1264-1276.

BOULANGER, Y., S. GAUTHIER, D. R. GRAY, H. LE GOFF, P. LEFORT et J. MORISSETTE. 2013. « Fire regime zonation under current and future climate over eastern Canada ». *Ecological Applications*, volume 23, numéro 4, pp. 904-923.

BRAGG, D. C. 2000. « Simulating catastrophic and individualistic large woody debris recruitment for a small riparian system ». *Ecology*, volume 81, numéro 5, pp. 1383-1394.

BREITENMOSER, P., J. BEER, S. BRÖNNIMANN, D. FRANK, F. STEINHILBER et H. WANNER. 2012. « Solar and volcanic fingerprints in tree-ring chronologies over the past 2000years ». *Palaeogeography, Palaeoclimatology, Palaeoecology*, volume 313-314, pp. 127-139.

BRIFFA, K. R., F. H. SCHWEINGRUBER, P. D. JONES, T. J. OSBORN, S. G. SHIYATOV et E. A. VAGANOV. 1998. « Reduced sensitivity of recent tree-growth to temperature at high northern latitudes ». *Nature*, volume 391, numéro 6668, pp. 678-682.

BRIFFA, K. R. 2000. « Annual climate variability in the Holocene: interpreting the message of ancient trees ». *Quaternary Science Reviews*, volume 19, numéro 1-5, pp. 87-105.

BRIFFA, K. R., T. J. OSBORN, F. H. SCHWEINGRUBER, I. C. HARRIS, P. D. JONES, S. G. SHIYATOV et E. A. VAGANOV. 2001. « Low-frequency temperature variations from a northern tree ring density network ». *Journal of*

Geophysical Research D: Atmospheres, volume 106, numéro D3, pp. 2929-2941.

BRIFFA, K. R. et J. A. MATTHEWS. 2002. « ADVANCE-10K: a European contribution towards a hemispheric dendroclimatology for the Holocene ». *Holocene*, volume 12, numéro 6, pp. 639-642.

BRIFFA, K. R., T. J. OSBORN et F. H. SCHWEINGRUBER. 2004. « Large-scale temperature inferences from tree rings: a review ». *Global and Planetary Change*, volume 40, numéro 1-2, pp. 11-26.

BÜNTGEN, U., J. ESPER, D. C. FRANK, K. NICOLUSSI et M. SCHMIDHALTER. 2005. « A 1052-year tree-ring proxy for Alpine summer temperatures ». *Climate Dynamics*, volume 25, numéro 2-3, pp. 141-153.

CARCAILLET, C., P. J. H. RICHARD, Y. BERGERON, B. FŔCHETTE et A. A. ALI. 2010. « Resilience of the boreal forest in response to Holocene fire-frequency changes assessed by pollen diversity and population dynamics ». *International Journal of Wildland Fire*, volume 19, numéro 8, pp. 1026-1039.

CHEN, X., X. WEI et R. SCHERER. 2005. « Influence of wildfire and harvest on biomass, carbon pool, and decomposition of large woody debris in forested streams of southern interior British Columbia ». *Forest Ecology and Management*, volume 208, numéro 1-3, pp. 101-114.

COLE-DAI, J., D. FERRIS, A. LANCIKI, J. SAVARINO, M. BARONI et M. H. THIEMENS. 2009. « Cold decade (AD 1810-1819) caused by Tambora (1815) and another (1809) stratospheric volcanic eruption ». *Geophysical Research Letters*, volume 36, numéro 22, L22703.

COLLIER, K. J., B. J. SMITH et N. J. HALLIDAY. 2004. « Colonization and use of pine wood versus native wood in New Zealand plantation forest streams: Implications for riparian management ». *Aquatic Conservation: Marine and Freshwater Ecosystems*, volume 14, numéro 2, pp. 179-199.

COLLINS, B. D., D. R. MONTGOMERY, K. L. FETHERSTON et T. B. ABBE. 2012. « The floodplain large-wood cycle hypothesis: A mechanism for the

physical and biotic structuring of temperate forested alluvial valleys in the North Pacific coastal ecoregion ». *Geomorphology*, volume 139-140, pp. 460-470.

COOK, E. R., J. ESPER et R. D. D'ARRIGO. 2004. « Extra-tropical Northern Hemisphere land temperature variability over the past 1000 years ». *Quaternary Science Reviews*, volume 23, numéro 20-22, pp. 2063-2074.

COOK, E. R., C. A. WOODHOUSE, C. M. EAKIN, D. M. MEKO et D. W. STAHLE. 2004. « Long-term aridity changes in the western United States ». *Science*, volume 306, numéro 5698, pp. 1015-1018.

COOK, E. R., B. M. BUCKLEY, J. G. PALMER, P. FENWICK, M. J. PETERSON, G. BOSWIJK et A. FOWLER. 2006. « Millennia-long tree-ring records from Tasmania and New Zealand: A basis for modelling climate variability and forcing, past, present and future ». *Journal of Quaternary Science*, volume 21, numéro 7, pp. 689-699.

D'ARRIGO, R., R. WILSON et G. JACOBY. 2006. « On the long-term context for late twentieth century warming ». *Journal of Geophysical Research D: Atmospheres*, volume 111, numéro D3, D03103.

D'ARRIGO, R., R. WILSON, B. LIEPERT et P. CHERUBINI. 2008. « On the 'Divergence Problem' in Northern Forests: A review of the tree-ring evidence and possible causes ». *Global and Planetary Change*, volume 60, numéro 3-4, pp. 289-305.

D'ARRIGO, R., G. JACOBY, B. BUCKLEY, J. SAKULICH, D. FRANK, R. WILSON, A. CURTIS et K. ANCHUKAITIS. 2009. « Tree growth and inferred temperature variability at the North American Arctic treeline ». *Global and Planetary Change*, volume 65, numéro 1-2, pp. 71-82.

D'ARRIGO, R., R. WILSON et K. J. ANCHUKAITIS. 2013. « Volcanic cooling signal in tree ring temperature records for the past millennium ». *Journal of Geophysical Research D: Atmospheres*, volume 118, numéro 16, pp. 9000-9010.

D'ARRIGO, R. D. et G. C. JACOBY. 1993. « Secular trends in high northern latitude temperature reconstructions based on tree rings ». *Climatic Change*, volume 25, numéro 2, pp. 163-177.

DE LAFONTAINE, G. et S. PAYETTE. 2010. « The Origin and Dynamics of Subalpine White Spruce and Balsam Fir Stands in Boreal Eastern North America ». *Ecosystems*, volume 13, numéro 6, pp. 932-947.

DOUGLASS, A. E. 1929. « The secret of the Southwest solved by talkative tree rings ». *National Geographic Magazine*, volume 56, numéro 6, pp. 736-770.

DY, B. 2008. « Mécanismes d'apport et temps de résidence des débris ligneux grossiers dans la zone littorale de deux lacs nord boréaux au Québec ». Mémoire de maîtrise en gestion de la faune et de ses habitats, Rimouski: Université du Québec à Rimouski, 67 p.

ERONEN, M., P. ZETTERBERG, K. R. BRIFFA, M. LINDHOLM, J. MERILAINEN et M. TIMONEN. 2002. « The supra-long Scots pine tree-ring record for Finnish Lapland: Part 1, chronology construction and initial inferences ». *Holocene*, volume 12, numéro 6, pp. 673-680.

ESPER, J., E. R. COOK et F. H. SCHWEINGRUBER. 2002. « Low-frequency signals in long tree-ring chronologies for reconstructing past temperature variability ». *Science*, volume 295, numéro 5563, pp. 2250-2253.

ESPER, J., D. C. FRANK, M. TIMONEN, E. ZORITA, R. J. S. WILSON, J. LUTERBACHER, S. HOLZKÄMPER, N. FISCHER, S. WAGNER, D. NIEVERGELT, A. VERSTEGE et U. BÜNTGEN. 2012. « Orbital forcing of tree-ring data ». *Nature Climate Change*, volume 2, numéro 12, pp. 862-866.

ESPER, J., L. SCHNEIDER, P. J. KRUSIC, J. LUTERBACHER, U. BÜNTGEN, M. TIMONEN, F. SIROCKO et E. ZORITA. 2013. « European summer temperature response to annually dated volcanic eruptions over the past nine centuries ». *Bulletin of Volcanology*, volume 75, numéro 7, pp. 1-14.

EVERETT, R. A. et G. M. RUIZ. 1993. « Coarse woody debris as a refuge from predation in aquatic communities - An experimental test ». *Oecologia*, volume 93, numéro 4, pp. 475-486.

FAUSCH, K. D. et T. G. NORTHCOTE. 1992. « Large woody debris and salmonid habitat in a small coastal British Columbia stream ». *Canadian Journal of Fisheries and Aquatic Sciences*, volume 49, numéro 4, pp. 682-693.

FERGUSON, C. W. 1979. « Dendrochronology of bristlecone pine, *Pinus longaeva* ». *Environment International*, volume 2, numéro 4-6, pp. 209-214.

FERGUSON, C. W. et D. A. GRAYBILL. 1983. « Dendrochronology of bristlecone pine: a progress report ». *Radiocarbon*, volume 25, numéro 2, pp. 287–288.

FILION, L., S. PAYETTE, L. GAUTHIER et Y. BOUTIN. 1986. « Light rings in subarctic conifers as a dendrochronological tool ». *Quaternary Research*, volume 26, numéro 2, pp. 272-279.

FRANKE, J., D. FRANK, C. C. RAIBLE, J. ESPER et S. BRÖNNIMANN. 2013. « Spectral biases in tree-ring climate proxies ». *Nature Climate Change*, volume 3, numéro 4, pp. 360-364.

FRIEDRICH, M., S. REMMELEL, B. KROMER, J. HOFMANN, M. SPURK, K. F. KAISER, C. ORCEL et M. KUPPERS. 2004. « The 12,460-year Hohenheim oak and pine tree-ring chronology from central Europe - A unique annual record for radiocarbon calibration and paleoenvironment reconstructions ». *Radiocarbon*, volume 46, numéro 3, pp. 1111-1122.

GAO, C., A. ROBOCK et C. AMMANN. 2008. « Volcanic forcing of climate over the past 1500 years: An improved ice core-based index for climate models ». *Journal of Geophysical Research D: Atmospheres*, volume 113, numéro 23, D23111.

GENNARETTI, F., D. ARSENEAULT et Y. BÉGIN. 2014. « Millennial stocks and fluxes of large woody debris in lakes of the North American taiga ». *Journal of Ecology*, volume 102, numéro 2, pp. 367–380.

GIRARD, F., S. PAYETTE et R. GAGNON. 2008. « Rapid expansion of lichen woodlands within the closed-crown boreal forest zone over the last 50 years caused by stand disturbances in eastern Canada ». *Journal of Biogeography*, volume 35, numéro 3, pp. 529-537.

GLAZ, P. N. 2008. « Dynamique spatio-temporelle des macroinvertébrés des débris ligneux lentiques. ». Mémoire de maîtrise en gestion de la faune et de ses habitats, Rimouski: Université du Québec à Rimouski, 66 p.

GLAZ, P. N., C. NOZAIS et D. ARSENEAULT. 2009. « Macroinvertebrates on coarse woody debris in the littoral zone of a boreal lake ». *Marine and Freshwater Research*, volume 60, numéro 9, pp. 960-970.

GRUDD, H., K. R. BRIFFA, W. KARLEN, T. S. BARTHOLIN, P. D. JONES et B. KROMER. 2002. « A 7400-year tree-ring chronology in northern Swedish Lapland: natural climatic variability expressed on annual to millennial timescales ». *Holocene*, volume 12, numéro 6, pp. 657-665.

GUYETTE, R. P. et W. G. COLE. 1999. « Age characteristics of coarse woody debris (Pinus strobus) in a lake littoral zone ». *Canadian Journal of Fisheries and Aquatic Sciences*, volume 56, numéro 3, pp. 496-505.

GUYETTE, R. P., W. G. COLE, D. C. DEY et R. M. MUZIKA. 2002. « Perspectives on the age and distribution of large wood in riparian carbon pools ». *Canadian Journal of Fisheries and Aquatic Sciences*, volume 59, numéro 3, pp. 578-585.

GUYETTE, R. P., D. C. DEY et M. C. STAMBAUGH. 2008. « The temporal distribution and carbon storage of large oak wood in streams and floodplain deposits ». *Ecosystems*, volume 11, numéro 4, pp. 643-653.

HANTEMIROV, R. M. et S. G. SHIYATOV. 2002. « A continuous multimillennial ring-width chronology in Yamal, northwestern Siberia ». *Holocene*, volume 12, numéro 6, pp. 717-726.

HARMON, M. E., J. F. FRANKLIN, F. J. SWANSON, P. SOLLINS, S. V. GREGORY, J. D. LATTIN, N. H. ANDERSON, S. P. CLINE, N. G.

AUMEN, J. R. SEDELL, G. W. LIENKAEMPER, K. CROMACK JR et K. W. CUMMINS. 2004. « Ecology of Coarse Woody Debris in Temperate Ecosystems ». *Advances in Ecological Research*, volume 34, pp. 59-234.

HASLER, A. D. 1975. *Coupling of Land and Water Systems.* 1e édition. New York, Heidleberg & Berlin: Springer-Verlag. 308 p.

HELAMA, S., M. LINDHOLM, M. TIMONEN, J. MERILAINEN et M. ERONEN. 2002. « The supra-long Scots pine tree-ring record for Finnish Lapland: Part 2, interannual to centennial variability in summer temperatures for 7500 years ». *Holocene*, volume 12, numéro 6, pp. 681-687.

HÉON, J. 2009. « Chevauchements des feux dans la taïga du Québec ». Mémoire de maîtrise en gestion de la faune et de ses habitats, Rimouski: Université du Québec à Rimouski, 76 p.

HOLMES, R. L. 1983. « Computer-assisted quality control in tree-ring dating and measurement ». *Tree-Ring Bulletin*, volume 43, pp. 69-78.

HRODEY, P. J., B. J. KALB et T. M. SUTTON. 2008. « Macroinvertebrate community response to large-woody debris additions in small warmwater streams ». *Hydrobiologia*, volume 605, numéro 1, pp. 193-207.

JACOBY, G. C., I. S. IVANCIU et L. D. ULAN. 1988. « A 263-year record of summer temperature for northern Quebec reconstructed from tree-ring data and evidence of a major climatic shift in the early 1800's ». *Palaeogeography, Palaeoclimatology, Palaeoecology*, volume 64, numéro 1-2, pp. 69-78.

JACOBY, G. C. et R. D. D'ARRIGO. 1995. « Tree ring width and density evidence of climatic and potential forest change in Alaska ». *Global Biogeochemical Cycles*, volume 9, numéro 2, pp. 227-234.

JANSEN, E., J. OVERPECK, K. R. BRIFFA, J.-C. DUPLESSY, F. JOOS, V. MASSON-DELMOTTE, D. OLAGO, B. OTTO-BLIESNER, W. R. PELTIER, S. RAHMSTORF, R. RAMESH, D. RAYNAUD, D. RIND, O. SOLOMINA, R. VILLALBA et D. ZHANG. 2007. « Palaeoclimate ». Dans *Climate Change 2007: The Physical Science Basis. Contribution of Working*

Group I to the Fourth Assessment Report of the Intergovernmental Panel on Climate Change. pp. 433-497. Cambridge & New York: Cambridge University Press

JOHNSON, E. A. 1992. « Fire and vegetation dynamics: studies from the North American boreal forest ». *Fire and vegetation dynamics: studies from the North American boreal forest*.

JOHNSTONE, J. F. et F. S. CHAPIN. 2006. « Fire interval effects on successional trajectory in boreal forests of northwest Canada ». *Ecosystems*, volume 9, numéro 2, pp. 268-277.

JOHNSTONE, J. F. 2006. « Response of boreal plant communities to variations in previous fire-free interval ». *International Journal of Wildland Fire*, volume 15, numéro 4, pp. 497-508.

JOHNSTONE, J. F., T. N. HOLLINGSWORTH, F. S. CHAPIN et M. C. MACK. 2010. « Changes in fire regime break the legacy lock on successional trajectories in Alaskan boreal forest ». *Global Change Biology*, volume 16, numéro 4, pp. 1281-1295.

JONES, P. D., T. J. OSBORN et K. R. BRIFFA. 2001. « The evolution of climate over the last millennium ». *Science*, volume 292, numéro 5517, pp. 662-667.

JONES, P. D., K. R. BRIFFA, T. J. OSBORN, J. M. LOUGH, T. D. VAN OMMEN, B. M. VINTHER, J. LUTHERBACHER, E. R. WAHL, F. W. ZWIERS, M. E. MANN, G. A. SCHMIDT, C. M. AMMANN, B. M. BUCKLEY, K. M. COBB, J. ESPER, H. GOOSSE, N. GRAHAM, E. JANSEN, T. KIEFER, C. KULL, M. KUTTEL, E. MOSLEY-THOMPSON, J. T. OVERPECK, N. RIEDWYL, M. SCHULZ, A. W. TUDHOPE, R. VILLALBA, H. WANNER, E. WOLFF et E. XOPLAKI. 2009. « High-resolution palaeoclimatology of the last millennium: a review of current status and future prospects ». *Holocene*, volume 19, numéro 1, pp. 3-49.

JUCKES, M. N., M. R. ALLEN, K. R. BRIFFA, J. ESPER, G. C. HEGERL, A. MOBERG, T. J. OSBORN et S. L. WEBER. 2007. « Millennial temperature

reconstruction intercomparison and evaluation ». *Climate of the Past*, volume 3, numéro 4, pp. 591-609.

KELLY, P. M., H. H. LEUSCHNER, K. R. BRIFFA et I. C. HARRIS. 2002. « The climatic interpretation of pan-European signature years in oak ring-width series ». *Holocene*, volume 12, numéro 6, pp. 689-694.

KUNIHOLM, P. I. 2000. « Dendrochronology (Tree-Ring Dating) of Panel Paintings ». Dans *The Science of Paintings*. pp. 206–215. New York: Springer-Verlag

LARSEN, C. P. S. 1997. « Spatial and temporal variations in boreal forest fire frequency in northern Alberta ». *Journal of Biogeography*, volume 24, numéro 5, pp. 663-673.

LAVIGNE, F., J.-P. DEGEAI, J.-C. KOMOROWSKI, S. GUILLET, V. ROBERT, P. LAHITTE, C. OPPENHEIMER, M. STOFFEL, C. M. VIDAL, SURONO, I. PRATOMO, P. WASSMER, I. HAJDAS, D. S. HADMOKO et E. DE BELIZAL. 2013. « Source of the great A.D. 1257 mystery eruption unveiled, Samalas volcano, Rinjani Volcanic Complex, Indonesia ». *Proceedings of the National Academy of Sciences of the United States of America*, volume 110, numéro 42, pp. 16742-16747.

LAVOIE, L. et L. SIROIS. 1998. « Vegetation Changes Caused by Recent Fires in the Northern Boreal Forest of Eastern Canada ». *Journal of Vegetation Science*, volume 9, numéro 4, pp. 483-492.

LE GOFF, H. et L. SIROIS. 2004. « Black spruce and jack pine dynamics simulated under varying fire cycles in the northern boreal forest of Quebec, Canada ». *Canadian Journal of Forest Research*, volume 34, numéro 12, pp. 2399-2409.

LESTER, R. E., W. WRIGHT et M. JONES-LENNON. 2007. « Does adding wood to agricultural streams enhance biodiversity? An experimental approach ». *Marine and Freshwater Research*, volume 58, numéro 8, pp. 687-698.

LEUSCHNER, H. H., U. SASS-KLAASSEN, E. JANSMA, M. G. L. BAILLIE et M. SPURK. 2002. « Subfossil European bog oaks: population dynamics and

long-term growth depressions as indicators of changes in the Holocene hydro-regime and climate ». *Holocene*, volume 12, numéro 6, pp. 695-706.

MANN, M. E., R. S. BRADLEY et M. K. HUGHES. 1998. « Global-scale temperature patterns and climate forcing over the past six centuries ». *Nature*, volume 392, numéro 6678, pp. 779-787.

MANN, M. E. et P. D. JONES. 2003. « Global surface temperatures over the past two millennia ». *Geophysical Research Letters*, volume 30, numéro 15, 1820.

MANN, M. E., J. D. FUENTES et S. RUTHERFORD. 2012. « Underestimation of volcanic cooling in tree-ring-based reconstructions of hemispheric temperatures ». *Nature Geoscience*, volume 5, numéro 3, pp. 202-205.

MARBURG, A. E., M. G. TURNER et T. K. KRATZ. 2006. « Natural and anthropogenic variation in coarse wood among and within lakes ». *Journal of Ecology*, volume 94, numéro 3, pp. 558-568.

MARCHAND, D., Y. T. PRAIRIE et P. A. DEL GIORGIO. 2009. « Linking forest fires to lake metabolism and carbon dioxide emissions in the boreal region of Northern Quebec ». *Global Change Biology*, volume 15, numéro 12, pp. 2861-2873.

MARGRETH, A., A. S. DYKE, J. C. GOSSE et A. M. TELKA. Sous presse. « Neoglacial ice expansion and late Holocene cold-based ice cap dynamics on Cumberland Peninsula, Baffin Island, Arctic Canada ». *Quaternary Science Reviews*.

MCINTYRE, S. et R. MCKITRICK. 2005. « Hockey sticks, principal components, and spurious significance ». *Geophysical Research Letters*, volume 32, numéro 3, L03710.

MILLER, G. H., A. GEIRSDÓTTIR, Y. ZHONG, D. J. LARSEN, B. L. OTTO-BLIESNER, M. M. HOLLAND, D. A. BAILEY, K. A. REFSNIDER, S. J. LEHMAN, J. R. SOUTHON, C. ANDERSON, H. BJÖRNSSON et T. THORDARSON. 2012. « Abrupt onset of the Little Ice Age triggered by

volcanism and sustained by sea-ice/ocean feedbacks ». *Geophysical Research Letters*, volume 39, numéro 2, L02708.

MITCHELL, T. D. et P. D. JONES. 2005. « An improved method of constructing a database of monthly climate observations and associated high-resolution grids ». *International journal of climatology*, volume 25, numéro 6, pp. 693-712.

MOBERG, A., D. M. SONECHKIN, K. HOLMGREN, M. H. DATSENKO et W. KARLÉN. 2005. « Highly variable Northern Hemisphere temperatures reconstructed from low- and high-resolution proxy data ». *Nature*, volume 433, numéro 7026, pp. 613-617.

MORNEAU, C. et S. PAYETTE. 1989. « Postfire lichen-spruce woodland recovery at the limit of the boreal forest in northern Quebec ». *Canadian Journal of Botany*, volume 67, numéro 9, pp. 2770-2782.

NAIMAN, R. J. et H. DÉCAMPS. 1997. « The ecology of interfaces: Riparian zones ». *Annual Review of Ecology and Systematics*, volume 28, pp. 621-658.

NAURZBAEV, M. M., E. A. VAGANOV, O. V. SIDOROVA et F. H. SCHWEINGRUBER. 2002. « Summer temperatures in eastern Taimyr inferred from a 2427-year late-Holocene tree-ring chronology and earlier floating series ». *Holocene*, volume 12, numéro 6, pp. 727-736.

OTTERÅ, O. H., M. BENTSEN, H. DRANGE et L. SUO. 2010. « External forcing as a metronome for Atlantic multidecadal variability ». *Nature Geoscience*, volume 3, numéro 10, pp. 688-694.

PAGES 2K CONSORTIUM. 2013. « Continental-scale temperature variability during the past two millennia ». *Nature Geoscience*, volume 6, numéro 5, pp. 339-346.

PAYETTE, S. et R. GAGNON. 1985. « Late Holocene deforestation and tree regeneration in the forest-tundra of Québec ». *Nature*, volume 313, numéro 6003, pp. 570-572.

PAYETTE, S., L. FILION, L. GAUTHIER et Y. BOUTIN. 1985. « Secular climate change in old-growth tree-line vegetation of northern Quebec ». *Nature*, volume 315, numéro 6015, pp. 135-138.

PAYETTE, S., C. MORNEAU, L. SIROIS et M. DESPONTS. 1989. « Recent Fire History of the Northern Quebec Biomes ». *Ecology*, volume 70, numéro 3, pp. 656-673.

PAYETTE, S. et C. MORNEAU. 1993. « Holocene Relict Woodlands at the Eastern Canadian Treeline ». *Quaternary Research*, volume 39, numéro 1, pp. 84-89.

PAYETTE, S. 1993. « The Range Limit of Boreal Tree Species in Quebec-Labrador - an Ecological and Paleoecological Interpretation ». *Review of Palaeobotany and Palynology*, volume 79, numéro 1-2, pp. 7-30.

PAYETTE, S., L. FILION et A. DELWAIDE. 2008. « Spatially explicit fire-climate history of the boreal forest-tundra (Eastern Canada) over the last 2000 years ». *Philosophical Transactions of the Royal Society B: Biological Sciences*, volume 363, numéro 1501, pp. 2301-2316.

PAYETTE, S., A. DELWAIDE, A. SCHAFFHAUSER et G. MAGNAN. 2012. « Calculating long-term fire frequency at the stand scale from charcoal data ». *Ecosphere*, volume 3, numéro 7, pp. art59.

POLIS, G. A., W. B. ANDERSON et R. D. HOLT. 1997. « Toward an integration of landscape and food web ecology: The dynamics of spatially subsidized food webs ». *Annual Review of Ecology and Systematics*, volume 28, pp. 289-316.

ROWE, J. S. et G. W. SCOTTER. 1973. « Fire in the boreal forest ». *Quaternary Research*, volume 3, numéro 3, pp. 444-464.

ROY, R., L. MATHIER et B. BOBÉE. 1995. « Analyse probabiliste des conditions de faible hydraulicité dans une perspective de production hydro-électrique (mars 1995) ». *Science et changements planétaires / Sécheresse*, volume 6, numéro 4, pp. 355-363.

RUDOLPH, T. D. et P. R. LAIDLY. 1990. « Pinus banksiana Lamb. ». Dans *Silvics of North America: 1. Conifers; 2. Hardwoods. Agriculture Handbook 654.* pp. 555-586. Washington, DC: U.S. Department of Agriculture, Forest Service

RUTHERFORD, S., M. E. MANN, T. J. OSBORN, R. S. BRADLEY, K. R. BRIFFA, M. K. HUGHES et P. D. JONES. 2005. « Proxy-based Northern Hemisphere surface temperature reconstructions: Sensitivity to method, predictor network, target season, and target domain ». *Journal of Climate*, volume 18, numéro 13, pp. 2308-2329.

SANTER, B. D., C. BONFILS, J. F. PAINTER, M. D. ZELINKA, C. MEARS, S. SOLOMON, G. A. SCHMIDT, J. C. FYFE, J. N. S. COLE, L. NAZARENKO, K. E. TAYLOR et F. J. WENTZ. 2014. « Volcanic contribution to decadal changes in tropospheric temperature ». *Nature Geoscience*, volume 7, numéro 3, pp. 185-189.

SARGENT, L. W., S. W. GOLLADAY, A. P. COVICH et S. P. OPSAHL. 2011. « Physicochemical habitat association of a native and a non-native crayfish in the lower Flint river, Georgia: Implications for invasion success ». *Biological Invasions*, volume 13, numéro 2, pp. 499-511.

SAUCIER, J.-P., P. GRONDIN, A. ROBITAILLE et J.-F. BERGERON. 2003. « Zones de végétation et domaines bioclimatiques du Québec ». Québec: Gouvernement du Québec, Ministère des Ressources naturelles, de la Faune et des Parcs. En ligne. <https://www.mrn.gouv.qc.ca/forets/inventaire/inventaire-zones.jsp>. Consulté le 07/03/2014

SCEALY, J. A., S. J. MIKA et A. J. BOULTON. 2007. « Aquatic macroinvertebrate communities on wood in an Australian lowland river: Experimental assessment of the interactions of habitat, substrate complexity and retained organic matter ». *Marine and Freshwater Research*, volume 58, numéro 2, pp. 153-165.

SCHLEUSSNER, C. F. et G. FEULNER. 2013. « A volcanically triggered regime shift in the subpolar North Atlantic Ocean as a possible origin of the Little Ice Age ». *Climate of the Past*, volume 9, numéro 3, pp. 1321-1330.

SCHMIDT, G. A., D. T. SHINDELL et K. TSIGARIDIS. 2014. « Reconciling warming trends ». *Nature Geoscience*, volume 7, numéro 3, pp. 158-160.

SCIEM. 2007. *OSM 3. On Screen Measuring and Image Analysis. Version 3.65 User Manual.* Vienna, Austria: 58 p.

SCIEM. 2011. *PAST4. Personal Analysis System for Treering Research. Version 4.3 Instruction Manual.* Vienna, Austria: 161 p.

SENICI, D., A. LUCAS, H. Y. H. CHEN, Y. BERGERON, A. LAROUCHE, B. BROSSIER, O. BLARQUEZ et A. A. ALI. 2013. « Multi-millennial fire frequency and tree abundance differ between xeric and mesic boreal forests in central Canada ». *Journal of Ecology*, volume 101, numéro 2, pp. 356-367.

SHAO, X., S. WANG, H. ZHU, Y. XU, E. LIANG, Z. Y. YIN, X. XU et Y. XIAO. 2009. « A 3585-year ring-width dating chronology of Qilian juniper from the northeastern Qinghai-Tibetan Plateau ». *IAWA Journal*, volume 30, numéro 4, pp. 379-394.

SIDOROVA, O. V., M. SAURER, A. ANDREEV, D. FRITZSCHE, T. OPEL, M. M. NAURZBAEV et R. SIEGWOLF. 2013. « Is the 20th century warming unprecedented in the Siberian north? ». *Quaternary Science Reviews*, volume 73, pp. 93-102.

SIROIS, L. 1997. « Distribution and dynamics of balsam fir (Abies balsamea L. Mill.) at its northern limit in the James Bay area ». *Ecoscience*, volume 4, numéro 3, pp. 340-352.

SPURK, M., H. H. LEUSCHNER, M. G. L. BAILLIE, K. R. BRIFFA et M. FRIEDRICH. 2002. « Depositional frequency of German subfossil oaks: climatically and non-climatically induced fluctuations in the Holocene ». *Holocene*, volume 12, numéro 6, pp. 707-715.

STENCHIKOV, G., T. L. DELWORTH, V. RAMASWAMY, R. J. STOUFFER, A. WITTENBERG et F. ZENG. 2009. « Volcanic signals in oceans ». *Journal of Geophysical Research D: Atmospheres*, volume 114, numéro D16, D16104.

STOCKER, T. F., D. QIN, G.-K. PLATTNER, M. TIGNOR, S.K. ALLEN, J. BOSCHUNG, A. NAUELS, Y. XIA, V. BEX et P. M. MIDGLEY. 2013. *IPCC, 2013: Climate Change 2013: The Physical Science Basis. Contribution of Working Group I to the Fifth Assessment Report of the Intergovernmental Panel on Climate Change*. Cambridge, United Kingdom and New York, NY, USA: Cambridge University Press. 1535 p.

STOCKS, B. J., J. A. MASON, J. B. TODD, E. M. BOSCH, B. M. WOTTON, B. D. AMIRO, M. D. FLANNIGAN, K. G. HIRSCH, K. A. LOGAN, D. L. MARTELL et W. R. SKINNER. 2003. « Large forest fires in Canada, 1959-1997 ». *Journal of Geophysical Research D: Atmospheres*, volume 108, numéro D1, 8149.

SWETNAM, T. W., C. H. BAISAN, A. C. CAPRIO, P. M. BROWN, R. TOUCHAN, R. S. ANDERSON et D. J. HALLETT. 2009. « Multi-millennial fire history of the Giant Forest, Sequoia National Park, California, USA ». *Fire Ecology*, volume 5, numéro 3, pp. 120-150.

TANK, J. L. et J. R. WEBSTER. 1998. « Interaction of substrate and nutrient availability on wood biofilm processes in streams ». *Ecology*, volume 79, numéro 6, pp. 2168-2179.

TINGLEY, M. P. et P. HUYBERS. 2013. « Recent temperature extremes at high northern latitudes unprecedented in the past 600 years ». *Nature*, volume 496, numéro 7444, pp. 201-205.

TROUET, V., H. F. DIAZ, E. R. WAHL, A. E. VIAU, R. GRAHAM, N. GRAHAM et E. R. COOK. 2013. « A 1500-year reconstruction of annual mean temperature for temperate North America on decadal-to-multidecadal time scales ». *Environmental Research Letters*, volume 8, numéro 2, 024008.

VADEBONCOEUR, Y. et D. M. LODGE. 2000. « Periphyton production on wood and sediment: Substratum-specific response to laboratory and whole-lake nutrient manipulations ». *Journal of the North American Benthological Society*, volume 19, numéro 1, pp. 68-81.

VIAU, A. E., M. LADD et K. GAJEWSKI. 2012. « The climate of North America during the past 2000 years reconstructed from pollen data ». *Global and Planetary Change*, volume 84-85, pp. 75-83.

VIERECK, L. A. et W. F. JOHNSTON. 1990. « Picea mariana (Mill.) B. S. P. ». Dans *Silvics of North America: 1. Conifers; 2. Hardwoods. Agriculture Handbook 654*. pp. 443–464. Washington, DC: U.S. Department of Agriculture, Forest Service

WARDLE, D. A., L. R. WALKER et R. D. BARDGETT. 2004. « Ecosystem properties and forest decline in contrasting long-term chronosequences ». *Science*, volume 305, numéro 5683, pp. 509-513.

WILMKING, M., R. D'ARRIGO, G. C. JACOBY et G. P. JUDAY. 2005. « Increased temperature sensitivity and divergent growth trends in circumpolar boreal forests ». *Geophysical Research Letters*, volume 32, numéro 15, L15715.

ZANCHETTIN, D., C. TIMMRECK, H. F. GRAF, A. RUBINO, S. LORENZ, K. LOHMANN, K. KRÜGER et J. H. JUNGCLAUS. 2012. « Bi-decadal variability excited in the coupled ocean-atmosphere system by strong tropical volcanic eruptions ». *Climate Dynamics*, volume 39, numéro 1-2, pp. 419-444.

ZHONG, Y., G. H. MILLER, B. L. OTTO-BLIESNER, M. M. HOLLAND, D. A. BAILEY, D. P. SCHNEIDER et A. GEIRSDOTTIR. 2011. « Centennial-scale climate change from decadally-paced explosive volcanism: A coupled sea ice-ocean mechanism ». *Climate Dynamics*, volume 37, numéro 11-12, pp. 2373-2387.